

ALLIGATOR RIVERS ANALOGUE PROJECT



ISBN 0-642-59941-6

DOE/HMIP/RR/92/085

SKI TR 92:20-15

FINAL REPORT VOLUME 15

GEOCHEMISTRY OF ^{239}Pu , ^{129}I , ^{99}Tc AND ^{36}Cl

1992

AN OECD/NEA INTERNATIONAL PROJECT MANAGED BY:
AUSTRALIAN NUCLEAR SCIENCE AND TECHNOLOGY ORGANISATION

Legacy - 70

ALLIGATOR RIVERS ANALOGUE PROJECT

FINAL REPORT

VOLUME 15

GEOCHEMISTRY OF ^{239}Pu , ^{129}I , ^{99}Tc AND ^{36}Cl

Lead Author: J.T. Fabryka-Martin¹

Contributing Author: D.B. Curtis¹

¹Los Alamos National Laboratory,
Isotope and Nuclear Chemistry Division,
Mail Stop J514, Los Alamos, New Mexico, 87545, USA

~~Ineos Heights, New South Wales, Australia~~
Research Lab, A
Private Mail Bag 1,
Memai, NSW 2234

PREFACE

The Koongarra uranium ore deposit is located in the Alligator Rivers Region of the Northern Territory of Australia. Many of the processes that have controlled the development of this natural system are relevant to the performance assessment of radioactive waste repositories. An Agreement was reached in 1987 by a number of agencies concerned with radioactive waste disposal, to set up the International Alligator Rivers Analogue Project (ARAP) to study relevant aspects of the hydrological and geochemical evolution of the site. The Project ran for five years.

The work was undertaken by ARAP through an Agreement sponsored by the OECD Nuclear Energy Agency (NEA). The Agreement was signed by the following organisations: the Australian Nuclear Science and Technology Organisation (ANSTO); the Japan Atomic Energy Research Institute (JAERI); the Power Reactor and Nuclear Fuel Development Corporation of Japan (PNC); the Swedish Nuclear Power Inspectorate (SKI); the UK Department of the Environment (UKDoE); and the US Nuclear Regulatory Commission (USNRC). ANSTO was the managing participant.

This report is one of a series of 16 describing the work of the Project; these are listed below:

No.	Title	Lead Author(s)
1	Summary of Findings	P Duerden, D A Lever, D A Sverjensky and L R Townley
2	Geologic Setting	A A Snelling
3	Geomorphology and Paleoclimatic History	K-H Wyrwoll
4	Geophysics, Petrophysics and Structure	D W Emerson
5	Hydrogeological Field Studies	S N Davis
6	Hydrogeological Modelling	L R Townley
7	Groundwater Chemistry	T E Payne
8	Chemistry and Mineralogy of Rocks and Soils	R Edis
9	Weathering and its Effects on Uranium Redistribution	T Murakami
10	Geochemical Data Bases	D G Bennett and D Read
11	Geochemical Modelling of Secondary Uranium Ore Formation	D A Sverjensky
12	Geochemical Modelling of Present-day Groundwaters	D A Sverjensky
13	Uranium Sorption	T D Waite
14	Radionuclide Transport	C Golian and D A Lever,
15	Geochemistry of ^{239}Pu , ^{129}I , ^{99}Tc and ^{36}Cl	J T Fabryka-Martin
16	Scenarios	K Skagius and S Wingefors

CONTENTS

	Page
EXECUTIVE SUMMARY	
ACKNOWLEDGMENTS	
1 INTRODUCTION	1
1.1 Research Objectives	1
1.2 Relevance to Performance Assessment Activities for Geologic Repositories	1
1.3 Overview of Approach	4
2 CHARACTERISATION OF ORE SAMPLES	6
2.1 Description of Ore Deposits and Samples	6
2.1.1 Koongarra, Australia	6
2.1.2 Oklo, Gabon	10
2.1.3 Cigar Lake, Canada	10
2.1.4 Key Lake, Canada	11
2.1.5 Shinkolobwe, Zaire	11
2.1.6 Beaverlodge, Canada	11
2.2 Mineralogy	12
2.3 Elemental Composition	12
2.4 Uranium Concentrations and Isotopic Composition	17
2.5 Neutron Production Rates	18
3 MEASURED NRP CONCENTRATIONS IN ORES AND GROUNDWATERS	20
3.1 Analytical Methods for Ore Samples	20
3.1.1 Plutonium-239	20
3.1.2 Iodine-129	20
3.1.3 Technetium-99	21
3.1.4 Chlorine-36	21
3.2 NRP Concentrations in Ores	21
3.2.1 Plutonium-239 in ores	21
3.2.2 Iodine-129 in ores	24
3.2.3 Technetium-99 in ores	24
3.2.4 Chlorine-36 in ores	24

	Page
3.3 NRP Concentrations in Groundwater	24
3.3.1 Plutonium-239 in groundwater	26
3.3.2 Iodine-129 in groundwater	30
3.3.3 Technetium-99 in groundwater	31
3.3.4 Chlorine-36 in groundwater	34
4 MODELLING NRP SOURCE TERMS	38
4.1 NRP Production Mechanisms	38
4.1.1 Spontaneous fission of ^{238}U	38
4.1.2 Neutron-induced fission of ^{235}U and ^{238}U	38
4.1.3 Neutron-capture reactions	40
4.2 Source-Term Model Description	40
4.2.1 General approach	40
4.2.2 Results of the infinite model	42
4.2.3 Estimated uncertainties in abundances predicted by the infinite model	47
4.3 Effect of Stratigraphy on NRP Abundances	51
4.3.1 Koongarra	55
4.3.2 Key Lake	58
4.3.3 Cigar Lake	58
4.3.4 Oklo	59
4.4 Conclusions about Modelling Capability	61
4.4.1 Capability to predict absolute NRP abundances	61
4.4.2 Uncertainties in predictions of absolute abundances	64
4.4.3 Capability to predict relative NRP abundances	64
4.5 Other Radionuclides in Koongarra Groundwaters	72
4.5.1 Tritium	72
4.5.2 Carbon-14	72
5 CONCLUSIONS: APPLICABILITY OF URANIUM OREBODIES AS NATURAL ANALOGUES FOR HLW REPOSITORIES	73
5.1 Applicability for Testing Release-Rate Models	73
5.2 Directions for Future Work	74
6 REFERENCES	76

LIST OF TABLES

	Page
2.1 Source deposits for primary ore samples	8
2.2 Description of secondary ore samples, Koongarra deposit	10
2.3 Dominant mineralogy of primary ore samples	13
2.4 Methods and detection limits for elemental analyses of uranium ore samples	14
2.5 Elemental analyses of certified reference materials and sample replicates	15
2.6 Elemental analyses of primary ore samples	16
2.7 Uranium concentrations and activity ratios of primary ore samples	17
2.8 Measured rates of neutron production in uranium ores	19
3.1 Plutonium-239 concentrations in primary ores, corrected for background	22
3.2 Plutonium-239 concentrations in weathered Koongarra ores	23
3.3 Iodine-129 concentrations in primary uranium ores	25
3.4 Chlorine-36 in uranium ores	26
3.5 Plutonium-239 concentrations in Koongarra groundwaters	29
3.6 Iodine-129 and chlorine-36 in Koongarra groundwaters, pre-existing boreholes, 1983-91	32
3.7 Chlorine-36 in Koongarra groundwaters, new boreholes, 1989-91	35
4.1 Bounding concentrations of H (ppm) used for sensitivity analyses	42
4.2 Uranium fission rates and NRP abundances predicted by MCNP for infinite ore bodies	43
4.3 Comparison of measured and predicted NRP concentrations for Shinkolobwe pitchblende	45
4.4 Results of sensitivity analyses for infinite ore bodies	48
4.5 Effects of ore geometry on NRP abundance predictions	54
4.6 Predicted production rate of ^{129}I and ^{99}Tc , assuming negligible contribution from induced fission of ^{238}U	70

LIST OF FIGURES

		Page
1.1	Actinide and fission product geochemical cycle	3
2.1	Procedure for characterising ore samples	7
2.2	Map of Koongarra drillholes from which ore samples were obtained for this study	9
3.1	Map of Koongarra boreholes from which water samples were obtained for this study	27
4.1	Model for predicting nuclide production rates	39
4.2	Comparison of measured and predicted NRP concentrations for Shinkolobwe pitchblende	46
4.3	Variation in predicted $^{239}\text{Pu}/\text{U}$ ratios and ^{235}U fission rates in samples from various ore deposits as a function of HREE and H contents	49
4.4	Comparison of measured and predicted ^{239}Pu concentrations for primary uranium ores	52
4.5	Comparison of measured and predicted ^{129}I concentrations for primary uranium ores	53
4.6	Geometry model: predicted distribution of $^{239}\text{Pu}/\text{U}$, $^{129}\text{I}/\text{U}$, $^{36}\text{Cl}/\text{Cl}$ and $^{99}\text{Tc}/\text{U}$ ratios in a profile through G2698	56
4.7	Geometry model: predicted distribution of $^{239}\text{Pu}/\text{U}$, $^{129}\text{I}/\text{U}$, $^{36}\text{Cl}/\text{Cl}$ and $^{99}\text{Tc}/\text{U}$ ratios in a profile through G4674	57
4.8	Geometry model: predicted distribution of ^{235}U and ^{238}U induced fission rates, and $^{239}\text{Pu}/\text{U}$, $^{129}\text{I}/\text{U}$, $^{99}\text{Tc}/\text{U}$ and $^{36}\text{Cl}/\text{Cl}$ ratios in a profile of Cigar Lake Hole 220	60
4.9	Geometry model: predicted distribution of (a) ^{235}U induced fission rates, (b) $^{36}\text{Cl}/\text{Cl}$ ratios, (c) $^{239}\text{Pu}/\text{U}$ ratios and (d) ^{238}U induced fission rates in the Oklo Reactor Zone 9 ore seam	62
4.10	Predicted correlation between ^{235}U fission rate and $^{36}\text{Cl}/\text{Cl}$ in primary uranium ores, as a function of H/U atom ratio	65
4.11	Predicted correlation between ^{235}U fission rate and $^{36}\text{Cl}/\text{Cl}$ in the Oklo Reactor Zone 9 ore seam, as a function of location	66
4.12	Predicted fraction of (a) total and (b) induced fissions attributable to ^{238}U induced fission in primary uranium ores, as a function of H/U atom ratio	68
4.13	Predicted correlation between $^{239}\text{Pu}/\text{U}$ ratios and ^{238}U fission rates, as a function of H/U atom ratio	69
4.14	Comparison of measured and predicted ^{129}I concentrations for primary uranium ores, assuming negligible contribution from induced fission of ^{238}U	71

EXECUTIVE SUMMARY

Among the most persistent radioactive constituents of high-level wastes (HLW) from nuclear fission power reactors are plutonium-239 ($t_{1/2}$, 24,100 a), technetium-99 ($t_{1/2}$, 2.1×10^5 a), and iodine-129 ($t_{1/2}$, 1.6×10^7 a). The extent to which such long-lived constituents will be retained by a waste repository will be a function of their retention by the waste matrix and canister, by backfill materials, and by the natural geologic environment of the repository. Natural analogues, particularly uranium ore deposits, offer a means to evaluate the geochemical transport and retention properties of these radionuclides in analogous natural materials. In these natural environments, plutonium and fission-product elements have a unique geochemical history. They are produced by nuclear processes in minerals. Under certain hydrogeochemical conditions, they may be released from their host minerals, transported from their site of production, and retained at another location. In order for the effects of these processes to be manifest, they must occur on a timescale that is significantly less than a few mean lifetimes of the radioactive nuclides. For ^{239}Pu , ^{99}Tc and ^{129}I , the timescales must be less than about 10^5 a, 10^6 a, and 10^7 a, respectively. Hence, studies of the geochemistry of these three nuclides provide specific information about the chemical mass transport of elements that comprise long-term constituents of HLW on timescales that are directly relevant to the assessment of the effectiveness of geologic repositories for nuclear waste isolation.

In this report, measured abundances of natural ^{239}Pu , ^{99}Tc and ^{129}I in uranium ores are compared to calculated abundances in order to evaluate the degree of retention of these radionuclides by the ore. Measured ^{129}I concentrations in all samples of unweathered primary ore investigated in this study exceed the minimum concentrations predicted from spontaneous fission of ^{238}U . However, the concentrations are variably less than the amounts predicted by the source-term model under a wide variety of assumptions. Although the production of ^{129}I by neutron-induced fission of ^{235}U and ^{238}U is difficult to estimate with any accuracy, the measurements suggest that ^{129}I may be depleted to a larger extent in samples from the shallow Koongarra orebody than in samples from the deeper Cigar Lake deposit. Samples from weathered primary ore from Koongarra contain quantities of ^{129}I that are well below the minimum allowable abundance for in-situ production, an unambiguous indicator of loss of this fission product from its site of production, possibly in response to the alteration processes that have occurred in this region of the deposit. The mobility of radioiodine is also apparent from its high concentrations in the groundwaters flowing through the Koongarra deposit.

Predictions of the source-term model indicate that ^{99}Tc production in uranium ores is dominated by spontaneous fission of ^{238}U . In the ore samples studied, production of this fission product by induced fission of ^{235}U is 5-25% of the total, and that by neutron-induced fission of ^{238}U is generally $\leq 4\%$. The dominance of the spontaneous fission component should simplify interpretation of measured ^{99}Tc concentrations in uranium minerals. The validity of the source-term model prediction is borne out by two analyses of ^{99}Tc in primary ores, which had ^{99}Tc abundances at the levels predicted by the model, about 10% above that expected for spontaneous fission alone. Release of ^{99}Tc from the ore during weathering is suggested by its presence at measurable concentrations in water from one of the Koongarra boreholes.

Source-term models predicting ^{239}Pu abundances in uranium minerals lead to ambiguous conclusions. Several model-dependent evaluations of ^{239}Pu concentrations are compared with measured abundances in primary uranium minerals that are believed to have been closed systems with respect to ^{239}Pu and U. Measured abundances are generally within the range of predicted values. However, the results indicate that, in very heterogeneous media such as that typical of uranium ore deposits, the chemical parameters critical for determination of ^{239}Pu abundances are difficult to characterise with sufficient accuracy to use the results for evaluating the degree of retention or loss of ^{239}Pu from the orebody. The model predictions are particularly sensitive to spatial variations of U, H and Gd concentrations within a radius of about 20-40 cm of the sample. Consequently, current methods for estimating ^{239}Pu production rates are limited to estimates that are no better than a factor of 2 of the true rate, which is not sufficiently precise to provide unambiguous measures of Pu retention.

Alternative methods for evaluating Pu mobility are being investigated, including its measurement in groundwaters. Attempts to characterise the aqueous geochemistry of plutonium in Koongarra groundwater indicated the presence of the element in two wells at very low concentrations, on the order of 10^{-18} M. The source of the plutonium in one of the wells is unknown and may be anthropogenic fallout rather than natural plutonium derived from the orebody. The results suggest that mobile plutonium may be in particulate matter and in anionic form. Establishing the validity of these observations, and a less ambiguous interpretation, would require additional, more sophisticated, sampling.

The feasibility of uranium minerals as analogues for the behaviour of nuclear reaction products (NRP) in spent fuel relies upon a capability to characterize NRP concentrations in source minerals. Extensive modelling work documented in this report emphasizes the need to include as much information as possible about sample environs in any NRP production rate model. Even with detailed compositional information, however, uncertainties in model predictions will often be too large to provide reliable estimates of absolute NRP abundances in heterogeneous geologic systems. To address this limitation, one of the most useful conclusions of the modelling study has been to show the extent to which various NRP should be correlated to one another, such that one constrains the production rate of another. For example, ^{36}Cl ($t_{1/2}$, 3.0×10^5 a), another long-lived neutron-capture product found in uranium ores, is shown to be an ideal in-situ monitor of the ^{235}U fission rate, which is the dominant source term for ^{129}I and possibly a significant one for ^{99}Tc . Similarly, $^{239}\text{Pu}/\text{U}$ ratios can be used to establish limits on the ^{238}U neutron-induced fission rate; the ratios measured in this study suggest that ^{238}U induced fission comprises $< 4\%$ of the total fissions in most of the ore samples studied. These two correlations are only valid if the H/U atom ratio in the sample or in its immediate environs exceeds 6, which roughly corresponds to 6000 ppm H.

ACKNOWLEDGMENTS

This research has been supported by the U.S. Department of Energy, Office of Basic Energy Sciences, Division of Engineering and Geosciences (DOE/OBES); Alligator Rivers Analogue Project (ARAP); and the U.S. Department of Energy, Office of Civilian Waste Management, Office of Strategic Planning and International Programs (DOE/OCWM). The continued participation of Los Alamos National Laboratory in this research was made possible by the energetic programmatic support of George Kolstad (DOE/OBES), George Birchard and Linda Kovach (U.S. Nuclear Regulatory Commission), and Bob Levich and Tom Isaacs (DOE/OCWM).

The oft-thankless role of providing critical technical and administrative coordination was capably managed by Peter Duerden, with the efficient assistance of Robin Lowerson (Australian Nuclear Science and Technology Organisation (ANSTO)). Koongarra samples were selected with the assistance of Andrew Snelling and Peter Airey (ANSTO). Samples from Cigar Lake were provided by Jan Cramer (Atomic Energy of Canada Ltd (AECL)). Alex Gancarz (LANL) collected or assisted in the collection of samples from Oklo and Key Lake. The NBL-6 sample was provided to us through the courtesy of Fred Brauer and Robert Strebin, Jr. (Battelle-Pacific Northwest Laboratories). Jan Cramer (AECL) and David Bish and Ernest Gladney (LANL) assisted in determining some of the sample properties. Field collection of groundwater samples was only possible due to the skill, ingenuity, careful planning and patience applied to this problem by Tim Payne and Robert Edis (ANSTO).

1 INTRODUCTION

1.1 Research Objectives

Geologic repositories will be required to contain some constituents of high-level nuclear waste for 10^4 years or more. Concepts of redundant containment are being developed to attain the desired results. In such repositories, it is envisaged that waste will be immobilised in a stable matrix selected to inhibit the rate of release of radioactive constituents to the environment. The waste matrix will be surrounded by engineered barriers and emplaced in a geologic setting selected to restrict the movement of long-lived radionuclides from the waste to the accessible environment in the event that an accidental release occurs. Such multiple barriers are intended to ensure that the waste materials will be introduced into the human environment at a sufficiently low rate so as to allow the radioactive constituents to decay or be diluted below some predetermined acceptable threshold activity.

The long times required for containment and the complex physical and chemical processes make it difficult to assess the effectiveness of the multiple barrier concept. Assessments are being done using computer-based models that integrate the processes controlling the rate of release and movement of radioactive materials in the repository environment. The models predict the probability of radioactive constituents being introduced into the accessible environment. Uncertainties in such assessments are difficult to quantify - but are undoubtedly large - because they arise from an imperfect understanding of the processes, the nature of their interactions, and the accuracy with which the models simulate them.

One means of reducing the uncertainties associated with assessments of repository effectiveness is to compare the results, or the assumptions upon which the results are based, with observable consequences of natural processes that have occurred over times and/or in complex systems that are analogous to those anticipated for the lifetime of the repository. This report describes the quantitative determination of natural ^{239}Pu , ^{99}Tc and ^{129}I in rocks and groundwaters from uranium deposits. The usefulness of such analyses are evaluated for quantifying changes in relative concentrations of these nuclides and uranium in rocks over the last hundred thousand years, and for characterising the chemical and physical nature of these nuclides in groundwater. This work establishes the foundation for a comprehensive characterisation of ^{239}Pu and fission-product geochemistry in systems with a variety of geochemical and hydrogeochemical properties.

1.2 Relevance to Performance Assessment Activities for Geologic Repositories

Natural analogues are not meant to provide an analogue for an entire repository but rather only for a small subset of the processes or materials expected to be present in a repository. They provide a means to corroborate that long-term or large-scale processes that form the basis for risk assessment operate in nature and that there is a consistency between natural systems, laboratory experiments, and theoretical constructs of the models. Results from analogues indicate conditions under which processes occur, and to what magnitude. They provide data that can be used, in

conjunction with data from laboratory or smaller-scale field studies, to assign probabilities to occurrences of specific scenarios. They also provide a guidepost pointing the way to rigorous experiments that provide the verification of models of repository behavior (Ewing, 1990). In addition to the longer timescale and larger spatial scale, natural analogues differ from smaller-scale field experiments and laboratory experiments in that they commonly reflect the effects of coupling among processes.

Several aspects of uranium ore deposits, including Koongarra, may have parallels to geologic repositories and hence suggest the appropriateness of these deposits as analogues for materials or processes expected in repositories (Airey and Ivanovich, 1986; Birchard and Alexander, 1983; Chapman et al., 1984; Chapman and Smellie, 1986; Petit, 1991). Geochemical processes of interest are illustrated in Figure 1.1; those specifically relevant to uranium orebodies are as follows:

- (a) Analogue for spent fuel. Uraninite in primary ore zones may be considered as an analogue for spent fuel, in which one may study the uraninite to determine the extent to which radionuclides are redistributed by diffusion from the matrix or during mineral dissolution or alteration.
- (b) Transport and/or retardation modelling. Samples from secondary ore zones or zones of dispersed uranium down-gradient of primary ore bodies provide a means to assess the extent to which mobilisation of nuclear reaction products (NRP) may be limited by sorption onto clays or other active surfaces, by inclusion in structural sites of minerals, and by co-precipitation with U minerals.
- (c) Aqueous speciation modelling for groundwater. Geochemical analyses of groundwater samples from within and down-gradient of deposits may be used to assess the validity of the thermodynamic data base associated with aqueous speciation codes.

The limitations of natural analogues need always to be kept in mind. No experiment or observation can validate a predicted performance, e.g., the ability of a geologic repository to contain radioactive wastes for some specified time interval. In common with most other geologic analogues (Pearcy and Murphy, 1991), uranium deposits as analogues have a number of limitations, some serious, some relatively negligible, with respect to the applications described in this report:

- (a) Inadequate constraint on initial and boundary conditions. Flow paths and rates, now and in past, cannot be unambiguously determined, nor can the rate of advance of the weathering front. Consequently, one cannot know how much material has been involved in transport of nuclear reaction products (NRP).
- (b) The source term (i.e., original distribution of NRP elements of interest) is not well constrained for the primary ore zone. This problem is minor for ^{99}Tc , moderate for ^{129}I , and serious for ^{239}Pu . The consequence is a limited ability to quantify the extent of retention or loss of ^{239}Pu or ^{129}I from this zone.

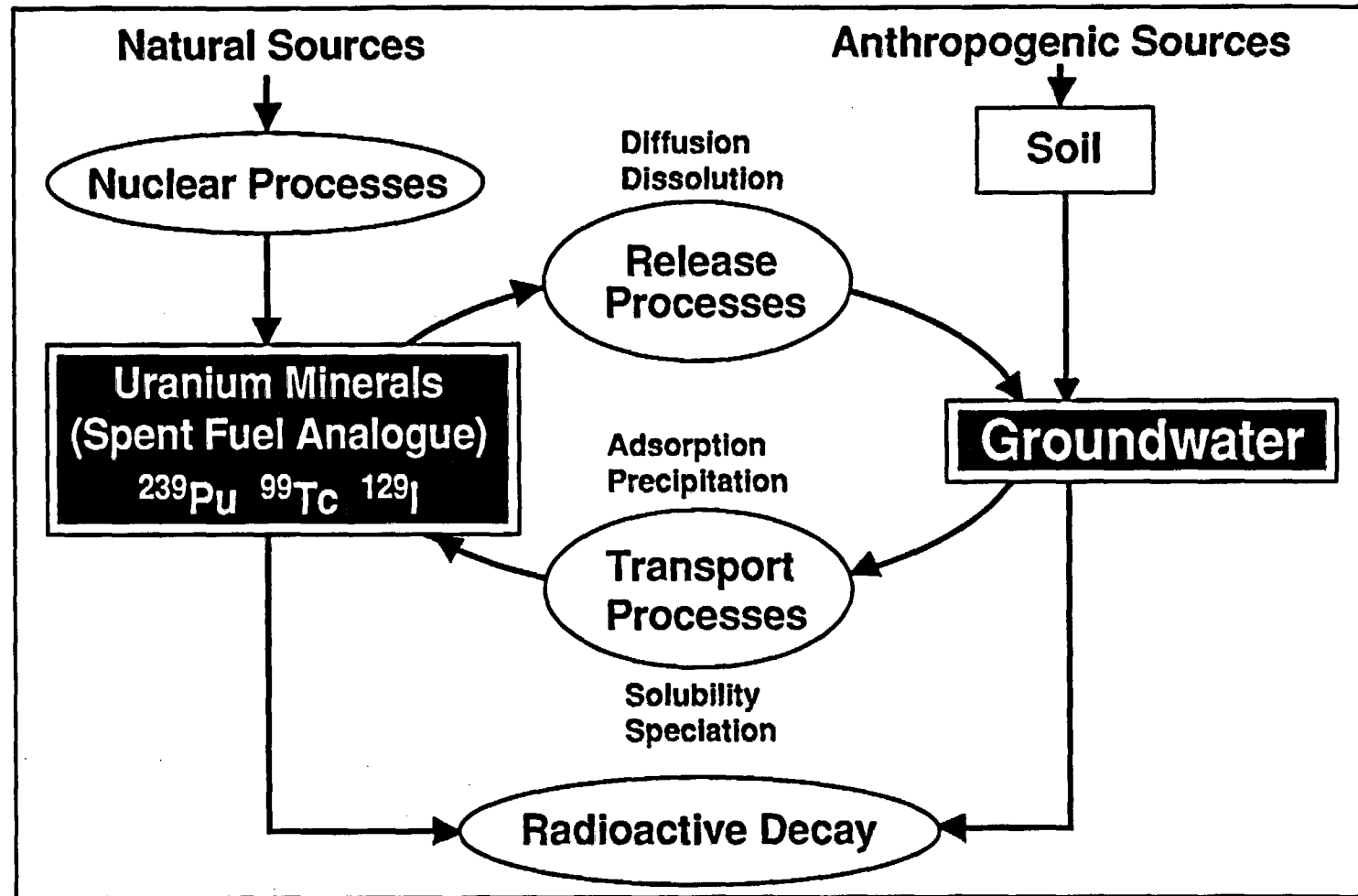


Figure 1.1 Actinide and fission product geochemical cycle

- (c) Geochemical conditions over the relevant time period may have varied in an unknown way.
- (d) The results may reflect overlapping effects from other processes that are not expected to be present in a repository.
- (e) Interpretation of results is not unique; more than one combination of processes and events are generally consistent with the observations.
- (f) Elements and materials studied in natural analogues are only crude approximations of those in a radioactive-waste repository. For example, uraninite is a good analogue to the bulk composition and crystal form of spent fuel (Finch and Ewing, 1989; Pearcy and Murphy, 1991, p. 45) but does not contain internal phase segregations present in spent fuel or a substantial transuranic component (Pearcy and Manaktala, 1992).

At best, analogues allow broad limits to be set on specific processes. No analogue can prove a geologic hypothesis regarding long-term phenomena such as NRP retention by spent fuel; analogue studies can only approach a limited kind of proof by showing compatibility of the hypothesis with a large body of independent observations (Ewing and Jercinovic, 1987), i.e., by showing that the hypothesis is not invalidated under a given set of conditions. Consequently, it is important that a variety of geochemical environments be studied in order to develop a large data base of independent observations. For this reason, this report presents results for samples from several uranium ore deposits in addition to that at Koongarra.

1.3 Overview of Approach

The overall objective of the work described herein is to test assumptions about the geochemistries of ^{239}Pu , ^{99}Tc and ^{129}I , collectively called NRP (nuclear reaction products). The approach is: (a) to measure concentrations of these radionuclides in different geochemical environments; (b) to compare measured concentrations with those predicted by a source-term model, assuming closed or static systems; and (c) to interpret measured concentrations in terms of retention by the ore, migration in groundwater, or retardation down-gradient of the ore body.

The approach is described in more detail using ^{239}Pu as an example; an analogous discussion could be given for the fission products ^{99}Tc or ^{129}I . Among the elements, natural plutonium is unusual in that it has no surviving primordial component. All modern natural plutonium is juvenile, a monoisotopic element, ^{239}Pu , produced by ^{238}U capture of neutrons. Unlike most elements, which are exclusively primordial, plutonium typically has a simple natural history. In a static or closed system, the element resides at its site of production with a mean lifetime of 3.5×10^4 yr until it decays by α -emission to ^{235}U . In a system that has been undisturbed for about 10^5 yr (i.e., several ^{239}Pu half-lives), the relative abundances of the plutonium product and the uranium target reach a constant saturation value that is exclusively a function of the rate of plutonium production. This in turn is a function of the neutronics - the fluence and energy distribution of neutrons - that induce the nuclear reaction. The relative abundances of plutonium and uranium

under this condition are analogous to the more familiar condition referred to as secular equilibrium in the systematics of radioactive decay: plutonium production and decay proceed at equal rates. At secular equilibrium, the relative abundances of plutonium and uranium can be calculated if the neutronics can be defined.

If the relative rate of plutonium gain or loss due to processes in an open system is greater than its rate of production and decay by nuclear processes at secular equilibrium, then a condition of disequilibrium will develop in which the relative abundances of plutonium and uranium differ from those at secular equilibrium. Theoretically, comparison of abundances of plutonium and uranium under a condition of disequilibrium with those that would exist if the system were in secular equilibrium provides the means to quantify differential rates of change of plutonium and uranium concentrations produced by open-system processes over the last hundred thousand years. To test this approach, the relative abundances of plutonium and uranium have been measured in rocks from several natural uranium deposits. The measurements, expressed as the ratio $^{239}\text{Pu}/\text{U}$, are then compared with calculated values of the relative abundances of the two elements in a condition of secular equilibrium. The comparison is formalised by calculating the fractionation factor α , which is the ratio of ratios shown in the equation below:

$$\alpha = (^{239}\text{Pu}/\text{U})_{\text{M}} / (^{239}\text{Pu}/\text{U})_{\text{SE}} \quad (1.1)$$

The subscript M refers to measured element ratios; the subscript SE refers to element ratios calculated for conditions of secular equilibrium. The factor α is a measure of the extent of any change in plutonium concentration relative to uranium over several ^{239}Pu half-lives, i.e., a period of about 1×10^5 years. An α -value of 1 manifests no fractionation between the two actinide elements. Values less than 1 suggest preferential loss of Pu relative to U, and values greater than 1 suggest preferential gain of Pu relative to U.

This report focusses on samples from unweathered and unaltered zones in several different primary ore deposits, i.e., samples believed to approximate closely systems which are closed with respect to retention of nuclear reaction products. A wide range of uranium contents and ore mineralogies was selected in order to test our understanding of factors controlling nuclide production rates and degrees of nuclide retention. In addition to Koongarra, the deposits include Key Lake, Cigar Lake, and Beaverlodge, Canada; Oklo, Gabon; and Shinkolobwe, Zaire. To some extent, these ores can also be considered as natural analogues of spent fuel and its alteration as well as source terms for radionuclide migration in groundwater. A few analyses are also reported for NRP concentrations in samples from dynamic open systems: specifically, ores from the altered and weathered zones of the Koongarra deposit, and groundwaters from Koongarra.

2 CHARACTERISATION OF ORE SAMPLES

In order to assess NRP mobility, measured NRP concentrations are compared to those expected if the ores had behaved as closed systems with respect to uranium and its products. Under conditions of secular equilibrium in closed systems, NRP concentrations are solely a function of neutron flux, uranium content, and NRP decay rates. Fission products ^{99}Tc and ^{129}I are produced by three mechanisms: spontaneous fission of ^{238}U , which is a function of the uranium concentration, and neutron-induced fission of ^{235}U and ^{238}U . For ^{239}Pu , the only production mechanism is neutron-capture by ^{238}U ; ^{36}Cl is produced by neutron-capture by ^{35}Cl and is of interest as a possible in-situ monitor of the neutron flux and as an indigenous water tracer. The physical and chemical properties that affect the in-situ neutron flux were measured in each sample (Figure 2.1). These properties include the abundances of major elements, selected minor and trace elements, and the rate of primary neutron production.

This report summarises data collected on the primary and secondary ore samples from several ore deposits, including Koongarra (Tables 2.1 and 2.2). A brief description of each source deposit for these samples is provided in section 2.1. Each sample was first analysed for its neutron production rate by a passive technique described in section 2.5. Then, for the primary ore samples, initial sample preparation consisted of grinding about 20-100 g of each sample to a fine powder in order to homogenise it. Small aliquots of the ground samples were then allocated for various analyses: mineralogy (section 2.2), elemental composition (section 2.3), uranium analyses and isotopic composition (sections 2.4 and 2.6), ^{239}Pu , ^{129}I and ^{99}Tc concentrations and $^{36}\text{Cl}/\text{Cl}$ ratios (section 3).

2.1 Description of Ore Deposits and Samples

2.1.1 Koongarra, Australia

The Koongarra deposit has been studied by ANSTO as a natural analogue since 1981. Geologic and hydrogeologic characterisation of the deposit is found in Volumes 2 and 5 of this series, respectively. The deposit occurs in a chloritised zone of quartz muscovite schist. The ore is elongated and dips 55° parallel to the plane of the reverse fault which juxtaposes the Cahill schist against Kombolgie sandstone and which serves as a nearly impermeable groundwater barrier between them. Dispersed secondary mineralization extends to depths of 25-30 m and forms a fan in the weathered schist extending ~80 m downslope from the deposit. Transport of U from the primary U ore zone is an ongoing process. Uranium is being leached from rocks in the unsaturated zone and deposited just below the top of the water table in the weathered, oxidised zone (Airey, 1986). Most of the U is associated with Fe phases. In addition to vertical redistribution, U has also been remobilised to form a roll front-type deposit extending away from the area of primary mineralization (Airey et al., 1987). Water chemistry in the weathered zone is undersaturated with respect to uraninite and other U minerals present in the deposit, consistent with the idea that present groundwaters may still be dissolving and dispersing the U (Volumes 11 and 12 of this series). The Koongarra samples used in this study were selected from the core library with the guidance of A. Snelling, and consisted of coarse fragments of drillpulp.

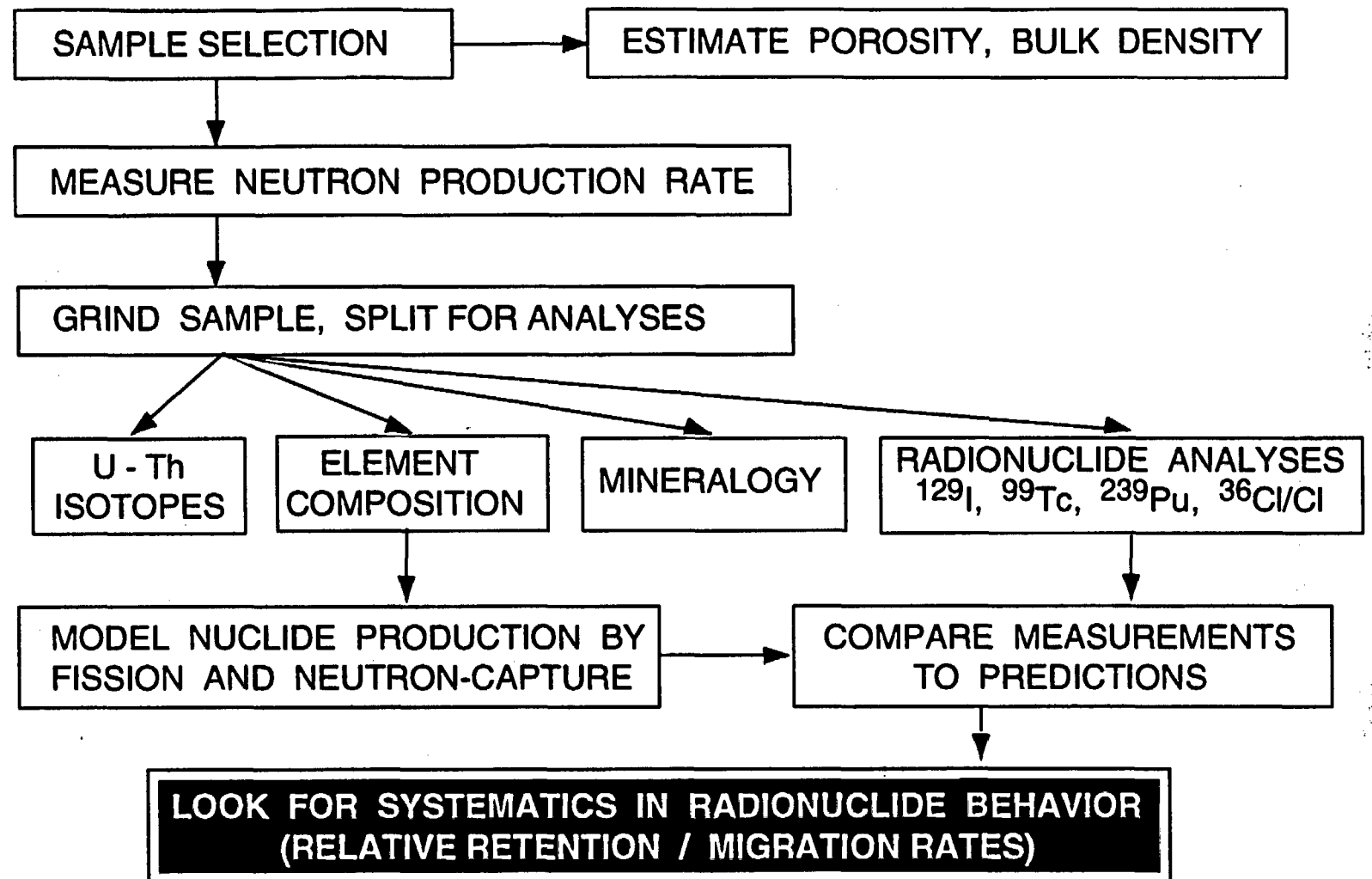
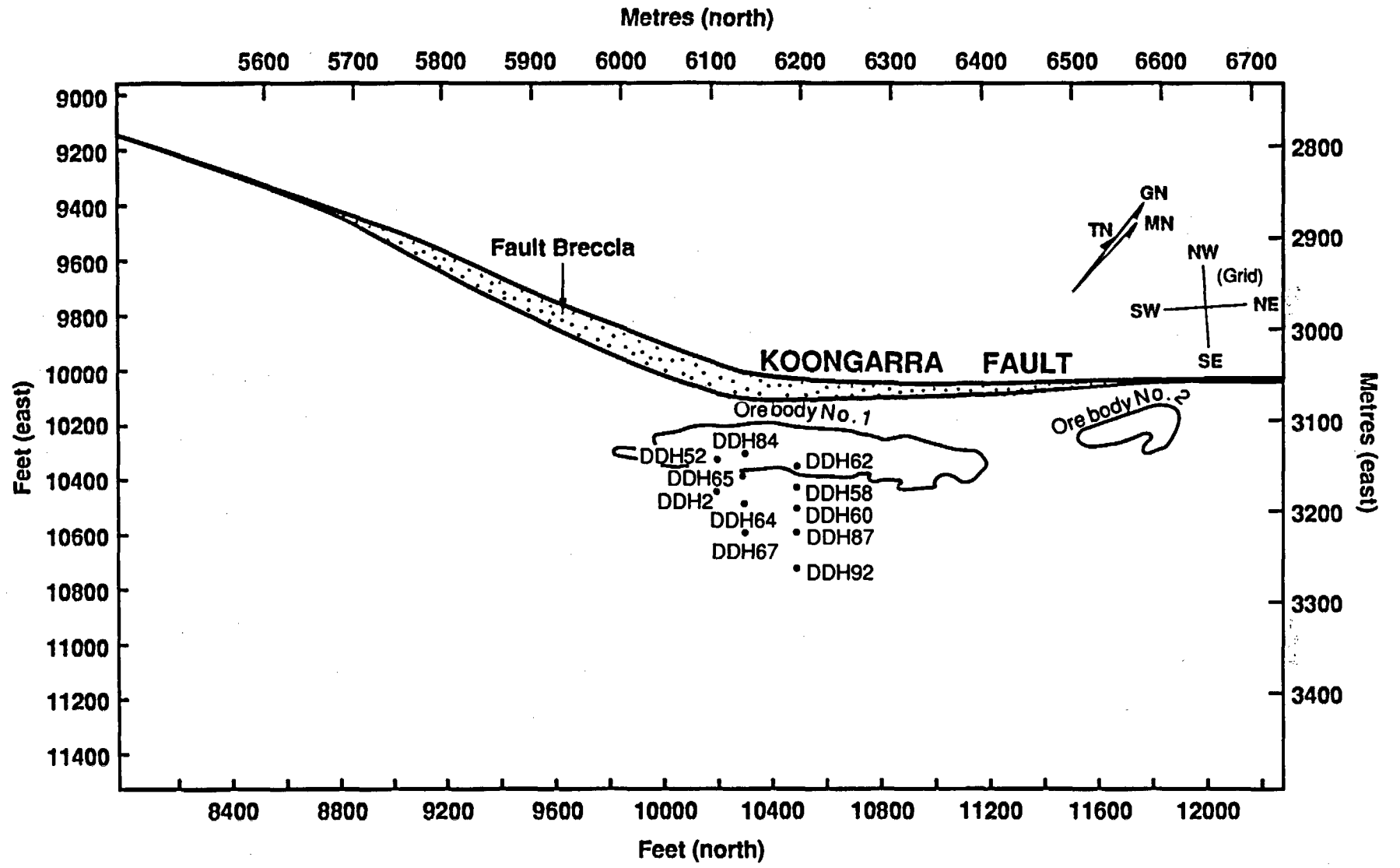


Figure 2.1 Procedure for characterising ore samples

TABLE 2.1

SOURCE DEPOSITS FOR PRIMARY ORE SAMPLES

Sample	Borehole and Depth (Note 1)	Analyses Reported (Note 2)
Koongarra, Orebody No. 1, Northern Territory, Australia (see Figure 2.2)		
G2698	DDH 58, 40.6 - 41.0 m	Element, neut, α , XRD, Pu, ^{129}I
G2759	DDH 60, 59.4 - 61.0 m	Neut, ^{129}I
G3608	DDH 64, 56.4 - 57.9 m	Neut, ^{129}I
G3624	DDH 64, 79.2 - 80.8 m	Neut, ^{129}I
G4674	DDH 87, 91.4 - 92.2 m	Element, neut, α , XRD, Pu, ^{129}I , ^{36}Cl , Tc
Key Lake, Deilmann Orebody, Athabasca Basin, Canada		
KL756	Hole 756, 100 m	Element, neut, α , XRD, Pu
KL785	Hole 785, 139 m	Element, neut, α , XRD, Pu, ^{129}I
Cigar Lake, Athabasca Basin, Canada		
CS235L	Hole 113, 419.50 m	Element, neut, α , XRD, Pu, ^{129}I
W83A	Hole 145, 441.15 m	Element, neut, α , XRD, Pu, ^{129}I , Tc
W83C	Hole 145, 441.20 m	Element, neut, α , XRD, Pu, ^{129}I
Oklo Reactor Zone 9, Gabon		
Z9-005	Curtis et al. [1989]	Element, neut, α , Pu
Z9-028	Curtis et al. [1989]	Element, neut, α , XRD, Pu, ^{129}I
Shinkolobwe (Katanga), Zaire		
NBL-6	Reference uranium ore distributed by New Brunswick Laboratory	Neut, α , Pu, ^{129}I
Beaverlodge, Saskatchewan, Canada		
BL-3	Reference uranium ores distributed by CANMET	Element
BL-5		Element, neut, α , Pu
Notes:		
1) Depths given are measured along drillholes. Drillholes at Koongarra are inclined about 50° to the northwest (Volume 2 of this series), such that vertical depths for these samples are approximately 76% of the reported depths. Drillhole locations for Koongarra are shown in Figure 2.2		
2) Analyses: Element - elemental analysis, Tables 2.5 and 2.6; Neut - measured neutron production rate, Table 2.8; α - α -spectroscopy used to obtain uranium concentrations and uranium-thorium activity ratios, Table 2.7; XRD - mineralogic analysis by X-ray diffraction, Table 2.3; Pu - ^{239}Pu analysis, Tables 3.1 and 3.2; ^{129}I - ^{129}I analysis, Table 3.3; ^{36}Cl - $^{36}\text{Cl}/\text{Cl}$ analysis, Table 3.4; Tc - ^{99}Tc analysis, see text in section 3.2.3.		



6

Figure 2.2 Map of Koongarra drillholes from which ore samples were obtained for this study

TABLE 2.2

DESCRIPTION OF SECONDARY ORE SAMPLES, KOONGARRA DEPOSIT

Sample	Borehole / Depth (m)	Analyses Reported	Description
G2806	DDH 62 / 20 - 21	Neutron Pu ³⁶ Cl	Red hematite and decomposed quartz chlorite schist with urano-phosphates. Possibly extension of primary ore zone into weathered zone and hence the source of secondary uranium dispersed down-gradient
G2683	DDH 58 / 18 - 20	Pu	Weathered schist down-gradient from G2806; predominantly red-stained quartz mica schist
G2747	DDH 60 / 18 - 20	Pu	Weathered schist down-gradient of G2683. Sericitic clays.
Notes: 1) Depths given are reported in a data base provided to ANSTO by the Denison mining company and are measured along drillholes. Because drillholes at Koongarra are inclined about 50° to the northwest (Volume 2 of this series), vertical depths for these samples are approximately 76% of the reported depths. Drillhole locations are shown in Figure 2.2. 2) Analyses reported: Neutron - neutron production rate, Table 2.8; Pu - ²³⁹ Pu analyses, Table 3.2; ³⁶ Cl - ³⁶ Cl/Cl analysis, Table 3.4			

2.1.2 Oklo, Gabon

The Oklo deposit is the site of the only known natural nuclear reactor and has been extensively studied. Uranium is contained in deltaic sediments overlying fluvial deposits of coarse sandstone and conglomerates which are the source rocks for the uranium (Gauthier-Lafaye and Ohmoto, 1989). The host rocks consist of organic-rich impure shales with high carbonate contents (Brookins, 1976). The reactor zones range from 10-20 m in length and are about 1 m thick (De Laeter, 1985). The mineralogy of the reactors consists of uraninite, chlorite, illite and carbonates; little organic carbon or quartz is present (Brookins, 1976). Large samples of solid ore were collected from the mine by A. Gancarz (LANL) in 1979. The two samples selected for this study, Z9-005 and Z9-028, are from reactor zone 9 and represent about the highest grade present.

2.1.3 Cigar Lake, Canada

The Cigar Lake deposit has been studied by Atomic Energy of Canada Ltd (AECL) as a natural analogue since 1982 (Cramer et al., 1987). Uranium ore occurs as a lens 2 km

long and 25-100 m wide at a depth of 400 m (Vilks et al., 1988) at the unconformable contact between the Athabasca Sandstone and basement rock. Dominant U minerals are uraninite and coffinite; average grade is about 15-20% U. Primary mineralization has been dated at 1.3 Ga (Sunder et al., 1987). The deposit is surrounded by a 5-30 m thick alteration zone consisting of illite, kaolinite, quartz and minor rutile, all of which is covered by a quartz-cemented cap (Goodwin et al., 1988). The surrounding sandstone is highly porous, conveying a high groundwater flux. A combination of hydrogeologic, geochemical and mineralogical factors has limited the migration of radionuclides away from the deposit (Cramer, 1986). Present fluids are chemically reducing, so little dissolution of uraninite or associated fission products has occurred (Cramer, 1986). Any radionuclides which might dissolve and migrate out of the ore zone encounter a naturally sorptive barrier in the form of a clay alteration zone (Cramer, 1986). The samples used in this study, CS-235L, W83A and W83C, were provided to LANL as solid drillcore by J. Cramer (AECL) in 1987.

2.1.4 Key Lake, Canada

The two Key Lake uranium-nickel orebodies are located along the rim of the Athabasca Basin and occur at the unconformity between the Athabasca sandstone and the underlying metasediments and in fault zones within the metasediments. The mineralization is dated at 1.3 Ga, with alterations occurring at ~250 Ma (Trocki et al., 1984). Ore minerals consist of uranium oxides and silicates and nickel sulfides and arsenides (Dahlkamp, 1978); the average ore grade is 2.7% U (Trocki et al., 1984). The host rock is kaolinite mylonite and Fe-rich chlorite mylonite (Curtis and Gancarz, 1980). The samples in this report were selected from the LANL archive of drill core samples collected from the Key Lake core shed (for the Deilmann orebody) by A. Gancarz and D. Curtis in 1978.

2.1.5 Shinkolobwe, Zaire

The Shinkolobwe U deposit is about 1.8 Ga old and is hosted by dolomitic shales, siliceous dolostones, and chloritic siltstones (Finch and Ewing, 1989). The deposit has been exposed to surface weathering for the last 60 Ma and to highly oxidising alteration such that uraninite crystals form alteration zones. The deposit may be considered an analogue to the weathering of spent fuel. In the older literature, this ore has been called Katanga or Belgian Congo pitchblende and was the source deposit used during World War II to produce the first manmade nuclear reactor at the University of Chicago. The sample analysed in this study, NBL-6, was finely ground, homogenised powder prepared in 1956 and distributed by New Brunswick Laboratory as a uranium standard. The sample was provided to LANL by F. Brauer and R. Strebin (Battelle-Pacific Northwest Laboratories). It is of interest primarily because NRP analyses of this sample or of other samples presumed to be from the same deposit have been published in the literature.

2.1.6 Beaverlodge, Canada

A problem encountered with NRP studies is that no geologic standards exist for these rare nuclides, and most samples are unique with respect to NRP concentrations such that demonstration of the accuracy of the analytical results is difficult. For this reason,

commercially-available uranium ore standards are included in the analytical suite in order to make it possible to acquire a long-term data base of replicate results and to permit other laboratories to compare their results to those reported here. Two low-grade concentrates from Beaverlodge, Saskatchewan, were obtained from the Canada Centre for Mineral and Energy Technology (CANMET). The samples (BL-3 and BL-5) were prepared in large batches by CANMET as finely ground, homogenised material. The major mineralogical components, in decreasing order of abundance, are plagioclase feldspars, hematite, quartz, calcite and dolomite, chlorite and muscovite (CANMET, no date). Samples are in secular equilibrium with respect to uranium-series nuclides.

2.2 Mineralogy

X-Ray Diffraction (XRD) patterns were obtained for most of the primary ores. Minerals identified from the patterns are reported in Table 2.3. In Koongarra sample G2698, the primary uranium mineral is sklodowskite; otherwise, the dominant uranium mineral in these samples is uraninite with minor or trace amounts of alteration products such as coffinite. Co-existing minerals fall into three categories: those in which chlorite/illite clays are dominant, those in which sulfide-rich, silica-poor minerals prevail, and those in which uraninite is so prevalent that no other minerals can be discerned in the XRD scans.

2.3 Elemental Composition

Elemental compositions are required for the NRP production model (Section 4). With few exceptions, noted in table footnotes, these analyses were obtained from X-Ray Assay Laboratories (XRAL). Table 2.4 lists the method of analysis and detection limit reported by XRAL for each element. Table 2.5 reports XRAL results for the samples submitted for quality control:

- SRM 1633a, a coal fly ash certified for several trace elements by the National Institute of Science and Technology (NIST);
- BL-3 and BL-5, two low-grade reference ores from Beaverlodge, Saskatchewan, certified for U by CANMET (Ingles et al., 1977; Steger, 1986); and
- replicate analyses of Koongarra G2698.

Results from this table are used in Section 4 as the basis for estimating uncertainties to be used for Gd and Sm in the sensitivity and uncertainty analyses with the source-term model. Finally, Table 2.6 reports XRAL results for ten primary uranium ores. NBL-6 was not submitted for analysis due to insufficient sample quantity. Subtotals listed at the bottom of the table, which exclude oxygen. Typical rocks contain 40-50% oxygen, while the richest of these ores contain less than 10%. The elemental compositions are generally consistent with the mineralogy of each sample.

TABLE 2.3

DOMINANT MINERALOGY OF PRIMARY ORE SAMPLES

Sample	Minerals identified in XRD scans
Koongarra	
G2698	Major sklodowskite, quartz, Mg-Fe chlorite, illite; minor uraninite
G4674	Major quartz, chlorite, muscovite, uraninite
Key Lake	
KL785	Major illite/smectite, Fe-Mg chlorite, goethite
KL756	Major gersdorffite, coffinite; possible trace feldspar
Cigar Lake	
CS235L	Major uraninite, chlorite, illite, kaolinite
W83A	Major uraninite, gersdorffite, calcite; minor coffinite
W83C	Major uraninite; minor gersdorffite, calcite, coffinite
Oklo Reactor Zone 9	
Z9-005	No XRD analysis done
Z9-028	Major uraninite; minor galena
Shinkolobwe	
NBL-6	Major uraninite, uranyl uranium oxide sulfate hydrate; minor curite
<p>Source and interpretation of XRD scans: G4674, G2698, KL785, CS235L -- D. Bish, LANL/ESS-1 W83A, CS235L, NBL-6, PDC-1 -- J. Cramer, Atomic Energy of Canada Ltd. KL756, W83C, Z9-028 -- X-Ray Assay Laboratories, Don Mills, Ontario</p>	

TABLE 2.4

METHODS AND DETECTION LIMITS FOR ELEMENTAL ANALYSES
OF URANIUM ORE SAMPLES

Element	Method	Detection Limit	Element	Method	Detection Limit
Li	AAA	0.01 %	TiO ₂	DCPA	0.01 %
B	DCPA	0.01 %	MnO	DCPA	0.01 %
C	LECO	0.01 %	Fe ₂ O ₃	DCPA	0.01 %
F	Wet	0.01 %	Ni	XRF	0.01 %
Na ₂ O	DCPA	0.01 %	Cu	XRF	0.01 %
MgO	DCPA	0.01 %	As	XRF	0.01 %
Al ₂ O ₃	DCPA	0.01 %	Mo	XRF	0.01 %
SiO ₂	DCPA	0.01 %	Sm	ICPMS	0.1 ppm
P ₂ O ₅	DCPA	0.01 %	Gd	ICPMS	0.1 ppm
S	Wet	0.01 %	Pb	XRF	0.01 %
Cl	Wet	0.01 %	ThO ₂	XRF	0.005 %
K ₂ O	DCPA	0.01 %	U	XRF	0.01 %
CaO	DCPA	0.01 %			

TABLE 2.5

**ELEMENTAL ANALYSES OF CERTIFIED REFERENCE MATERIALS
AND SAMPLE REPLICATES**

Element	SRM 1633a		REFERENCE ORE BL-3			REF. ORE BL-5		SAMPLE G2698	
	NIST value	XRAL 880419	CANMET value	XRAL 880419	XRAL 890130	CANMET value	XRAL 890130	XRAL 880419	XRAL 890130
Li %	---	0.018	---	0.0017	<0.01	---	<0.01	0.01	0.01
B %	---	0.005	---	0.003	<0.01	---	<0.01	<0.01	0.01
C %	---	0.27	---	1.22	1.32	1.9	1.95	0.05	0.22
F ppm	---	40	---	600	400	---	500	400	600
Na %	0.17	0.30	4.2	4.1	2.8	3.6	2.3	0.02	<0.01
Mg %	0.455	0.446	1.4	1.4	1.6	1.5	2.0	2.85	4.70
Al %	14.3	14.2	7.3	6.9	7.0	6.0	5.9	2.91	3.76
Si %	22.8	22.5	27.8	26.5	28.0	22.0	22.5	19.9	24.2
P %	---	0.17	---	0.08	0.10	0.07	0.09	0.07	0.07
S %	0.18	0.15	0.36	0.32	0.36	0.3	0.32	0.06	0.16
Cl ppm	---	160	---	530	300	---	700	380	200
K %	1.88	1.90	0.66	0.60	0.32	0.4	0.20	0.31	0.16
Ca %	1.11	1.11	2.9	3.1	3.2	4.0	4.1	0.19	0.40
Ti %	0.8	0.83	---	0.40	0.42	0.4	0.36	0.09	0.09
Mn %	0.018	0.02	---	0.06	0.07	0.05	0.06	0.12	0.15
Fe %	9.4	9.5	5.3	5.1	5.6	5.9	6.0	3.16	3.49
Sm ppm	---	19	---	7.0	6.9	---	14.5	83	65
Gd ppm	---	18	---	6.7	5.6	---	14.5	182	152
Pb %	0.0072	0.0064	0.17	0.12	0.20	1.5	1.68	1.78	1.70
Th ppm	25	24	15	13	<100	40	<100	7	<100
U %	0.0010	0.0012	1.02	0.94	1.57	7.09	8.38	19.0	20.8

--- Value not reported

Notes on samples:

- (a) SRM 1633a, coal fly ash from National Institute of Standards and Technology (NIST). Certified for Na, Mg, Al, Si, K, Ca, Mn, Fe, Pb, Th, U. Other analyses provided on certificate for information purposes only.
- (b) Uranium Ore BL-3, reference material certified for U by CANMET. Other analyses are reported for information purposes only in CANMET Report 77-64 [Ingles et al., 1977].
- (c) Uranium Ore BL-5, reference material certified for U by CANMET. Other analyses reported for information purposes only in CANMET catalog, CM84-14E [Steger, 1986].

TABLE 2.6

ELEMENTAL ANALYSES OF PRIMARY ORE SAMPLES

	G2698	G4674	KL785	KL756	CS235L	W83A	W83C	Z9-05	Z9-28	NBL-6
Li %	0.01	0.01	0.01	<0.01	<0.01	<0.01	<0.01	0.01	0.01	---
B %	0.01	0.02	0.16	0.02	0.05	0.03	0.04	0.02	0.02	---
C %	0.22	1.14	0.33	0.56	0.46	0.63	0.21	0.60	0.58	---
F %	0.06	0.06	0.28	0.11	0.11	0.07	0.07	0.11	0.08	---
Na %	<0.01	<0.01	0.04	<0.01	0.01	<0.01	<0.01	<0.01	<0.01	0.01
Mg %	4.70	9.11	2.76	2.04	5.74	4.20	4.51	5.75	5.80	0.006
Al %	3.76	7.04	10.8	0.59	1.37	1.04	1.10	1.70	1.06	---
Si %	24.2	16.7	15.3	1.94	3.12	3.01	2.48	2.07	1.44	15.7
P %	0.07	0.06	0.03	0.03	0.09	0.11	0.13	0.25	0.23	0.013
S %	0.16	0.18	<0.01	11.0	0.34	6.66	5.10	0.62	1.55	0.75
Cl %	0.02	0.04	0.01	<0.01	0.19	0.06	0.11	0.08	0.09	0.032
K %	0.16	0.36	1.29	<0.01	0.17	<0.01	<0.01	0.07	0.06	0.01
Ca %	0.40	2.16	0.43	0.56	2.11	2.89	1.23	1.53	1.41	0.54
Ti %	0.09	0.34	0.77	0.07	0.23	0.89	0.80	0.21	0.22	---
Mn %	0.15	0.11	0.12	0.01	0.11	0.06	0.07	0.20	0.18	0.002
Fe %	3.49	5.50	9.93	0.23	3.70	4.36	4.83	1.09	0.90	0.11
Ni %	0.01	0.04	0.03	21.7	0.03	6.76	3.82	<0.01	<0.01	---
Cu %	0.14	0.11	<0.01	0.03	0.57	3.57	3.14	0.01	0.03	0.17
As %	0.01	0.01	0.04	15.9	0.02	7.22	5.13	0.04	0.09	0.068
Mo %	---	---	---	0.02	---	0.03	0.03	---	---	0.37
Pb %	1.70	1.09	0.23	1.63	6.94	3.78	6.55	6.76	10.9	6.5
Th %	<0.01	<0.01	<0.01	<0.01	<0.01	0.01	0.01	<0.01	<0.01	<0.01
U %	20.8	13.9	10.6	27.5	64.6	41.6	55.8	70.2	74.0	42.1
Sm ppm	65	50	33	144	59	44.5	57	457	633	110
Gd ppm	152	99	91	358	247	204	252	283	148	180
Sub-total%	60.2	58.0	53.2	84.0	90.0	87.0	95.2	91.4	98.7	66.4
--- Not analysed										
Data sources:										
(a) For all samples excluding NBL-6: Ni, Cu and As in G2698, G4674, KL785, Z9-005, Z9-028, CS235L were analysed by The Mineral Lab (Lakewood, Colorado) using XRF. All other analyses are by X-Ray Assay Laboratories (Don Mills, Ontario), using methods listed in Table 2.4.										
(b) Elemental analyses for NBL-6 assumed to be approximated by those reported for Shinkolobwe pitchblende in Kenna and Attrep (1966). Value reported above for Gd is actually the sum for elements 63-71.										
(c) Subtotal excludes oxygen.										

2.4 Uranium Concentrations and Isotopic Composition

Because concentrations of ^{129}I , ^{99}Tc and ^{239}Pu are interpreted relative to U, accurate U analyses are as important to the research program as are accurate analyses of rarer radionuclides. The U concentrations adopted for the primary ores in this study were obtained by α -spectrometry (Table 2.7), except for those samples for which certified values are available. For secondary ores, values reported in drilling logs were used.

TABLE 2.7
URANIUM CONCENTRATIONS AND ACTIVITY RATIOS
OF PRIMARY ORE SAMPLES

Sample ID	Total Uranium wt. %	Total Thorium wt. %	$^{234}\text{U}/^{238}\text{U}$ Activity Ratio (AR)	$^{230}\text{Th}/^{234}\text{U}$ Activity Ratio (AR)
G2698	19.1	< 1000	0.99	1.00
G4674	11.5	< 1000	1.05	1.03
KL756	22.4	2137	1.02	1.02
KL785	9.0	1232	1.02	1.02
CS235L	54.6	---	0.98	1.02
W83A	40.8	---	0.95	0.98
W83C	46.8	---	0.98	1.01
Z9-005	62.8	6700	0.90	1.07
Z9-028	62.2	6050	0.94	1.03
NBL-6	46.0	---	0.98	1.01
BL-5	7.2	1777	1.02	1.00

Notes:

- (a) 1σ error bars for activity ratios are ± 0.02 .
- (b) BL-5 is certified by CANMET to contain 7.09% U.
- (c) NBL-6 was certified in 1956 by New Brunswick Laboratory to contain 53.55% U_3O_8 (equivalent to 45.4% U).
- (d) Source of data: Letter report from J.J. Cramer (Atomic Energy of Canada, Ltd.) to J. Fabryka-Martin, 23 January 1989, GACB-89-051. Additional data reported by J.J. Cramer to J. Fabryka-Martin, 24 April and 21 July 1989.

All of the primary ores being studied have formation ages on the order of 10^8 years or more, sufficiently old to have allowed secular equilibrium to have been attained. The assumption of undisturbed uranium was confirmed for each sample by the lack of secondary mineralisation in XRD scans and by activity ratios $^{234}\text{U}/^{238}\text{U}$ and $^{230}\text{Th}/^{234}\text{U}$ that are essentially 1.0 (Table 2.7). The analytical procedure used was adapted from the method described by Gascoyne and Larocque (1984) (J. Cramer, pers. commun., 1989). Nearly all of the samples in Table 2.7 have activity ratios $^{234}\text{U}/^{238}\text{U}$ and $^{230}\text{Th}/^{234}\text{U}$

within 3σ of 1.00, the only exceptions being the two Oklo ores which appear to be significantly depleted in ^{234}U relative to ^{238}U and ^{230}Th .

2.5 Neutron Production Rates

Prediction of radionuclide production rates is complicated by the need to estimate the neutron flux as a function of energy. In uranium ores, neutrons arise by two major processes: spontaneous fission of ^{238}U and neutron emission in (α, n) reactions on light nuclei. In the latter case, the α -particles derive from members of the ^{235}U and ^{238}U α -decay series; in uranium ores, those produced by ^{232}Th α -decay can be neglected. Neutron production from spontaneous fission can be calculated directly, with an average of 2.0 neutrons emitted per fission event. However, the contribution of neutrons from (α, n) reactions is not readily amenable to calculations. An approach to modelling (α, n) reaction rates in rocks was developed by Feige et al. (1968); updated neutron yield factors were compiled by Andrews et al. (1989) and Heaton et al. (1989). However, the few published attempts made thus far to apply these neutron-production models to the prediction of neutron fluxes in rocks have met with only mixed success (Andrews et al., 1989; Fabryka-Martin, 1988; Fabryka-Martin et al., 1987c, 1988; Kuhn et al., 1984).

A reason for the disparity between calculated and measured neutron fluxes is easy to surmise but difficult to test. The neutron-production models assume that α -emitters and targets are homogeneously distributed throughout the rock. However, because of the short range of α -particles in rocks, at most only a few tens of microns, neutron yields are quite sensitive to the micro-distribution of elements, typically quite heterogeneous. Neutron yields might therefore be dominated by the elemental composition of the uranium-bearing minerals, as opposed to that of the bulk rock.

In this study, neutron production rates in the uranium ore samples were measured directly using a neutron coincidence counter (Fabryka-Martin et al., 1993). A Monte Carlo Neutron/Photon Transport Code (MCNP) (Briesmeister, 1986) is then used to track the fate of these neutrons (Section 4). The neutron coincidence detection system distinguishes between fission neutrons and those arising from (α, n) reactions by gross and coincidence neutron counting measurements. The coincidence count rate results from spontaneous fission of ^{238}U and is therefore a direct measure of the quantity of uranium present in the sample.

Neutron counting results are shown in Table 2.8. In pure uranium metal, only spontaneous fission of ^{238}U produces neutrons, at a measured rate of 0.015 n/s/g ^{238}U . The relative importance of (α, n) reactions can be seen by comparing this to the rates measured for the ores, which range from 0.021 to 0.032 n/s/g ^{238}U . The (α, n) reactions thus account for 30 to 60% of the total neutron production in these samples. When normalised to uranium content, highest rates are seen for those ores containing aluminosilicate minerals such as illite and chlorite, and lowest rates for those ores hosted by metal sulfides in the absence of aluminosilicates. The enhancement seen in the silicate-hosted ores reflects the influence of α -targets with larger cross-sections for (α, n) reactions than O, particularly Mg, Al, Si, B and F. Neutron production rates in sulfide ores are comparatively low because, except for a minor contribution from Fe, metals and sulfur do not produce neutrons by (α, n) reactions due to a high threshold energy.

TABLE 2.8

MEASURED RATES OF NEUTRON PRODUCTION IN URANIUM ORES

Sample	% U See Note	Total Rate of Neutron Production		Neutron Production due to (α,n) Reactions	
		n/10 ⁴ s per g ore	n/10 ⁴ s per g ²³⁸ U	n/10 ⁴ s per g ²³⁸ U	% of total
Koongarra					
G2698	19.8 ± 0.6	56 ± 1	285 ± 9	139 ± 9	49
	18.1 ± 1.0	53 ± 1	293 ± 16	147 ± 16	50
G2759	6.2 ± 0.4	17 ± 1	270 ± 22	124 ± 22	46
G2806	1.0 ± 0.3	4 ± 1	360 ± 154	214 ± 154	59
G3608	24.7 ± 0.8	62 ± 1	253 ± 9	107 ± 9	42
	24.1 ± 2.4	63 ± 3	263 ± 31	117 ± 31	44
G3624	6.7 ± 0.5	18 ± 1	269 ± 24	123 ± 24	46
G4674	12.8 ± 0.5	37 ± 1	293 ± 13	147 ± 13	50
Key Lake					
KL756	24.2 ± 0.7	65 ± 1	270 ± 8	124 ± 8	46
KL785	9.4 ± 0.5	29 ± 1	316 ± 19	170 ± 19	54
	9.8 ± 0.6	32 ± 1	332 ± 22	186 ± 22	56
Cigar Lake					
CS235L	55.4 ± 1.5	164 ± 1	298 ± 8	152 ± 8	51
	57.1 ± 1.8	163 ± 1	287 ± 9	141 ± 9	49
W83A	37.2 ± 1.0	91 ± 1	246 ± 7	100 ± 7	41
W83C	46.8 ± 1.2	110 ± 1	237 ± 6	91 ± 6	38
Oklo reactor zone 9					
Z9-005	64.3 ± 1.7	135 ± 1	211 ± 6	65 ± 6	31
Z9-028	65.6 ± 1.7	135 ± 1	208 ± 5	62 ± 5	30
	64.4 ± 2.5	144 ± 5	225 ± 11	79 ± 11	35
Shinkolobwe					
NBL-6	46.4 ± 1.6	130 ± 2	283 ± 11	137 ± 11	48
Beaverlodge					
BL-5	6.7 ± 0.8	28 ± 1	416 ± 56	270 ± 56	56
Uranium metal					
SRM-960	100	145 ± 1	146 ± 1	0	0
Rates predicted for pure uranium oxides					
Pure UO ₂	88.1	141	161	24	16
Pure U ₃ O ₈	84.8	144	172	35	20
Note: U content of ore samples based on measured rate of coincident neutrons, normalised to rate measured for SRM-960, U metal of normal isotopic composition certified to be 99.975% pure by the National Institute of Standards and Technology (NIST). Prior to neutron measurement, the outer oxide layer was removed from the metal by acid-cleaning.					

3 MEASURED NRP CONCENTRATIONS IN ORES AND GROUNDWATERS

3.1 Analytical Methods for Ore Samples

The following provides a brief overview of the analytical procedures followed for each set of NRP analyses. Results are presented in section 3.2.

3.1.1 Plutonium-239 - *R. Aguilar, M. Attrep, Jr., and F. Roensch (LANL)*

Plutonium abundances were measured by isotope dilution mass spectrometry on masses of sample ranging from 0.5 to 7 grams for primary ores, up to 25 g for weathered ores. The ^{239}Pu measurements were calibrated with National Institute of Standards and Technology (NIST) plutonium standard 949. The procedure to extract and purify plutonium from rocks in preparation for mass spectrometric analysis is described by Attrep et al. (1992). Sample dissolution in hydrofluoric, nitric and perchloric acids was followed by various solvent extraction steps and ion-exchange techniques to isolate the plutonium from its matrix. The measurement of plutonium isotopic abundances by thermal ionization mass spectrometry is discussed by Perrin et al. (1985).

Measured quantities of plutonium were on the order of 10^9 atoms (10^{-12} g). The accuracy and precision of such small quantities are limited by the introduction of contaminant plutonium during sampling, storage, or preparation for analysis. Consequently, numerous air-monitoring, reagent, quartz and basalt blanks were periodically analysed. These show that the reagents are free of measurable Pu but that Pu contamination is introduced randomly from the environment during analysis. These blanks average about $8 (\pm 6) \times 10^7$ atoms ^{239}Pu (Curtis et al., 1992). The detection limit, defined as three standard deviations above the average background, is 3×10^8 atoms.

3.1.2 Iodine-129 - *J. Fabryka-Martin (LANL) and P. Sharma (University of Rochester)*

Iodine-129 measurements were obtained by accelerator mass spectrometry (AMS) at the Nuclear Structure Research Laboratory of the University of Rochester (Elmore et al., 1980). Quantities of 0.1 to 3 g of each sample were mixed with 20 to 400 mg of ^{127}I carrier. Although AMS only requires about 10 mg iodine or less for isotopic analysis, large quantities of carrier were necessary to dilute the $^{129}\text{I}/\text{I}$ ratio to levels less than 10^{-10} so as to minimise the potential for contaminating the instrument and other samples. The detection limit, expressed as $^{129}\text{I}/\text{I}$, is 1×10^{-14} , and ratios for the samples were in the range of 10^{-13} to 10^{-12} , corresponding to 10^8 to 10^9 atoms $^{129}\text{I}/\text{g}$.

Two methods were used for extraction of fission-product ^{129}I from the ore matrix: Na peroxide fusion and acid dissolution in a microwave. Sample digestion was nearly complete with the fusion procedure, but a variable background of unknown origin limited the usefulness of the analyses. The microwave procedure had negligible blank levels but did not dissolve the ore completely, leading to doubts as to whether the ^{129}I was completely released from the solid phase. Following dissolution of the matrix, iodine was extracted from the aqueous solutions by solvent extraction cycles (Kleinberg and Cowan, 1960, p. 32). Where duplicate samples were processed by both methods, results for the microwave method were 60-80% of those obtained by the fusion method.

Consequently, the fusion results are viewed as upper limits, and the microwave results as lower limits, for the true ^{129}I concentration.

3.1.3 Technetium-99 - *N. Schroeder and D. J. Rokop (LANL)*

Technetium-99 analyses were obtained by isotope dilution on a thermal ionization mass spectrometer on 1 g of material spiked with ^{97}Tc as a chemical yield tracer. Sample dissolution in hydrofluoric and nitric acids was followed by various solvent extraction steps and ion-exchange techniques to isolate the technetium from its matrix. The measurement of technetium isotopic abundances by thermal ionization mass spectrometry is discussed by Rokop et al. (1990).

Measured quantities of ^{99}Tc were on the order of 10^9 atoms (10^{-13} g). Analysis of numerous air-monitoring, reagent, quartz and basalt blanks indicated that contamination was introduced randomly from the environment during analysis, occasionally at levels exceeding those in the samples. Consequently, the results presented in section 3.2.3 are considered to be preliminary until blanks can be more carefully evaluated.

3.1.4 Chlorine-36 - *J. Fabryka-Martin (LANL) and P. Sharma (University of Rochester)*

Chlorine-36 was measured in one ore sample by accelerator mass spectrometry (AMS) at the Nuclear Structure Research Laboratory of the University of Rochester (Elmore et al., 1979). Seventy grams of sample were reacted with hydrofluoric and nitric acids, and the gas produced by the reaction was bubbled through a silver nitrate solution to precipitate silver chloride for isotopic analysis.

3.2 NRP Concentrations in Ores

3.2.1 Plutonium-239 in ores

Plutonium in primary ores. Plutonium abundances measured in the primary ore samples, corrected for the appropriate blanks, are reported in Table 3.1. Plutonium concentrations in the ores range from 0.3 to 6×10^9 atoms/g; $^{239}\text{Pu}/\text{U}$ ratios from 0.8 to 5×10^{-12} . The uncertainty in an individual result is one standard deviation and was calculated from the uncertainties in the isotopic abundance measurement and the blank. The average concentration in samples with multiple analyses was calculated by weighting each result by its associated standard deviation. The uncertainty of the average is one standard error of the mean.

Plutonium in weathered ores. Plutonium-239 analyses have also been made for three weathered primary ores from Koongarra with uranium concentrations of 0.2 to 1%. The results are all at the detection limit, with $^{239}\text{Pu}/\text{U}$ atom ratios $\leq 3 \times 10^{-13}$ (Table 3.2), or approximately an order of magnitude less than the ratios measured for the unweathered ores. If weathering of these samples had begun in the past few thousand years, one would interpret the lower $^{239}\text{Pu}/\text{U}$ ratios as evidence for preferential loss of ^{239}Pu relative to U in this oxidising environment. However, at present, no firm estimates exist of the timing of weathering for these samples. It is most likely that weathering occurred

TABLE 3.1

PLUTONIUM-239 CONCENTRATIONS IN PRIMARY ORES,
CORRECTED FOR BACKGROUND

Sample	% U	Date	²³⁹ Pu atoms/g x 10 ⁸	²³⁹ Pu/U ratio x 10 ⁻¹²
G2698	19.1	860916	11.3 ± 0.5	2.6 ± 0.1
		880321	12.8 ± 0.2	
		890630	11.1 ± 0.9	
		890630	15.2 ± 1.0	
		900112	9.9 ± 0.9	
		Average	12.5 ± 0.2	
G4674	11.5	870303	3.34 ± 0.65	1.4 ± 0.1
		890630	3.35 ± 0.81	
		890630	6.10 ± 1.03	
		890815	4.13 ± 0.19	
		Average	4.10 ± 0.18	
KL756	22.4	890830	14.8 ± 0.9	2.6 ± 0.2
KL785	9.0	890916	2.9 ± 0.2	1.3 ± 0.1
CS235L	54.6	880111	26.2 ± 0.2	1.9 ± 0.1
		890630	24.3 ± 0.9	
		Average	26.1 ± 0.2	
W83A	40.8	890830	31.0 ± 1.8	3.0 ± 0.2
W83C	46.8	890916	33.3 ± 0.9	2.8 ± 0.2
Z9-005	62.8	890916	13.3 ± 1.7	0.8 ± 0.1
Z9-028	62.2	890916	47.7 ± 1.7	3.0 ± 0.2
NBL-6	45.4	890630	58.9 ± 1.3	5.2 ± 0.1
		890815	62.8 ± 1.8	
		Average	60.2 ± 1.0	
BL-5	7.09	900315	5.57 ± 0.87	3.1 ± 0.4
		900720	5.25 ± 1.74	
		Average	5.51 ± 0.78	
Notes:				
1) % U from Table 2.7; certified values for NBL-6 and BL-5.2)				
2) Background correction applied to samples prepared prior to May 1987 is 2.9 (± 3.2) x 10 ⁸ atoms ²³⁹ Pu; that for samples prepared after May 1987 is 7.5 (± 6.6) x 10 ⁷ atoms ²³⁹ Pu.				
3) Average atomic concentrations are weighted and are reported ± one standard error of the mean. Average ²³⁹ Pu/U ratios are calculated from these values and include 5% uncertainty for U concentrations, except for NBL-6 and BL-5 for which the estimated uncertainty is 1%.				

sufficiently long ago ($> 10^5$ years) that the present-day ^{239}Pu abundances are in equilibrium with the lower U content and hence lower neutron flux; the measured abundances are consistent with the $^{239}\text{Pu}/\text{U}$ ratio predicted by the source-term model described in section 4.3.1.

TABLE 3.2

PLUTONIUM-239 CONCENTRATIONS IN WEATHERED KOONGARRA ORES

Sample	ppm U	^{239}Pu atoms/g	Calculated $^{239}\text{Pu}/\text{U}$	Reported $^{239}\text{Pu}/\text{U}$
G2683	2220	$1.0 \pm 0.7 \times 10^6$	$1.8 \pm 1.2 \times 10^{-13}$	$\leq 2 \times 10^{-13}$
G2747	2400	$1.3 \pm 0.8 \times 10^6$	$2.1 \pm 1.3 \times 10^{-13}$	$\leq 2 \times 10^{-13}$
G2806	11500	$7.9 \pm 4.5 \times 10^6$	$2.7 \pm 1.5 \times 10^{-13}$	$\leq 3 \times 10^{-13}$

Note: U concentrations from drillcore data provided to ANSTO by Denison.

Analytical precision. Analyses of replicate aliquots of G4674 and G2698 (Table 3.1) produced imprecise measures of plutonium abundances. The standard deviation of the results of four analyses of G4674 is 30% of the unweighted average. The unweighted average of five determinations of the plutonium abundance in G2698 has a standard deviation that is 17% of its value. The imprecision is the result of heterogeneity in the solid material from which the replicates were taken, not the imprecision of the plutonium measurement procedures. In order to test this assertion, the precision of the chemical analysis and instrumental detection was checked as follows. A 5-g sample was spiked with ^{242}Pu , dissolved and diluted to 200 mL in a volumetric flask. Three equal-sized aliquots were taken from this solution and chemically processed separately. Mass spectrometric analyses gave results of 9.96, 9.89, and 10.0 ($\times 10^8$) atoms $^{239}\text{Pu}/\text{g}$, averaging 9.95×10^8 atoms $^{239}\text{Pu}/\text{g}$ sample with a standard deviation of 0.6% (1σ).

Analytical accuracy. Properly executed, isotope dilution mass spectrometry is a highly accurate analytical procedure. In this case, the accuracy of the ^{239}Pu analyses cannot be evaluated because no relevant plutonium standard exists. Few opportunities are available to compare our results with those of other analysts. Although it is no longer available, NBL-6 has long served as a uranium standard distributed by the New Brunswick Laboratory. Other analysts have reported plutonium abundances in different samples from the same deposit (section 4.2.2, Table 4.3). The literature values encompass ours, having $^{239}\text{Pu}/\text{U}$ atom ratios ranging from 3 to 12×10^{-12} . None agrees with our value of 5.2×10^{-12} . These differences may indicate fractionation of ^{239}Pu and U in the sample treatment because some research groups worked with the mining company's aqueous waste stream. Alternatively, the differences may reflect variability of plutonium production within the ore body.

3.2.2 Iodine-129 in ores

Iodine-129 in primary ores. Results obtained for primary ore samples are listed in Table 3.3. All of the measured $^{129}\text{I}/\text{U}$ ratios are equal to or greater than the ratio of $6 (\pm 3) \times 10^{-13}$ expected for spontaneous fission of ^{238}U alone (assuming 0.035% mass ^{129}I yield). The results for the six Koongarra samples from the primary ore zone range from 1 to 3×10^{-12} , indicating that at least half of the ^{129}I production in these samples is attributable to induced fission of ^{235}U and/or ^{238}U .

Iodine-129 in weathered ores. In contrast to the case for primary ore samples, three Koongarra ores from the weathered zone all have $^{129}\text{I}/\text{U}$ ratios of 3×10^{-13} (Fabryka-Martin et al., 1987d), below the value for spontaneous fission alone (6×10^{-13}). Substantial loss of ^{129}I relative to U may thus have occurred in this part of the deposit.

3.2.3 Technetium-99 in ores

Technetium-99 in primary ores. The reliability of the ^{99}Tc analyses obtained by LANL for uranium ores is limited due to a spurious high blank of unknown origin. Thus, the measured $^{99}\text{Tc}/\text{U}$ atom ratios for samples G2698 and W83A are both reported as upper limits, $\leq 1.8 \times 10^{-12}$. This value is about 10% above the value of 1.6×10^{-12} predicted for pure spontaneous fission of ^{238}U and within the range of results expected for complete retention of ^{99}Tc relative to U (Section 4). The accompanying blank contained ^{99}Tc on the same order as that in the two ore samples. Twelve reagent blanks prepared subsequent to these samples contained negligible amounts of ^{99}Tc , suggesting that the process blank with the ores was not a typical background level. It is probable--although not certain--that the measured values for the ores represent their true ^{99}Tc contents.

3.2.4 Chlorine-36 in ores

Chlorine-36/chlorine ratios have been measured in several Koongarra ores from within and down-gradient of the primary ore body (Table 3.4). The ratios are about 1×10^{-10} within the primary ore, and decrease by a factor of 10-30 with distance away from it. In Section 3.4.4, the results are used to develop estimates of groundwater residence time in the primary ore zone.

3.3 NRP Concentrations in Groundwater

An accurate knowledge of concentration and physicochemical form in aqueous media is essential to assessing the transport rate of radioactive contaminants from nuclear waste repositories. For many radioactive species, the current understanding of these properties comes exclusively from laboratory studies and models that extrapolate the laboratory results to conditions at a repository site. Natural analogues provide the opportunity to assess whether the properties of actinides and fission products in natural aqueous media are consistent with the model interpretations of laboratory studies. The objective is to measure the concentration of these radionuclides and to characterise their chemical and physical form in waters from regions down-gradient of a source term. This work was first attempted at the Koongarra deposit and the results are reported here. At Koongarra, the upper portions of a lens of primary uranium has been altered and

TABLE 3.3

IODINE-129 CONCENTRATIONS IN PRIMARY URANIUM ORES

Sample	% U	Date	Sample ID	Preparation method	^{129}I at/g ore ($\times 10^9$)	$^{129}\text{I}/\text{U}$ ratio $\times 10^{-12}$
Koongarra						
G2698	19.1	8904	18912X	Fusion	0.84 ± 0.07	
			18953X	μ wave	0.65 ± 0.10	
			18957X	μ wave	0.46 ± 0.03	
			Average		0.65 ± 0.19	1.3 ± 0.4
G2759	6.2	8904	18935X	Fusion	0.31 ± 0.02	2.0 ± 0.2
G3608	24.6	8904	18936X	Fusion	1.6 ± 0.2	2.6 ± 0.2
G3624	6.7	8904	18919X	Fusion	0.19 ± 0.02	
			18937X	Fusion	0.26 ± 0.03	
			Average		0.23 ± 0.05	1.4 ± 0.3
G4674	11.5	8904	18913X	Fusion	0.38 ± 0.03	
			18954X	μ wave	0.25 ± 0.02	
			18958X	μ wave	0.22 ± 0.02	
			Average		0.28 ± 0.09	1.0 ± 0.3
Key Lake						
KL756	22.4	8904	18930X	Fusion	0.43 ± 0.04	0.75 ± 0.08
Cigar Lake						
CS235L	54.6	8904	18914X	Fusion	3.3 ± 0.3	
			18955X	μ wave	2.4 ± 0.2	
			18959X	μ wave	2.9 ± 0.2	
			Average		2.9 ± 0.5	2.1 ± 0.3
W83A	40.8	8904	18929X	Fusion	1.9 ± 0.2	1.8 ± 0.2
W83C	46.8	8904	18918X	Fusion	3.3 ± 0.3	2.8 ± 0.3
Oklo Reactor Zone 9						
Z9-028	62.2	8904	18917X	Fusion	4.2 ± 0.4	2.7 ± 0.3
Shinkolobwe						
NBL-6	45.4	8904	18911X	Fusion	9.6 ± 0.8	
			18920X	Fusion	9.0 ± 0.9	
			18931X	Fusion	9.3 ± 1.0	
			18952X	μ wave	6.2 ± 0.5	
			18956X	μ wave	7.3 ± 0.4	
			Average		8.3 ± 1.5	7.2 ± 1.3
Notes:						
1) Samples prepared at LANL and analysed at University of Rochester.						
2) Sources and uncertainty estimates for %U values: NBL-6, certified value, $\pm 1\%$; G2759, G3608, G3624 from neutron count rates, Table 2.8; all others from Table 2.7, $\pm 5\%$.						
3) Uncertainty estimates for $^{129}\text{I}/\text{U}$ ratios include analytical uncertainties for both ^{129}I and U measurements.						

TABLE 3.4
CHLORINE-36 IN URANIUM ORES

Sample	% U	$^{36}\text{Cl}/\text{Cl}$ $\times 10^{12}$	Drillhole/depth (m)	Mineralogy
G4674	12.2	84 ± 5	DDH87, 91.4 - 92.2	Unweathered primary ore
G2818	1.2	130 ± 3	DDH62, 38.1 - 39.6	Unweathered primary ore
G2806	1.1	60 ± 3	DDH62, 19.8 - 21.3	Weathered primary ore
G2537	0.07	7.6 ± 0.6	DDH52, 24.4	Weathered primary ore
G1136	0.12	2.7 ± 0.2	DDH2, 15.2 - 16.8	Dispersion fan

Notes:

- 1) Samples are listed approximately in order of the assumed groundwater flow path. See Figure 2.2.
- 2) Sources of data: G4674 - % U from Table 2.7; $^{36}\text{Cl}/\text{Cl}$ measured as part of present study; all other samples - % U from data base provided to ANSTO by Denison mining company; $^{36}\text{Cl}/\text{Cl}$ from Fabryka-Martin et al. (1987b).
- 3) Depths are from the data base provided to ANSTO by Denison mining company and are measured along drillholes. Because drillholes at Koongarra are inclined, vertical depths for these samples are approximately 76% of the measured depths.

redistributed by the flow of oxidising groundwater. The geochemistry of the altered part of the deposit has been extensively studied. Although the timing of the redistribution is ill-defined, it is believed to be geologically modern. Abundant measurements of disequilibrium between ^{238}U and its long-lived daughters ^{234}U and ^{230}Th indicate chemical disturbances in the last 10^6 yr (Dickson and Snelling, 1980; Payne and Waite, 1991).

As part of an extensive study of element migration at Koongarra, water samples were taken from numerous wells that penetrate the deposit and its immediate environs. Locations of wells referenced in this section are shown in Figure 3.1.

3.3.1 Plutonium-239 in groundwater - *R. Aguilar, M. Attrep, Jr., D. B. Curtis, R. E. Perrin and F. Roensch (LANL)*

On two occasions, an elaborate sampling scheme was implemented to characterise the nature of aqueous plutonium in these wells. The sampler was similar to the large-volume water sampler developed at the Battelle Pacific Northwest Laboratories (Silker et al., 1971). Water was passed through a series of particulate filters and then through a series of ion exchange resins to selectively isolate particulate, anionic, cationic and neutral species of plutonium from the water samples. The sampling system and results are described in the following subsections.

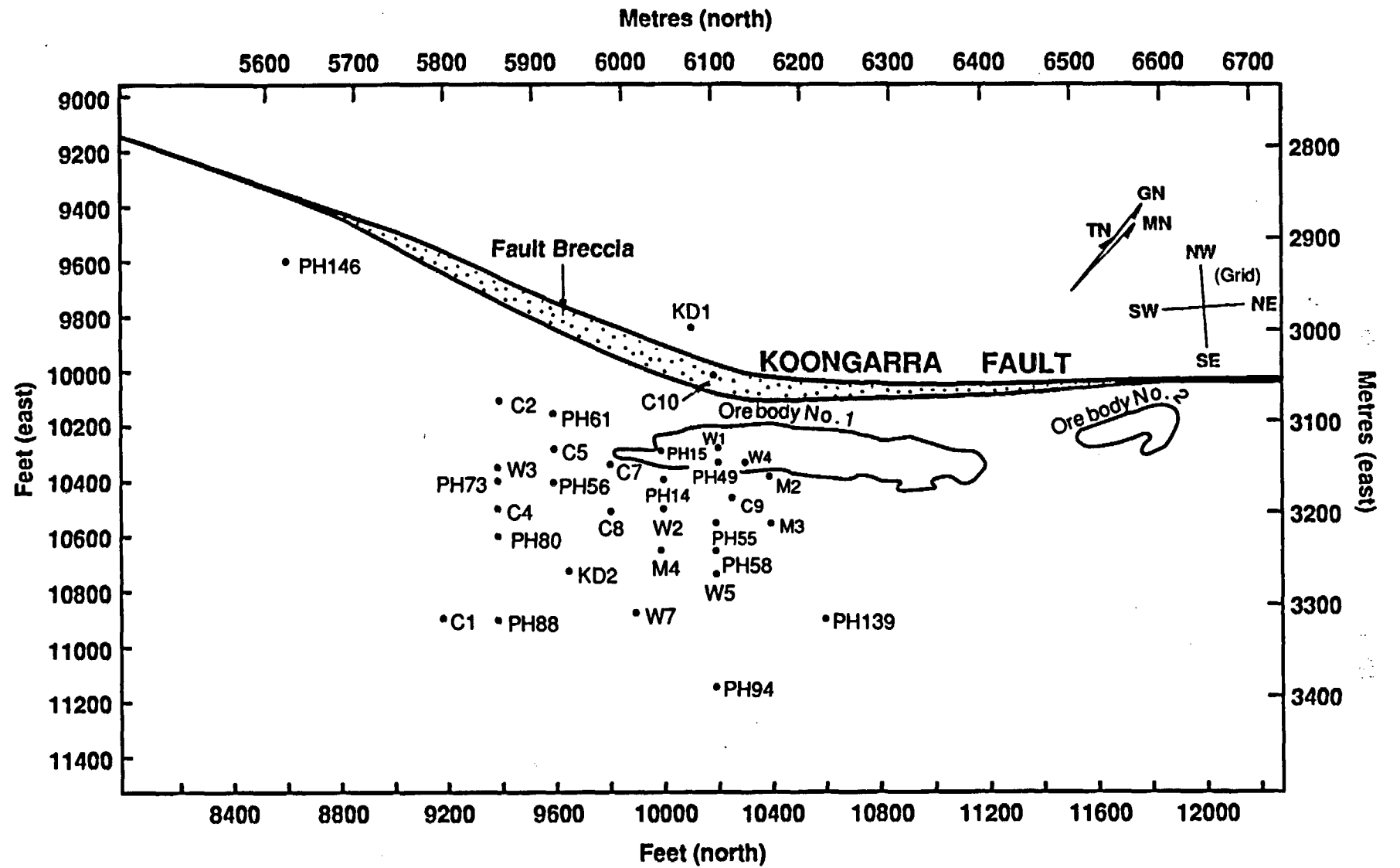


Figure 3.1 Map of Koongarra boreholes from which water samples were obtained for this study

3.3.1.1 Sample collection and processing

Two field trips involved the collection of groundwater samples for plutonium analysis. In September 1985, a suite of samples was collected from PH49 (unpacked), a well which intersects the primary ore body. The water was passed through 5- μ m and 1- μ m filters. A 2-litre solution of ^{244}Pu tracer (containing 5.15 ng Pu) was introduced slowly into the stream, and the water was split into 9 branches. One branch was connected to a series of resin beds: two beds of anion resin (AG1-X8, 100-200 mesh, chloride form), followed by two beds of cation resin (AG50W-X8, -200 mesh, ammonium form), and ending with a bed of neutral alumina (AG-7, 100-200 mesh). A total of 1936 litres of water was processed for ^{239}Pu collection in this manner. In addition, a 20-litre sample of water from this borehole was collected, evaporated to a small volume at ANSTO and sent to LANL for ^{239}Pu analysis.

In May 1989, a suite of samples was collected from wells in the vicinity of the Koongarra uranium ore deposit. Each suite consisted of seven samples: three filters (5- μ m paper filter, 1- μ m cloth filter, and 0.45- μ m capsule filter), two cation resin beds (AG, hydrogen form), followed by two anion resin beds. Analyses of resins and the 5- μ m filter for PH146 and PH49 (28-30-m depth) were completed and can be used to establish limits for the concentration of ^{239}Pu in these groundwaters (Sections 3.3.1.3 and 3.3.1.4). The analytical procedure for the resins and filters consisted of ashing each sample, adding ^{242}Pu tracer, and then following the same procedure as has been used for the uranium ore samples (Section 3.1.1). Background concentrations measured in the process blank samples (3.6×10^7 atoms, Table 3.5) are within the range of blanks measured with the ore samples in previous years ($7.5 \pm 6.6 \times 10^7$ atoms). Following are some general observations and conclusions from the analytical results for the groundwater samples.

3.3.1.2 Plutonium in PH49 water

Well PH49 penetrates the most uraniferous portions of the Koongarra deposit and water from it contained an average of 100 ppb of uranium. It seemed the most probable place to look for natural plutonium in aqueous media. Three samplings of this well were analysed: 40 litres of a whole water sample collected in 1985, and some of the filters and ion exchange resins collected in 1985 and in 1989. Analytical results are shown in Table 3.5. Only one of the samples show ^{239}Pu concentrations above instrumental background (1-5 μ m filter, September 1985 sampling, Table 3.5).

Based on the summation of the detection limits for the 5-micron filter, cation bed #1, and anion bed #1 for the 1989 sampling suite, the upper limit is estimated as follows:

$$\begin{aligned} &\leq 2 \times 10^8 \text{ atoms/692 litres} \\ &\leq 290 \text{ atoms/mL} \\ &\leq 5 \times 10^{-19} \text{ M} \end{aligned}$$

TABLE 3.5

PLUTONIUM-239 CONCENTRATIONS IN KOONGARRA GROUNDWATERS

Borehole	PH49	PH49	PH146
Depth interval	16 - 87 m	27.5 - 29.5 m	17 - 89 m
Collection date	Sept 85	May 89	May 89
Approx. U conc.	NA	107 ppb	1 ppb
Volume passed through resins	1936 litres	692 litres	700 litres
Measured ²³⁹ Pu Concentrations (atoms/litre)			
≥ 5 μm yarn filter	≤ 2 × 10 ⁶	≤ 1 × 10 ⁵	4 × 10 ⁵
1-5 μm filter	4 × 10 ⁵	na	na
Cation resin bed #1	≤ 1 × 10 ⁵	≤ 4 × 10 ⁴	≤ 3 × 10 ⁵
Cation resin bed #2	≤ 6 × 10 ⁴	≤ 1 × 10 ⁶	≤ 4 × 10 ⁶
Anion resin bed #1	≤ 1 × 10 ⁶	≤ 1 × 10 ⁵	1 × 10 ⁶
Anion resin bed #2	≤ 4 × 10 ⁴	≤ 9 × 10 ⁴	2 × 10 ⁶
Neutral alumina	na	nc	nc
Whole water (40 L)	≤ 5 × 10 ⁵	nc	nc
Notes:			
na - Sample not analysed			
nc - Sample not collected			
Results have not been corrected for background. Blanks measured for anion and cation resins averaged $4 \pm 2 \times 10^7$ atoms ²³⁹ Pu. Only three samples from PH146 had signals significantly above these background levels, such that the background signal was ≤ 10% of the total signal for these samples.			

The upper limit for the ²³⁹Pu/U ratio, assuming 107 ppb U, is 1.1×10^{-12} . This upper limit is approximately equal to or slightly less than the ²³⁹Pu/U ratio that has been measured for the Koongarra ores from the deep unweathered zone. Ore samples G2698 and G4674 had ratios of 2.6 and 1.3×10^{-12} , respectively, and came from depths (measured along the slanted borehole) of 41 and 92 metres. Thus, it appears that these results suggest that ²³⁹Pu is not preferentially lost relative to U in the unweathered zone. However, three ores from the weathered zone (20-m depths) all had ²³⁹Pu/U ratios $\leq 3 \times 10^{-13}$; hence, the PH49 groundwater result cannot be used to conclude anything about the relative mobility of ²³⁹Pu and U in this more oxidising environment. In addition, the collection system may not capture colloidal Pu or uncharged Pu species.

3.3.1.3 Plutonium in PH146 water

Well PH146 taps groundwater from the formation a few hundred metres away from the ore deposit (Figure 3.1). The borehole was not packed and hence drew water from the entire saturated zone, 17-89 m. The volume pumped through the collection system was

700 litres. Plutonium was detected in the particulate and anionic fractions from this well; unfortunately, low ^{242}Pu mass spectrometric signals for the two cation resin samples made it impossible to measure the 239/242 ratios in these samples, and the results for those samples can only be expressed as fairly high detection limits (Table 3.5).

A lower limit for ^{239}Pu in PH146 water was estimated, based on the filter and anion beds #1 and #2:

$$\begin{aligned} &\geq 2.0 \times 10^9 \text{ atoms/700 litres} \\ &\geq 2900 \text{ atoms/mL} \\ &\geq 5 \times 10^{-18} \text{ M} \end{aligned}$$

The lower limit for the $^{239}\text{Pu}/\text{U}$ ratio, assuming 1 ppb U, is 1.1×10^{-9} . This result suggests that Pu may be fairly mobile in this geochemical environment, and that its dominant forms may be anionic and particulate. However, it needs to be noted that the collection system may not be effective in capturing colloids or uncharged species. Also, because the second anion resin bed contained more ^{239}Pu than did the first one, suggesting that the collection system may not even be very efficient in capturing anionic forms of ^{239}Pu in this groundwater.

The measured $^{239}\text{Pu}/\text{U}$ ratio in water far exceeds any $^{239}\text{Pu}/\text{U}$ ratio seen in any natural rock sample in the present study by over two orders of magnitude (maximum in ore = 5×10^{-12} , NBL-6). If the Pu is derived from a natural source such as an ore deposit, then the PH146 result suggests that ^{239}Pu is more mobile than U in this geochemical environment. However, the more likely source of the ^{239}Pu in PH146 is global fallout. The Pu/U ratio of fallout is 10^{-5} to 10^{-7} and lower, depending upon the extent of dilution by U in the soil. Conceptual hydrologic models of the Koongarra deposit indicate that it is unlikely that water from the deposit flows toward PH146 (Volume 5 of this series). Plutonium-240 and -241, which are diagnostic indicators of global fallout, were not seen in these samples but their presence was probably obscured by the low ^{242}Pu current in the mass spectrometer. This borehole also had elevated levels of ^{36}Cl , about five times above background levels, which could indicate the presence of bomb-pulse nuclides (Table 3.7, discussed in Section 3.3.4). High ^{36}Cl values are not unambiguous, however, since they could also be a signal from the ore body. Tritium and ^{14}C results would probably be conclusive because these should be purely bomb pulse signals, not affected by the ore deposit. However, these results are not available.

3.3.2 Iodine-129 in groundwater - *J. Fabryka-Martin (LANL), and P. Sharma (University of Rochester)*

Published measurements of natural ^{129}I in groundwater include those reported in Fabryka-Martin et al. (1985, 1987a, 1987d, 1989). These results provided direct evidence that escape of fission-product ^{129}I from the rock into the water can be substantial. The interpretation of ^{129}I loss from the weathered zone (section 3.2.3) is supported by high ^{129}I concentrations in groundwater from the deposit. Results are available for groundwater samples collected in 1983, 1985 and 1986 (Table 3.6; data from Fabryka-Martin et al., 1987d). Although additional samples were collected, no new analyses have

been made since the 1987 report. Samples from the 1988 and 1989 field trips were not processed because reproducibly low reagent blanks could not be obtained.

The 1983-86 data clearly demonstrate that ^{129}I is being lost from some part of the ore body to a great extent, probably during weathering of the primary ore. In water from PH49 intersecting the primary ore body, $^{129}\text{I}/\text{I}$ ratios are higher by three orders of magnitude over background levels as represented by the 1983 sampling of KD-1. As a first approximation, the ratios can serve as surrogate measures for the ^{129}I concentration. Iodide concentrations in the waters were only measured for the 1983 and 1985 samples, in which they ranged from 1 to 3 ppb (Fabryka-Martin et al., 1987d). Iodine-129 concentrations ranged from a low of 2×10^4 and 3×10^5 atoms/L in KD-1, up to a maximum of 9×10^6 and 1.3×10^7 atoms/L in PH49, for the 1983 and 1985 samples, respectively (Fabryka-Martin et al., 1987d). Down-gradient, $^{129}\text{I}/\text{I}$ ratios in groundwater are lower than that in PH49 by factors of 2 to 7 but are still far above background. The down-gradient decrease is not systematic with distance from the ore body. The decrease probably reflects differing extents of dilution with meteoric waters which have not flowed through the deposit rather than evidence for sorptive losses of this radionuclide. The hypothesis of dilution is supported by the fact that a similar decrease occurs in the helium concentrations in the groundwater with increasing distance from the ore body (Gole et al. (1986); see also Volume 5 of this series).

Iodine-129 has other natural and anthropogenic sources, which can complicate the interpretation of fissiogenic ^{129}I in groundwater. Prior to the advent of nuclear testing, meteoric iodine had a $^{129}\text{I}/\text{I}$ ratio of 1×10^{-12} (Fabryka-Martin et al., 1987a). Since 1945, the ratio $^{129}\text{I}/\text{I}$ has increased in the environment due to contributions from above-ground nuclear weapons tests, operation of nuclear power plants, and nuclear-fuel reprocessing. Peak $^{129}\text{I}/\text{I}$ ratios reached about 10^{-7} in the 1960's and 1970's in biological samples from locations remote from nuclear facilities (NCRP, 1983, and references therein). However, levels of anthropogenic ^{129}I in waters immediately adjacent to the primary ore body are not likely to be significant, based upon the low tritium and ^{14}C levels.

3.3.3 Technetium-99 in groundwater - J. Fabryka-Martin and D. J. Rokop (LANL)

Only one measurement of natural ^{99}Tc in groundwater has been made, for groundwater collected from the Koongarra U ore deposit in September 1983. The method of collection used about 1 litre of anion-exchange resin (Dowex 1-X8, 100-200 mesh, chloride form). Laboratory testing of this resin confirmed its high efficiency for removing the $^{99}\text{TcO}_4^-$ anion from solution. The resin bed used in the field had a cross-sectional area of $\sim 600 \text{ cm}^2$ and was packed to a depth of $\sim 1.5 \text{ cm}$. About 1600 litres of groundwater were pumped from PH 49, through a $5\text{-}\mu\text{m}$ filter and through the resin blank. This sample was analysed at LANL in 1985. In the laboratory, ^{97}Tc tracer (19 pg ^{97}Tc) was added to the resin which was then ashed in a furnace. The ash was then treated in the same manner as the ore (section 3.1.3).

Four blanks analysed just prior to this sample indicated an average ^{99}Tc background of $7 (\pm 3) \times 10^9$ atoms. The blank-corrected result for the resin sample from PH 49 represents a concentration of $9 (\pm 2) \times 10^3$ atoms $^{99}\text{Tc}/\text{mL}$, assuming complete recovery

TABLE 3.6

IODINE-129 AND CHLORINE-36 IN KOONGARRA GROUNDWATERS,
PRE-EXISTING BOREHOLES, 1983-91

Bore-hole	Month -Year	Sample interval (m)	$^{129}\text{I}/\text{I}$ (10^{-12})	$^{36}\text{Cl}/\text{Cl}$ (10^{-15})	Cl^- mg/L	^3H T.U.	^{14}C pmC
PH 14	8-84	20-26	nc	356 ± 32	---	0.6	60
	8-86	20-26	298 ± 22	357 ± 23	---	---	--
	5-88	20-26	nc	nc	5.8	0.3	69
	5-89	20-26	nc	460 ± 15	6.8	---	--
PH 15	5-88	19-21	na	203 ± 19	2.7	0.3	69
PH 49	9-82	16-87	nc	nc	---	0.9	51
	9-83	16-87	645 ± 106	152 ± 22	---	---	--
	9-85	16-87	911 ± 134	169 ± 13 beg	---	---	--
				184 ± 29 end	---	---	--
	8-86	16-87	713 ± 44	406 ± 37	---	---	--
	5-88	28-30	na	231 ± 21	3.7	0.3	--
	5-89	27-29	na	112000 ± 2000	4.8	---	40
5-90	18-20	na	3470 ± 420	3.6	0.7	--	
PH 55	9-82	20-89	nc	nc	---	0.9	92
	9-83	20-89	45 ± 5	153 ± 17	---	---	--
	8-84	20-89	nc	886 ± 141	---	---	--
	9-85	20-89	106 ± 9	196 ± 18	---	---	--
	8-86	20-89	141 ± 9	403 ± 24	---	---	--
	5-88	26-28	na	177 ± 17	3.7	0.2	85
	5-88	40-42	nc	243 ± 22	3.8	0.2	88
PH 56	8-86	22-69	153 ± 9	nm	---	---	--
	5-88	26-28	nc	nc	4.7	0.3	76
	5-88	43-45	nc	nc	3.1	0.3	--
PH 58	8-84	25-27	nc	287 ± 56	---	---	--
	5-88	25-27	nc	nc	3.9	0.2	91
	5-88	38-40	nc	404 ± 33	3.8	0.4	--
PH 61	5-88	26-28	nc	103 ± 7	2.8	0.2	79
PH 73	9-82	14-85	nc	nc	---	---	94
	8-84	14-85	nc	351 ± 24	---	---	--
	8-86	14-85	108 ± 8	nm	---	---	--
PH 80	5-88	17-20	na	193 ± 21	4.3	0.4	84
	5-89	17-19	na	659 ± 17	5.0	---	--

TABLE 3.6 (continued)

Bore-hole	Month -Year	Sample interval (m)	$^{129}\text{I}/\text{I}$ (10^{-12})	$^{36}\text{Cl}/\text{Cl}$ (10^{-15})	Cl^- mg/L	^3H T.U.	^{14}C pmC	
PH 88	5-88	28-30	na	556 ± 42	3.6	0.8	100	
	5-88	38-40	nc	496 ± 38	3.8	1.2	102	
PH 94	9-82	24-76	nc	nc	---	4.7	101	
	9-83	24-76	nc	1723 ± 187	---	---	---	
	8-84	24-76	nc	11340 ± 910	---	---	---	
	5-88	26-28	na	nc	2.2	2.0	94	
PH 139	8-84	23-118	nc	802 ± 47	---	---	---	
	9-85	23-118	68 ± 8	392 ± 36	---	---	---	
PH 146	5-89	17-89	na	511 ± 17	3.6	---	---	
	4-91	17-89	na	3763 ± 204	2.1	---	---	
KD-1	9-82	70-120	nc	nc	---	1.0	64	
	9-83	70-120	6.4 ± 1.4	148 ± 20	---	---	---	
	9-85	70-120			267 ± 16 beg	---	---	---
					76 ± 9 end	---	---	---
5-88	80-82	nc	nc	2.6	0.4	83		
KD-2	8-86	?	178 ± 12	501 ± 34	---	---	---	
	11-90	24-32	nc	nc	3.0	0.5	---	

nc - either no sample was collected or else sample was lost prior to analysis
na - sample was collected but not analysed

Notes:

- 1) Analyses reported \pm one standard deviation
- 2) For 1985, the two $^{36}\text{Cl}/\text{Cl}$ results reported for PH49 and KD-1 represent samples collected at the beginning and end of large-volume sampling for ^{129}I , in order to monitor for changes in groundwater source during pumping.
- 3) Data for 1982-85 was previously reported in Fabryka-Martin et al. [1987]. Chloride, tritium and ^{14}C data are from Volume 7 of this series. Measurement errors are no more than 0.3 TU for tritium, and typically 5-10% for ^{14}C .
- 4) In 1985, a set of samples was collected and analysed for $^{36}\text{Cl}/\text{Cl}$ at the beginning and end of pumping large water volumes from PH49 and KD-1; these results are labelled "beg" and "end."

of ^{99}Tc by the anion-exchange resin used in the field for extracting this nuclide from the water. Such an assumption is considered fairly safe. The $^{99}\text{Tc}/\text{U}$ ratio in the water was on the order of 3×10^{-11} , more than an order of magnitude greater than the ratio predicted for equilibrium conditions (Section 4). The measured concentration and ratio relative to U both indicate that ^{99}Tc is being released to the water from some part of the deposit and that it is several times more mobile than U in this oxidising environment.

Other than U fission, no other natural production mechanism is known to produce significant quantities of ^{99}Tc . However, as for the case of other NRP, technological sources have contributed to a large atmospheric inventory of ^{99}Tc in the last few decades. The major sources have been above-ground testing of nuclear devices and atmospheric releases of volatile Tc compounds from U enrichment and fuel reprocessing plants. As with most other bomb-pulse nuclides, the atmospheric concentration of ^{99}Tc probably peaked in the early 1960's and decreased sharply after above-ground testing of nuclear weapons was banned. Concentrations measured in rainwater in 1961 to 1974 ranged from 10^8 to 10^{10} atoms/L (Ehrhardt and Attrep, 1978). Numerous studies document the wide-spread distribution of bomb-pulse ^{99}Tc in soils, marine and fresh-water sediments, and biota. As in the case of ^{129}I , however, the low levels of tritium and ^{14}C suggest that significant levels of technological ^{99}Tc are not likely to be present in PH49 water.

3.3.4 Chlorine-36 in groundwater - J. Fabryka-Martin (LANL), L. K. Fifield, G. L. Allan, E. Kiss, and T. R. Ophel (Australian National University), J. R. Bird, D. Fink, A. Jenkinson, A. Smith, and C. Tuniz (ANSTO), R. F. Davie (formerly with ANSTO), P. W. Kubik (Paul Scherrer Institute), and P. Sharma (University of Rochester)

Together with ^3H , measured $^{36}\text{Cl}/\text{Cl}$ ratios in Koongarra groundwaters provide a check for the presence of bomb-pulse radionuclides in the waters. The presence of bomb-pulse nuclides would complicate, if not negate, the use of ^{14}C for age dating at this site or the interpretation of ^{129}I , ^{99}Tc and ^{239}Pu concentrations in groundwater in terms of migration. Chlorine-36/chlorine ratios can also be used to constrain the residence time of groundwater in the ore deposit.

Results. Results of $^{36}\text{Cl}/\text{Cl}$ analyses are available for samples collected in 1983-91 for boreholes which were in existence as of 1983 (Table 3.6) as well as for samples collected during 1989-91 for boreholes which were constructed in 1989 (Table 3.7). All analyses were by accelerator mass spectrometry, first at the University of Rochester until 1987 and then at the Australian National University starting in 1988. A convenient unit of measurement for $^{36}\text{Cl}/\text{Cl}$ measurements is the CLU (Chlorine-36 Unit), where 1 CLU equals a $^{36}\text{Cl}/\text{Cl}$ ratio of 1×10^{-15} . For example, a ratio of 1×10^{-12} would be expressed as 1000 CLU. The results shown in Tables 3.6 and 3.7 span over four orders of magnitude, from 100 up to 10^6 CLU.

Meteoric background. The $^{36}\text{Cl}/\text{Cl}$ ratios of 100 and 64 CLU measured for PH61 and W1 (13-15 m, October 1989), respectively, are close to the value predicted for local water recharged prior to nuclear testing. This relatively low result for PH61 confirms the absence of significant bomb-pulse fallout in this shallow (26-28 m depth) part of the flow system and is also consistent with the hydrologic model presented in Volume 5 of this series, that most of the groundwater in this part of the flow system does not originate from the orebody. Although PH61 lies between PH146 and the orebody, the low $^{36}\text{Cl}/\text{Cl}$ ratio cannot be used to eliminate the possibility that the orebody may be the source for the ^{239}Pu observed in PH146 (Section 3.3.1.3) because the samples were collected from different depth intervals.

TABLE 3.7

CHLORINE-36 IN KOONGARRA GROUNDWATERS, NEW BOREHOLES, 1989-91

Bore hole	Sample date	Sampled interval, metres	$^{36}\text{Cl}/\text{Cl} \times 10^{-15}$ $\pm 1\sigma$	^{36}Cl atoms per μL	Cl ⁻ mg/L	Tritium (T.U.)	^{14}C pmC
M1	May 89	24-26	1726 \pm 43	160	5.5	---	70
M1	May 90	27-29	2646 \pm 78	110	2.4	0.3	--
M2	May 89	40-46	1160000 \pm 10000	100000	5.1	---	52
M2	May 90	42-44	95000 \pm 6300	3900	2.4	---	--
M2	Apr 91	36-40	45000 \pm 3000	1800	2.4	---	--
M3	May 89	20-22	1128 \pm 29	94	4.9	---	--
M3	May 89	34-40	7151 \pm 124	520	4.3	---	85
M4	May 89	34-40	2607 \pm 48	150	3.3	---	84
M4	May 90	28-30	nc	---	3.2	0.7	--
W1	Oct 89	13-15	64 \pm 4	7	6.8	0.6	96
W1	May 90	13-15	468 \pm 27	44	5.5	1.0	96
W1	Oct 89	23-25	1540 \pm 40	200	7.5	0.2	86
W1	May 90	23-25	3443 \pm 95	370	6.3	0.3	87
W2	May 90	13-15	447 \pm 42	26	3.4	0.3	--
W2	Oct 89	23-25	392 \pm 40	22	3.3	0.5	92
W2	May 90	23-25	288 \pm 29	15	3.1	0.6	80
W2	Apr 91	23-25	507 \pm 30	27	3.1	0.7	--
W3	Oct 89	13-15	130 \pm 9	13	6.1	2.8	98
W3	Oct 89	23-25	319 \pm 17	56	10.3	0.9	83
W4	Oct 89	13-15	194 \pm 22	20	6.1	1.2	85
W4	May 90	13-15	181 \pm 17	25	8.0	1.3	80
W4	Apr 91	13-15	195 \pm 13	31	9.4	---	--
W4	May 89	23-25	701 \pm 27	73	6.1	---	67
W4	May 90	23-25	6827 \pm 146	340	2.9	1.4	63
W4	Apr 91	23-25	324 \pm 25	23	4.1	1.3	--
W5	Oct 89	13-15	236 \pm 17	8	2.1	0.1	89
W5	Oct 89	23-25	432 \pm 23	71	9.7	0.3	92
W7	May 90	23-25	713 \pm 34	28	2.3	1.3	97
W7	Apr 91	23-25	723 \pm 49	27	2.2	1.0	--
C5	Oct 89	25-27	1903 \pm 40	58	1.8	0.1	67
C7	Oct 89	25-27	1581 \pm 60	59	2.2	0.1	97
C8	May 89	38-40	916 \pm 21	68	4.4	---	83
C9	May 89	34-40	2620 \pm 47	---	---	---	76
C9	May 90	28-30	370 \pm 25	33	5.2	0.4	79
C10	May 89	27-40	41357 \pm 445	2000	2.9	---	55

Note: Chlorine-36 sample analysis at Australian National University. Chloride, tritium and ^{14}C data from Volume 7 of this series.

Sources for ^{36}Cl in the groundwater. In the vicinity of the orebody, $^{36}\text{Cl}/\text{Cl}$ ratios are variably elevated above background (100 CLU) as represented by PH61. The high ratio in PH94 is bomb-pulse ^{36}Cl , as indicated by unambiguous bomb-pulse levels of tritium and ^{14}C in this well. The same is probably true for ^{36}Cl in PH88 and KD2. However, bomb-pulse ^{36}Cl is ruled out as a source for elevated signals in the vicinity of the orebody because concentrations of tritium and ^{14}C here are low. Most likely, high ^{36}Cl contents result from in-situ production of ^{36}Cl as a result of a combination of processes: direct production in the water in the orebody by neutron irradiation of dissolved Cl, production of ^{36}Cl in mineral grains, followed by diffusive loss or loss during weathering or alteration, and leaching of ^{36}Cl from mineral grains crushed and exposed by drilling activities.

Groundwater residence time in the orebody. The 1983-88 results can be used to estimate an upper limit for groundwater residence time in the orebody. If the elevated $^{36}\text{Cl}/\text{Cl}$ ratios result solely from direct production in the water, then the extent of ingrowth is directly proportional to the water residence time. Dissolved Cl in secular equilibrium with the orebody would have a ratio on the order of 1×10^{-10} or 1×10^5 CLU (section 3.2.4). Consequently, ratios of 150 to 460 CLU observed in water from the orebody (PH14, 15 and 49) suggest upper limits of a few hundred to a few thousand years, consistent with the ^{14}C results (Volumes 5 and 7 of this series). Leaching of ^{36}Cl from mineral grains would lead to overestimates of the water residence time; obviously, leaching of only a small quantity of chloride could cause a significant increase in the $^{36}\text{Cl}/\text{Cl}$ ratio in the water. Slightly higher chloride concentrations observed in ore-zone waters compared to waters outside the orebody (Volume 7 of this series) may be an indication that leaching has occurred. On the other hand, it is important to note that the zone of influence for these holes probably extended beyond the primary ore body, into the surrounding barren rock, because of the large water volumes typically pumped in the early years of the analogue project. Thus, high CLU signals reflecting long residence times in the primary ore body could have been diluted to an unknown extent by lower CLU signals from water outside the ore body.

In-situ production. The likelihood of leaching of ^{36}Cl from minerals following drilling is suggested by the dramatic changes seen in the ^{36}Cl distribution following drilling activities in 1989. In the 1989-91 suite of samples, measured $^{36}\text{Cl}/\text{Cl}$ ratios were generally considerably higher than for previous years, and ranged from 511 to 1.2×10^6 CLU (Table 3.7). The ratio measured for new borehole M2 is the highest ever seen in any terrestrial sample, including global fallout of bombpulse ^{36}Cl . The 1989 suite includes resampling of two boreholes; both showed order-of-magnitude increases in ^{36}Cl content. The ratio for PH49 ranged from 150 to 410 CLU during four previous years, and jumped to 112,000 CLU in 1989. The ratio for PH80 was 190 CLU in 1988, and 660 CLU in 1989. The extent to which new holes had elevated ratios was a function of their distance from M2, with the highest ratios having been collected closest to M2; wells with ratios > 5000 CLU were M2 (36-40 m, 42-43.5 m), PH49 (28-30 m), M3 (34-40 m), W4 (23-25 m), and C10 (27-40 m). Where two depths were sampled in a given well, the lower depths generally had higher ratios (e.g., M3, W1, W3, W4, W5, Table 3.7), suggesting that the ^{36}Cl derived from a subsurface source as opposed to a surface one such as a bomb-pulse signal. High ^{36}Cl levels persisted in subsequent years, although later concentrations generally showed increases or decreases of over a factor of two, consistent with the idea of a pulse input moving through the system.

Tracing the origin of these elevated ^{36}Cl levels is of key interest not only as a test of laboratory quality-control procedures, but also because of the implications for flow paths in the ore deposit. Cross-contamination during field collection, sample storage, or sample processing and analysis is judged remote due to the many precautions taken to minimise this possibility. Bomb-pulse ^{36}Cl is ruled out because measured levels exceed those for global fallout and because of low tritium and ^{14}C levels in this part of the flow system. One hypothesis is that limited pumping volumes from the new, packed holes may have been successful in collecting old, nearly stagnant water from the orebody with a minimum of mixing with water from surrounding barren rock. Given sufficient residence time, ingrowth of ^{36}Cl by neutron activation of dissolved chloride would give rise to $^{36}\text{Cl}/\text{Cl}$ ratios approaching that in the ore. It is difficult to test this hypothesis with available data; in-situ production of tritium and ^{14}C in the Koongarra orebody is negligible (Section 4.5), and therefore would not provide a useful test. Another hypothesis is leaching of in-situ-produced ^{36}Cl from mineral surfaces freshly exposed by drilling of new boreholes, particularly M2. The bottom of M2 extends into the primary ore body. Because the highest concentration of uraninite occurs just below the graphitic hanging wall unit, $^{36}\text{Cl}/\text{Cl}$ ratios at the bottom of M2 are expected to be of the order 10^5 to 10^6 CLU. Probably both of these hypotheses are valid.

Chlorine-36 as an indicator of groundwater movement. If the ^{36}Cl level in M2 were indeed released from the ores as a result of drilling and subsequent leaching by groundwater, then the drilling essentially initiated a tracer injection test, with M2 as the point source. Results for the other boreholes reflect the nature of the flow paths between them and M2. The prompt and dramatic increase in CLU values for down-gradient samples indicates the dominance of fracture flow during pumping and suggests direct connections between some of the boreholes, consistent with the results of aquifer tests (Volume 5 of this series) and downhole surveys of fracture networks (Volume 4 of this series). The variable connectivity between fracture networks is indicated by the variability of $^{36}\text{Cl}/\text{Cl}$ ratios observed for wells adjacent to one another or along a presumed flow line. For example, an elevated signal is obvious in wells M4, C7 and C8 in 1989, but appears largely to bypass W2.

The M2 scenario suggests that a similar increase in ^{36}Cl concentrations would have occurred following the drilling of the many exploration holes which intersect the deposit (1970-73 and 1978, Volume 2 of this series). The PH-series holes were drilled between September 1970 and September 1973 (Volume 5 of this series). The variability observed in the 1983-88 suite of results may thus reflect the limited extent to which groundwater entering the orebody has diluted or flushed out this in-situ-contaminated water and replaced it with meteoric chloride with a lower ^{36}Cl content over the subsequent 10-20 years. As such, the results provide additional evidence that the water in the orebody is almost static compared to the obvious rapid groundwater circulation around PH88 and PH94 (Volume 5 of this series).

Finally, consistently lower ratios in shallow (13-15 m) intervals compared to the deeper (23-25 m) intervals for two holes (W1, W3, W4, W5) provide evidence for a stratified flow system with minimal mixing between these layers. Thus, part of the weathered zone may behave as an aquitard, as postulated in Volumes 4 and 5 of this series and as assumed for some of the site-scale hydrologic model scenarios described in Volume 6.

4 MODELLING NRP SOURCE TERMS

4.1 NRP Production Mechanisms

Three types of nuclear processes are responsible for producing the radionuclides of interest to this study (Figure 4.1):

4.1.1 Spontaneous fission of ^{238}U

Spontaneous fission of ^{238}U produces fission products ^{99}Tc and ^{129}I , for which equilibrium abundances can be calculated from the relationship:

$$N_i = N_{238} \lambda_{sf} Y_{i,sf} / \lambda_i \quad (4.1)$$

where

N_i = concentration of fission product i (atoms/g)

N_{238} = concentration of ^{238}U (atoms/g)

λ_{sf} = ^{238}U spontaneous fission decay constant (8.49×10^{-17} /yr, DeCarvalho et al., 1982; Holden, 1981)

$Y_{i,sf}$ = spontaneous fission yield for product i (dimensionless)

λ_i = decay constant for product i (yr^{-1})

For Y_{99sf} , Rider (1981) recommends a value of 0.0606. A value of 3.5×10^{-4} is calculated for ^{129}I by multiplying the well-known chain yield for mass 136 (0.0584, Rider, 1981) times the experimental branching factor reported by Hebeda et al. (1987). Using these values, equilibrium atom ratios are $^{99}\text{Tc}/\text{U} = 1.57 \times 10^{-12}$ and $^{129}\text{I}/\text{U} = 6.7 \times 10^{-13}$.

4.1.2 Neutron-induced fission of ^{235}U and ^{238}U

Fission products ^{99}Tc and ^{129}I are also produced by neutron-induced fission of ^{235}U and ^{238}U , with equilibrium abundances determined by the relationship:

$$N_i = \int_0^{E_{\max}} \Phi_n(E) [N_{235} \sigma_{235f}(E) Y_{i,235f} + N_{238} \sigma_{238f}(E) Y_{i,238f}] dE / \lambda_i \quad (4.2)$$

where

N_{235} = concentration of ^{235}U (atoms/g)

N_{238} = concentration of ^{238}U (atoms/g)

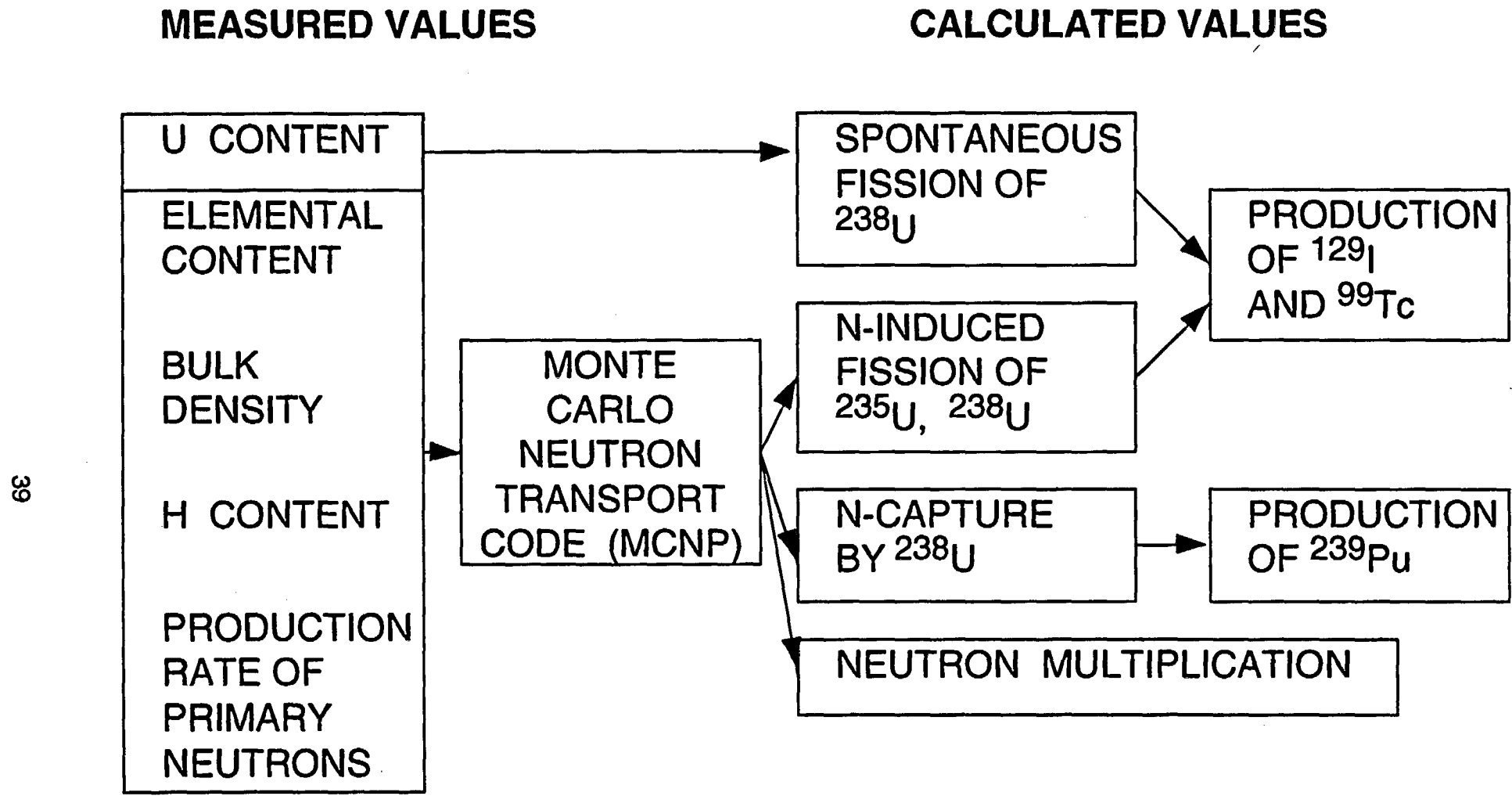
$\Phi_n(E)$ = neutron flux, as function of energy ($\text{n}/\text{cm}^2/\text{yr}$)

$\sigma_{235f}(E)$ = ^{235}U cross-section for fission, as function of energy (cm^2)

$\sigma_{238f}(E)$ = ^{238}U cross-section for fission, as function of energy (cm^2)

$Y_{i,235f}$ = ^{235}U induced fission yield for product i (dimensionless)

$Y_{i,238f}$ = ^{238}U induced fission yield for product i (dimensionless)



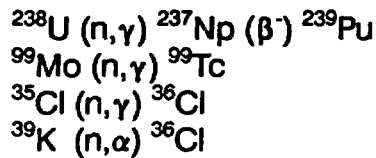
39

Figure 4.1 Model for predicting nuclide production rates

Although strictly speaking the induced fission yield is a function of neutron energy, for this study it was assumed that thermal-neutron induced fission yields would be an acceptable simplification. Mass yields for ^{235}U and ^{238}U induced fission are 0.0611 and 0.0618 for ^{99}Tc and 0.0075 and 0.0097 for ^{129}I , respectively (Rider, 1981).

4.1.3 Neutron-capture reactions

The following neutron-capture reactions produce ^{239}Pu , ^{99}Tc , and ^{36}Cl :



Of these, modeling calculations have shown that neutron-capture by ^{99}Mo and ^{39}K are negligible relative to other production mechanisms for ^{99}Tc and ^{36}Cl . Equilibrium abundances of these capture products are determined by the relationship:

$$N_i = \int_0^{E_{\max}} \Phi_n(E) N_{\text{tg}} \sigma_{\text{tg}}(E) dE / \lambda_i \quad (4.3)$$

where

N_{tg} = concentration of target isotope (atoms/g)

$\sigma_{\text{tg}}(E)$ = energy-dependent cross-section of target isotope (cm^2)

4.2 Source-Term Model Description

4.2.1 General approach

The accuracy with which NRP abundances can be calculated for a given sample is primarily a function of the accuracy with which the energy-dependent neutron flux can be estimated. The neutron flux is determined by the neutron production rate, which is a measured parameter in this study (Table 2.8), and by the energy-dependent cross-sections of the rock for neutron scattering and absorption. Calculations of neutron-activation products in common types of rocks are reasonably accurate using simple one or two-group neutron transport codes for highly thermalised systems and reactions with $1/v$ cross-sections in which the reaction cross-section is inversely proportional to the neutron energy or velocity (Lehmann et al., 1993). However, flux estimates for uranium ores are a particularly complicated problem because they are generally not well-thermalised systems; a significant proportion of the neutrons are absorbed by uranium at higher energies. Furthermore, the excitation function for ^{239}Pu production can not even be approximated by a simple $1/v$ relationship. For these reasons, it is necessary to use a multi-group neutron transport code combined with detailed information on the effective reaction cross-sections as a function of neutron energy in order to predict production rates with any accuracy. Consequently, the Monte Carlo Neutron and Photon (MCNP) transport code (Briesmeister, 1986) was used to calculate fluxes and neutron-capture reaction rates for the ore samples.

MCNP is a continuous-energy neutron/photon transport code based on the Monte Carlo method (Briesmeister, 1986). The user specifies the geometry of the problem, the elemental composition and density of the media, the cross-section evaluations which are to be used, characteristics of the neutron sources, and the type of answers desired (e.g., nuclear reaction rates). The objectives in using MCNP for this project are to estimate radionuclide concentrations expected for the ore samples, to identify the critical elemental parameters controlling radionuclide production rates, and to test for expected correlations among the radionuclide pairs.

Modelling was conducted for two geometries:

- (a) The "infinite model" was used to estimate NRP abundances by modelling the sample as homogeneous material with the elemental composition of the sample and infinite dimensions. In cases where the material surrounding the sample has a lower uranium concentration--which is true for nearly all of the samples in this study--the infinite model results should serve as upper limits for the true NRP abundances.
- (b) The "geometry model" was used to obtain more realistic estimates of NRP abundances. In these cases, each sample was modelled as high-grade material bordered by material with different, generally lower, U contents.

Uranium concentrations for the samples were taken from Table 2.7; other elemental compositions from Table 2.6. Because H was not measured, initial estimates of the H content of the solid phase for each sample were based on estimated proportions and stoichiometries of minerals (Table 4.1). The bulk composition and total H content of the ore were then adjusted to account for the addition of water in the porespace.

Neutron production rates were based on the measured values (Table 2.8), which were assumed to scale to the U content in the case of the adjacent intervals in the geometry model. A ^{238}U spontaneous fission spectrum was adopted to represent the shape of the initial neutron energy curve, with an average energy of 2 MeV, extending up to 20 MeV. This approach somewhat underestimates the average energy for neutrons produced by (α ,n) reactions, but the simplification does not lead to significant errors in the final results for the reactions of interest. Several different cross-section libraries are available in MCNP. Continuous-energy neutron cross-section data based on ENDF/B-V evaluations were used for the transport calculations (to calculate the neutron flux) and for the three reaction-rate calculations, $^{238}\text{U}(n,\gamma)$, $^{238}\text{U}(n,f)$ and $^{235}\text{U}(n,f)$. ENDF/B (Version V) is the Evaluated Nuclear Data File, an American effort coordinated by the National Nuclear Data Center at Brookhaven National Laboratory (Garber, 1975). For the reaction rate $^{35}\text{Cl}(n,\gamma)$, cross-section data from ACTL were used; ACTL is an evaluated neutron activation cross-section library from Lawrence Livermore National Laboratory (Gardner and Howerton, 1978).

TABLE 4.1

BOUNDING CONCENTRATIONS OF H (PPM) USED FOR SENSITIVITY ANALYSES

Sample	Mineral weight fractions				Grain dens. g/cm ³	ppm H in water as function of porosity		ppm H in mineral phases	
	UO ₂	PbO ₂	S	Rem.		2%	5%	Min.	Max.
G2698	0.22	0.02	0	0.76	3.70	609	1558	6008	10188
G4674	0.13	0.01	0	0.86	3.20	704	1798	6632	11362
KL756	0.25	0.02	0.49	0.24	5.57	406	1041	2150	3470
KL785	0.10	0	0	0.80	3.19	706	1803	6140	10540
CS235L	0.62	0.08	0	0.30	6.00	377	966	3118	4768
W83A	0.46	0.04	0.24	0.26	5.84	387	992	2594	4024
W83C	0.53	0.08	0.17	0.22	6.15	368	944	2392	3602
Z9-005	0.71	0.08	0.01	0.20	6.49	349	895	2494	3594
Z9-028	0.71	0.13	0.02	0.14	6.77	334	857	2044	2814
NBL-6	0.52	0.05	0.01	0.42	5.36	421	1080	3909	6246
BL-5	0.08	0.02	0	0.90	3.00	751	1916	6862	11812

Notes on calculations:

- 1) Mineral weight fractions - UO₂ calculated from U content (Table 2.7), other fractions estimated from elemental composition (Tables 2.5 and 2.6). For purposes of these calculations, all U is assumed to be present as UO₂, Pb as PbO₂, sulfides are calculated as sum of S+Cu+Ni+As and assumed to be present as NiAsS, remainder is assumed to be silicates (chlorite, illite, kaolinite). Exception: approximately 10% wt of KL785 is estimated to be present as FeOOH.
- 2) Grain density - assumes following densities (g/cm³) for each mineral fraction: UO₂ and PbO₂ - 7.5, NiAsS - 6, FeOOH - 4, silicates - 2.5
- 3) Mineral fraction, minimum H - assumes 0.75% H associated with silicate and FeOOH fractions (average measured for muscovite, chlorite, kaolinite, illite; Deer et al., 1966; Weaver and Pollard, 1973), 0.14% H in UO₂ fraction (Frondel, 1958, pp 16-17), no H associated with PbO₂ or sulfide fractions
- 4) Mineral fraction, maximum H - 1.3% H associated with silicate fraction (typical of chlorite), 0.14% H in UO₂ fraction, no H associated with PbO₂ or sulfide fractions

4.2.2 Results of the infinite model

In the infinite model, NRP abundances (Table 4.2) were estimated by assuming that the nuclear reaction rates take place in an infinitely homogeneous medium with the same composition as the sample. The base case was defined as 2% porosity, with 0.75% H in the silicate phase and 0.14% H in the uraninite phase (Table 4.1). A test of the general validity of this approach was conducted by comparing measured and predicted NRP abundances for pitchblende from Shinkolobwe. This ore has been heavily studied by nuclear chemists over the past 30 years such that a wealth of analyses of various fission products and neutron-capture products have been reported in the literature. Another

TABLE 4.2

URANIUM FISSION RATES AND NRP ABUNDANCES PREDICTED BY MCNP
FOR INFINITE ORE BODIES

Sample	% U	Predicted fissions / g ore / yr				Predicted atom ratios x 10 ⁻¹²			
		²³⁸ U spont.	²³⁵ U induced	²³⁸ U induced	Ratio, IF/TF	¹²⁹ I /U	⁹⁹ Tc /U	²³⁹ Pu /U	³⁶ Cl /Cl
G2698	19.1	41000	9590	1790	0.22	4.9	2.0	3.5	71
G4674	11.5	24700	5990	660	0.21	4.7	2.0	3.1	73
KL756	22.4	48100	3240	3110	0.12	2.9	1.8	2.9	15
KL785	9.0	19300	980	390	0.07	1.8	1.7	2.3	20
CS235L	54.6	117300	46200	26000	0.38	11	2.5	8.3	105
W83A	40.8	87600	16900	9400	0.23	5.5	2.1	4.2	50
W83C	46.8	100500	18400	13800	0.24	6.0	2.1	4.8	44
Z9-005	62.8	134900	45700	27900	0.35	9.2	2.4	7.0	88
Z9-028	62.2	133600	46000	28500	0.36	8.5	2.3	7.3	86
NBL-6	42.2	90600	36500	13000	0.35	9.2	2.4	6.8	118
BL-5	7.1	15230	6620	305	0.31	7.3	2.3	3.5	130

Notes:

- 1) Calculations assume 2% porosity and estimation of H associated with mineral phases as described in Table 3.1, footnote 3
- 2) Predicted fission rates calculated in the following manner:
 ^{238}U spontaneous fission = (^{238}U atoms/g) x (8.49×10^{-17} fissions/atom/year)
 [DeCarvalho et al., 1982]
 ^{235}U and ^{238}U neutron-induced fission rates = calculated by MCNP for specified elemental composition of ore and measured rate of primary neutron production (Table 2.8)
- 3) R, IF/TF = ratio, induced fissions/total fissions
- 4) Predicted concentrations of fission products calculated by multiplying fission rates times fission yields (below) times mean life of fission product
- 5) Assumed fission yields (Rider, 1981; Hebeda et al., 1987):
 ^{238}U spontaneous fission - 0.035% ^{129}I , 6.1% ^{99}Tc
 ^{235}U induced fission - 0.75% ^{129}I , 6.1% ^{99}Tc
 ^{238}U induced fission - 0.97% ^{129}I , 6.2% ^{99}Tc

advantage is that NBL-6 is a sample of well-homogenised material derived from a volume of rock that is probably large relative to the mean pathlength of a neutron. Consequently, for NBL-6 (and also BL-5), the validity of using the infinite model to characterise NRP production rates is easy to defend, making it an appropriate test for the model. In a later section, the case is made that the infinite model may not be valid for samples that were collected as hand specimens representative of a volume of rock that is small relative to neutron pathlengths.

In Table 4.3, model predictions for this ore are compared against published analyses for fission products ^{129}I , ^{99}Tc , ^{147}Pm , ^{149}Pm , ^{89}Sr and ^{90}Sr , and neutron-capture products ^{239}Pu and ^{36}Cl . The comparison is formalised in Figure 4.2 by calculating the fractionation factor α , which is the ratio of ratios shown in the equation below:

$$\alpha = (\text{NRP/Target})_{\text{M}} / (\text{NRP/Target})_{\text{SE}} \quad (4.4)$$

where NRP = nuclear reaction product (e.g. ^{239}Pu), Target = target element for the reaction (e.g., U), and subscript M = measured element ratios; and subscript SE refers to element ratios calculated for conditions of secular equilibrium. Log α is preferred so as to give equal weight to factors of under- or over-prediction, i.e., a measurement that is half or twice the predicted value has log α values of -0.3 and +0.3, respectively. Assuming that no fractionation between the NRP and target elements, then a log α value of 0 indicates that the model is able to accurately reproduce the NRP production rate. Negative log α values suggest that the model overpredicts NRP production, or that there has been preferential loss of the NRP relative to its target element. Positive log α values suggest that the model underpredicts NRP production, or that there has been preferential gain of the NRP relative to its target element; the latter possibility is considered improbable for these primary ores.

The agreement is excellent for all four short-lived fission products (^{149}Pm , ^{89}Sr , ^{147}Pm , ^{90}Sr) (Figure 4.2). Although the measured ^{89}Sr concentrations are roughly half of the predicted ones, such a discrepancy is expected because the rate of neutron-induced fission should be drastically reduced in hand samples of the ore, such that short-lived fission products should therefore be produced predominantly by spontaneous fission. In fact, the measured values for the three fission products with half-lives less than 3 years are within one standard deviation of the value predicted for spontaneous fission production alone. Agreement between measured and predicted values is quite variable for the longer-lived fission products and neutron-capture products. The ^{239}Pu and ^{129}I analyses conducted as part of the present study match the predicted concentrations quite well; other analyses lie within a factor of 3 of the predicted values. Any discrepancies could be a consequence of different sample sources, analytical problems, or an inaccurate representation of the elemental composition in the model:

- (a) Sampling issues. Only our analyses and the other ^{129}I analysis were conducted on NBL-6; the other analyses were conducted on processing plant concentrates or other source material and hence may not be derived from the same part of the deposit as NBL-6.

TABLE 4.3

COMPARISON OF MEASURED AND PREDICTED NRP CONCENTRATIONS
FOR SHINKOLOBWE PITCHBLENDE

Nuclide	Half-life (yr)	Predicted for ^{238}U fission only	Predicted total	Measured value	Ref. for measured value
$^{149}\text{Pm}/\text{U}$	6.06×10^{-3}	1.6×10^{-20}	$2.0 - 2.2 \times 10^{-20}$	$2.1 (\pm 0.8) \times 10^{-20}$	[3]
$^{89}\text{Sr}/\text{U}$	0.138	6.6×10^{-19}	$1.0 - 1.1 \times 10^{-18}$	$6.7 (\pm 1.0) \times 10^{-19}$	[1]
$^{147}\text{Pm}/\text{U}$	2.623	1.4×10^{-17}	1.8×10^{-17}	$1.7 (\pm 0.3) \times 10^{-17}$	[2]
$^{90}\text{Sr}/\text{U}$	29	1.9×10^{-16}	$2.8 - 3.0 \times 10^{-16}$	$2.7 (\pm 0.3) \times 10^{-16}$	[1]
$^{239}\text{Pu}/\text{U}$	2.41×10^4	---	$5.2 - 7.2 \times 10^{-12}$	$12 (\pm ?) \times 10^{-12}$ $15 (\pm 2) \times 10^{-12}$ $3.1 (\pm 0.1) \times 10^{-12}$ $5.3 (\pm 0.1) \times 10^{-12}$	[7] [9] [8] [10]
$^{99}\text{Tc}/\text{U}$	2.13×10^5	1.6×10^{-12}	$2.3 - 2.5 \times 10^{-12}$	$1.6 (\pm 0.2) \times 10^{-12}$	[6]
$^{36}\text{Cl}/\text{Cl}$	3.01×10^5	---	$1.1 - 1.3 \times 10^{-10}$	$0.9 (\pm 0.1) \times 10^{-10}$	[5]
$^{237}\text{Np}/\text{U}$	2.14×10^6	---	$1.0 - 1.4 \times 10^{-12}$	$2.2 (\pm 0.1) \times 10^{-12}$	[8]
$^{129}\text{I}/\text{U}$	1.57×10^7	0.6×10^{-12}	$8.0 - 9.9 \times 10^{-12}$	$19 (\pm ?) \times 10^{-12}$ $7.2 (\pm 1.3) \times 10^{-12}$	[4] [10]
References					
[1] Arino and Kuroda, 1968		[6] Kenna and Kuroda, 1964			
[2] Attrep, 1965, p. 68		[7] Levine and Seaborg, 1951			
[3] Attrep and Kuroda, 1968		[8] Myers and Lindner, 1971			
[4] Brauer and Strebin, 1982		[9] Peppard et al., 1951			
[5] Kenna and Kuroda, 1960		[10] This report, Tables 3.1 and 3.3			

- (b) Analytical problems. Reported uncertainties may not accurately express the true uncertainty of some of the analyses. The early ^{239}Pu results, for example, used α -spectroscopy such that a Pu tracer could not be added to the sample during processing to track the yield. Results were adjusted for chemical yields determined on samples other than the one being reported, and these yields were often low.
- (c) Elemental composition. The quantity of NBL-6 available to us was insufficient for an elemental determination. Hence, modelling was based upon analyses reported in a 1939 paper, as cited by Kenna and Attrep (1966). The degree to which this material has the same composition as NBL-6 is unknown.

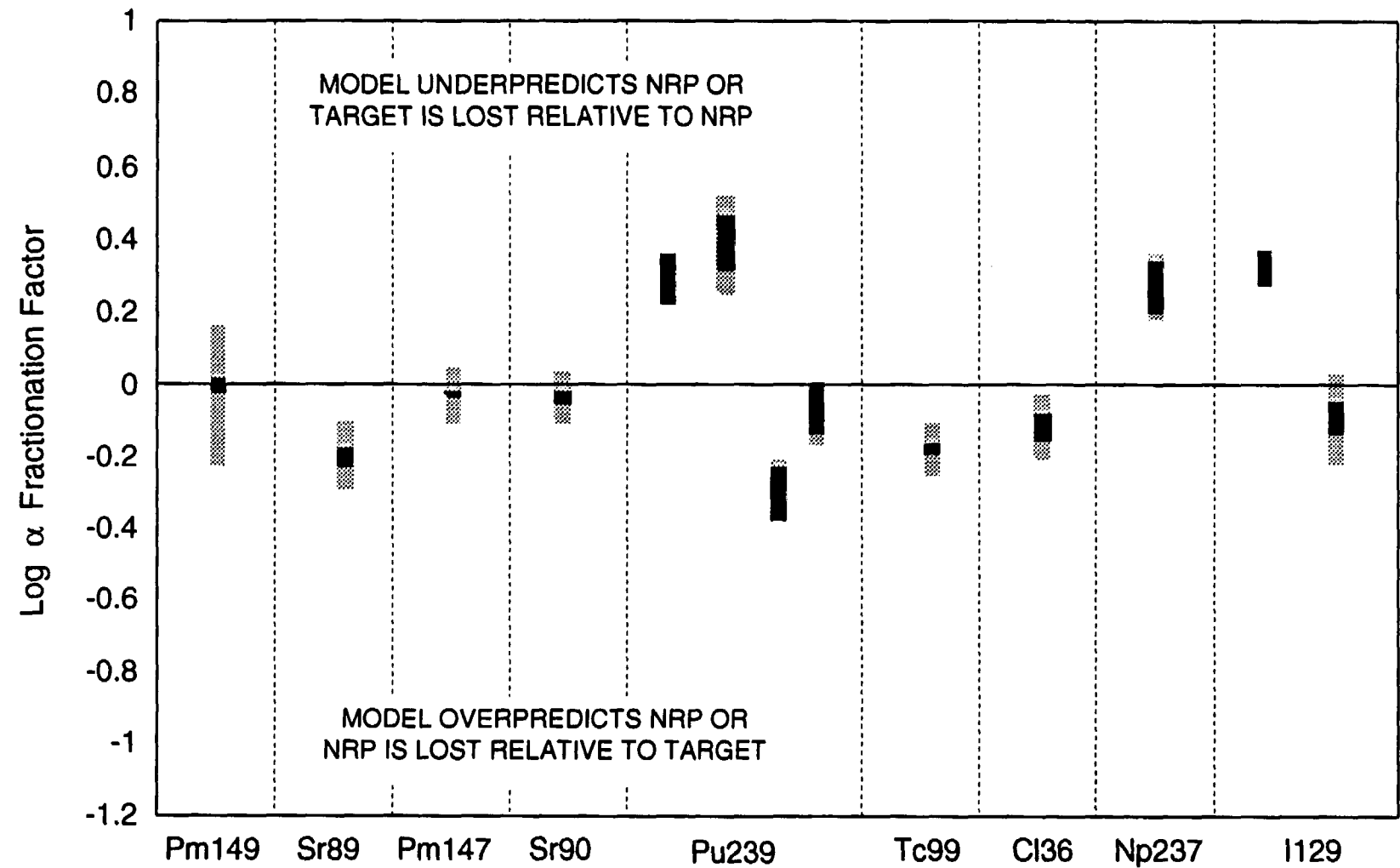


Figure 4.2 Comparison of measured and predicted NRP concentrations for Shinkolobwe pitchblende. The black portion of each line represents variability in log α attributable to uncertainties in model predictions; the shaded portion is the additional variability attributable to analytical uncertainties. Calculated from data in Table 4.3; see Table 4.4 footnote for definition of α .

Considering these limitations, the degree of agreement between the measurements and model calculations is encouraging.

4.2.3 Estimated uncertainties in abundances predicted by the infinite model

Uncertainties in the predictions of the infinite source-term model arise from uncertainties in the concentrations for those elements which have the greatest controlling influence on moderating the neutron flux: H, Sm, Gd. Bounding concentrations were estimated as follows:

- (a) Hydrogen (Table 4.1) - Porosities of the ores have not been measured; however, a range of 0 to 5% by volume seems reasonable. A more important source of H in these ores is probably that associated with the clay minerals, chlorite and illite. A range of 0.75 to 1.3% by weight was assumed for these mineral fractions.
- (b) Heavy rare earth elements (HREE) - Only Sm and Gd have been measured in these ore samples. Concentrations of other HREE were estimated by assuming that the chondrite-normalised patterns of the samples are the same as those measured for sample 75080180 by McLennan and Taylor (1980); however, model calculations showed that the difference in results when other HREE were included was insignificant compared to the results when only Sm and Gd were included. Based upon the XRAL analyses of duplicate samples (Table 2.5), a maximum uncertainty of 20% was assumed for the Sm and Gd concentrations for each sample. MCNP model runs were conducted using 80% and 120% of the measured Sm and Gd values.

The results of the sensitivity analyses are tabulated in Table 4.4. The responses of each nuclear reaction rate to variations in HREE and H contents are plotted as "sensitivity polygons" in Figures 4.3A through 4.3D. First shown in Figures 4.3A and 4.3B are ^{235}U fission rates, normalised to ^{235}U content, and ^{36}Cl production rates, normalised to total Cl. Readily seen is the general trend of increasing reaction rate with decreasing Gd/U ratio. High Gd/U ratios, such as those for the Key Lake samples, suppress the low-energy component of the neutron flux where the cross-sections for the ^{235}U fission and ^{36}Cl production reactions are highest. Low Gd/U ratios, such as those for BL-5, NBL-6, CS235L and the 2 Oklo samples, allow a higher proportion of the low-energy neutrons to be captured by ^{235}U and ^{35}Cl . In samples with low Gd/U ratios, an uncertainty of 20% in the Gd concentration leads to a maximum uncertainty of 5% in the predicted ^{235}U fission rate; the uncertainty decreases with increasing Gd/U ratio.

The sensitivities of ^{235}U and ^{36}Cl production rates to variations in H content are similar, but less pronounced, to their responses to HREE contents (Figures 4.3A and 4.3B). For a given HREE concentration in a given sample, reaction rates are 0-4% higher for the upper range of H content than for the lower range of H content. Neutrons lose energy most quickly in samples with high H/U ratios, thereby increasing the proportion of low-energy neutrons available. Similar sensitivity polygon shapes would be obtained for $^{129}\text{I}/\text{U}$ or $^{99}\text{Tc}/\text{U}$ plotted against Gd/U ratio, although the ranges of y-axis values for the fission products would have to be expanded for the first and compressed to a narrower range for the second.

TABLE 4.4

RESULTS OF SENSITIVITY ANALYSES FOR INFINITE ORE BODIES

Ore Deposit	Sample	$^{36}\text{Cl}/\text{Cl}$ $\times 10^{-12}$	$^{99}\text{Tc}/\text{U}$ $\times 10^{-12}$	$^{129}\text{I}/\text{U}$ $\times 10^{-12}$	$^{239}\text{Pu}/\text{U}$ $\times 10^{-12}$
RANGE OF PREDICTED VALUES					
Koongarra	G2698	62 - 81	1.9 - 2.0	4.2 - 5.4	2.6 - 3.8
	G4674	67 - 75	1.9 - 2.0	4.3 - 4.9	2.3 - 3.2
Key Lake	KL756	12 - 22	1.8	2.8 - 2.9	2.6 - 3.0
	KL785	14 - 15	1.7 - 1.8	1.7 - 1.8	1.7 - 2.4
Cigar Lake	CS235L	98 - 117	2.4 - 2.6	9.2 - 11	6.5 - 8.6
	W83A	40 - 50	1.9 - 2.0	4.7 - 5.5	3.5 - 4.3
	W83C	40 - 51	2.0 - 2.1	5.6 - 6.0	4.2 - 4.8
Oklo	Z9-005	82 - 100	2.3 - 2.5	8.1 - 9.8	5.8 - 7.5
	Z9-028	81 - 103	2.4 - 2.5	7.8 - 9.7	6.2 - 7.9
Shinkolobwe	NBL-6	110 - 133	2.3 - 2.5	8.0 - 9.9	5.2 - 7.2
Beaverlodge	BL-5	113 - 137	2.2 - 2.3	6.4 - 7.7	2.5 - 3.5
LOG α FRACTIONATION FACTORS					
Koongarra	G2698	n.m.	≤ -0.02	-0.62 to -0.51	-0.16 to 0.00
	G4674	0.05 to 0.10	n.m.	-0.69 to -0.63	-0.39 to -0.25
Key Lake	KL756	n.m.	n.m.	-0.59 to -0.57	-0.08 to -0.02
	KL785	n.m.	n.m.	n.m.	-0.30 to -0.15
Cigar Lake	CS235L	n.m.	n.m.	-0.72 to -0.64	-0.65 to -0.53
	W83A	n.m.	≤ -0.05	-0.49 to -0.42	-0.13 to -0.04
	W83C	n.m.	n.m.	-0.33 to -0.30	-0.23 to -0.18
Oklo	Z9-005	n.m.	n.m.	n.m.	-0.97 to -0.85
	Z9-028	n.m.	n.m.	-0.56 to -0.48	-0.44 to -0.32
Shinkolobwe	NBL-6	n.m.	n.m.	-0.14 to -0.05	-0.13 to 0.01
Beaverlodge	BL-5	n.m.	n.m.	n.m.	-0.05 to 0.09
<p>Notes:</p> <p>n.m. - not measured</p> <p>α-fractionation factor: $\alpha = (\text{NRP}/\text{Target})_{\text{M}} / (\text{NRP}/\text{Target})_{\text{SE}}$, where</p> <p>NRP = nuclear reaction product (e.g., ^{239}Pu, ^{36}Cl)</p> <p>Target = elemental target for reaction (e.g., U, Cl)</p> <p>subscript M = measured ratio</p> <p>subscript SE = ratio calculated assuming secular equilibrium</p> <p>Log $\alpha < 0$ suggests that either the model is overpredicting NRP production, or else the NRP is being lost from the sample at a greater rate than is its target.</p> <p>Log $\alpha > 0$ suggests that either the model is underpredicting NRP production, or else the NRP is being lost from the sample at a lesser rate than is its target.</p>					

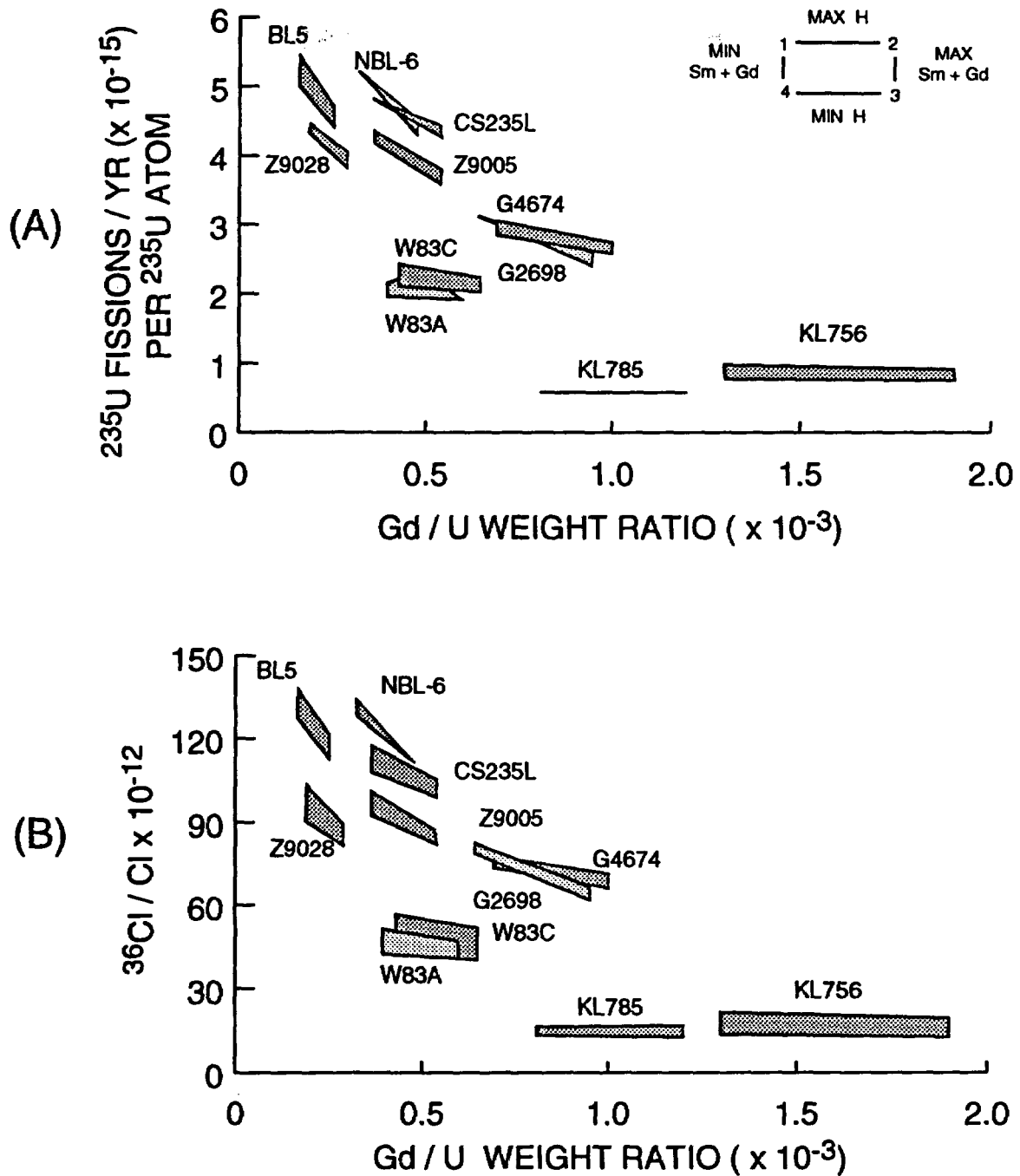


Figure 4.3 Variation in predicted nuclear reaction rates in primary ore samples as a function of HREE and H contents, plotted against Gd/U ratios. Plot (A) - ²³⁵U fission rates, Plot (B) - ³⁶Cl/Cl ratios, Plot (C) - ²³⁹Pu/U ratios, and Plot (D) - ²³⁸U fission rates. The limits of the "sensitivity polygons" in each plot are established by the following assumptions about H and HREE contents of the samples (refer to legend in Plot (A) or Plot (C)): (1) 5% porosity, maximum H content of mineral (Table 4.1), 80% of measured Sm+Gd value; (2) same as (1) but with 120% of measured Sm+Gd value; (3) 0% porosity, minimum H content of mineral phase, 120% of measured Sm+Gd value; (4) same as (3) but with 80% of measured Sm+Gd value.

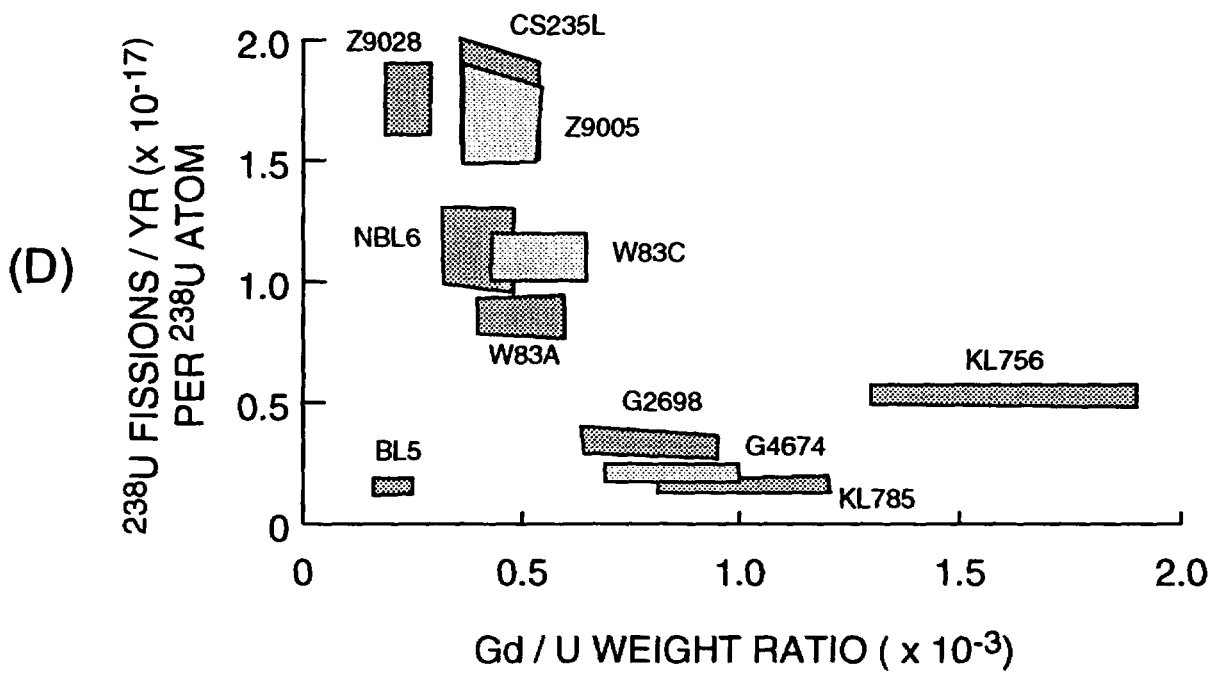
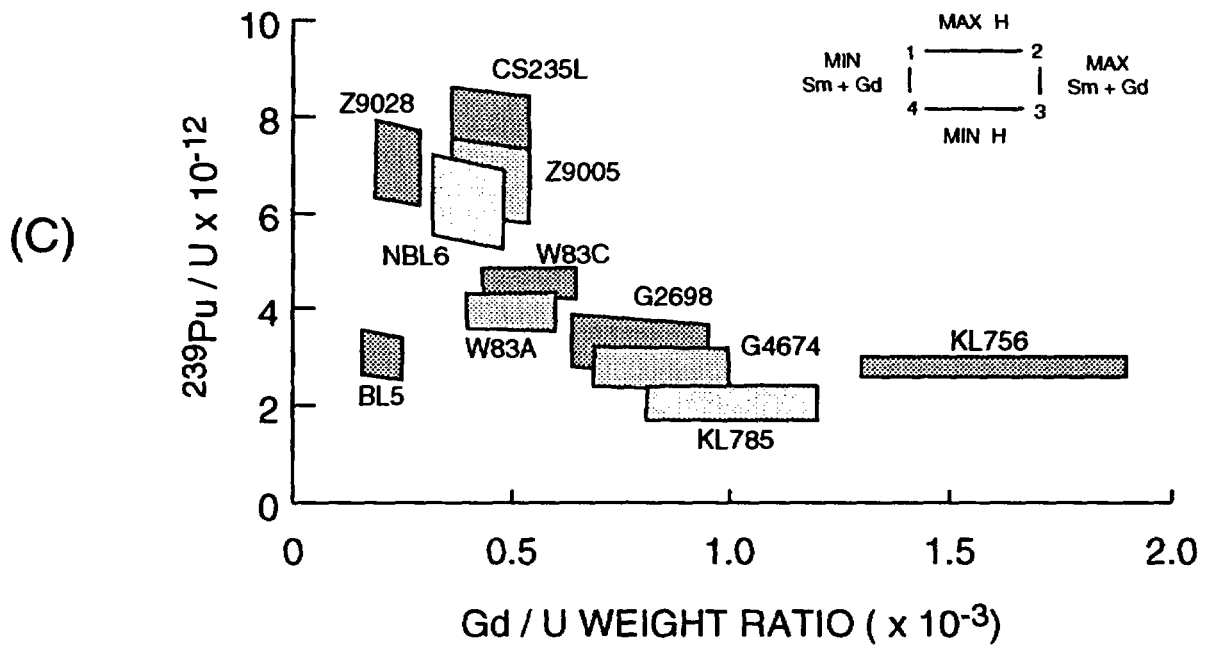


Figure 4.3 (continued)

Variations in ^{239}Pu production and ^{238}U induced fission rates are plotted as a function of Gd/U ratio in Figures 4.3C and 4.3D. In contrast to ^{235}U and ^{36}Cl , these nuclear reactions appear to be essentially independent of Gd content (within the range considered) but are comparatively more sensitive to variations in H content. Thus, these reactions are enhanced by moderation of the neutron flux but probably occur at neutron energies above the range in which Gd and Sm are effective absorbers.

Table 4.4 summarises the results of the sensitivity analyses by reporting the range of NRP production rates for each sample and by calculating log α factors for the samples. The log α values are plotted as shaded bars in Figures 4.4 (for ^{239}Pu) and 4.5 (for ^{129}I). With the exception of $^{36}\text{Cl}/\text{Cl}$ in G4674 and ^{239}Pu in BL-5 and NBL-6, the infinite model either greatly overpredicts NRP production rates, or else the NRP have been lost from the samples to a significant extent. The latter possibility is feasible for ^{129}I , but probably remote for ^{239}Pu in these primary ore environments. Consequently, the need for a more sophisticated model is indicated, as described in the next section.

4.3 Effect of Stratigraphy on NRP Abundances

Improved estimates of NRP production rates were obtained by incorporating as much detail as possible about ore stratigraphy into the source-term model geometry. NRP production rates are the result of nuclear processes within a radius of ~ 30 cm; most of our samples were hand specimens with dimensions on the order of a few centimetres or less. The material surrounding each sample generally has uranium contents, and hence neutron emission rates, considerably lower than those of the samples. As a first approximation, neutron emission rates can be assumed to scale directly with U content. Hence, a model that overestimates the uranium abundance in this volume of rock, and consequently overestimates the neutron production rate, will also overestimate NRP production rates.

The results of the geometry models are summarised in Table 4.5 and are discussed on a case-by-case basis in the following sections.

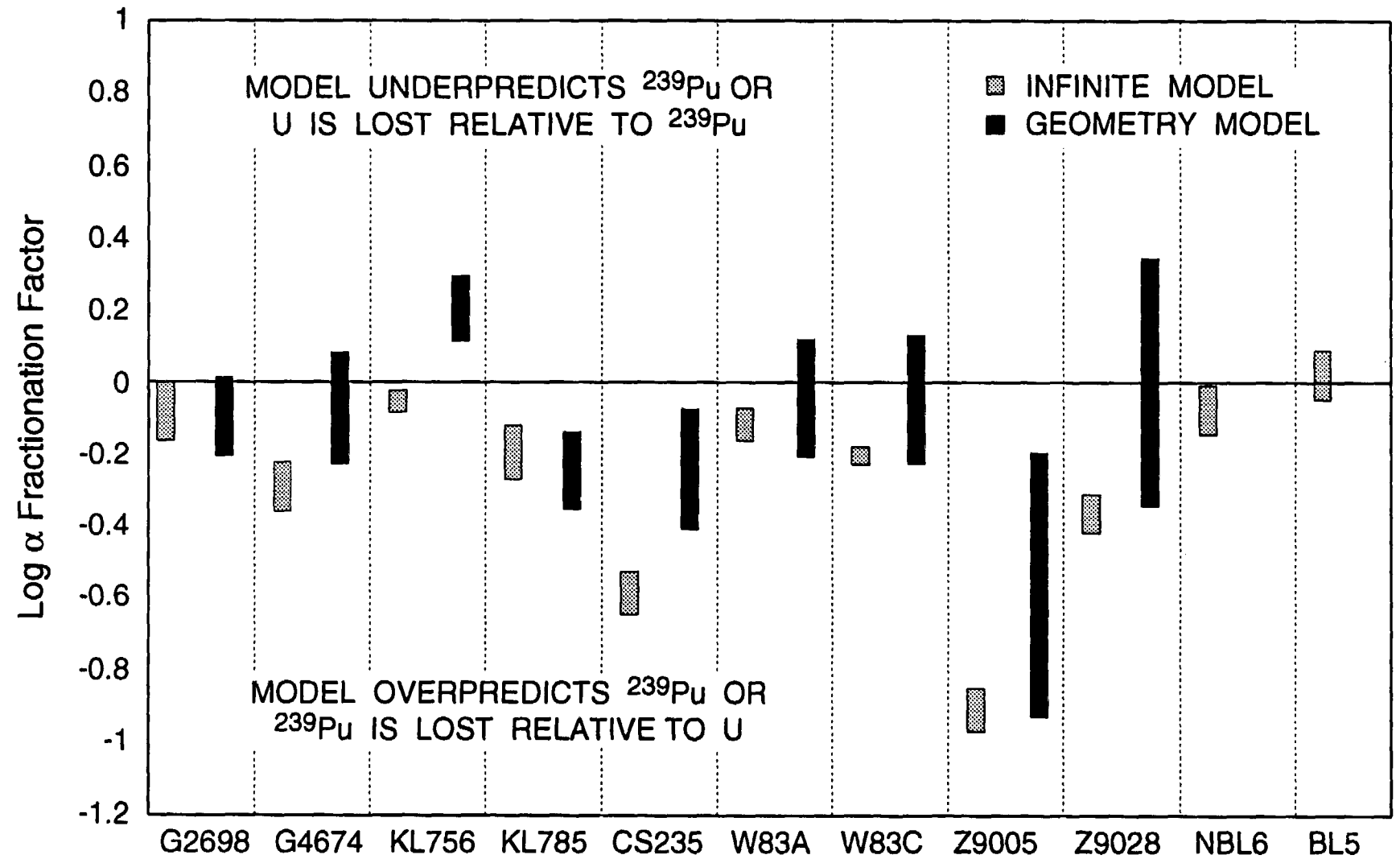


Figure 4.4 Comparison of measured and predicted ^{239}Pu concentrations for primary uranium ores. Calculated from data in Tables 4.4 and 4.5; see table footnotes for definition of α .

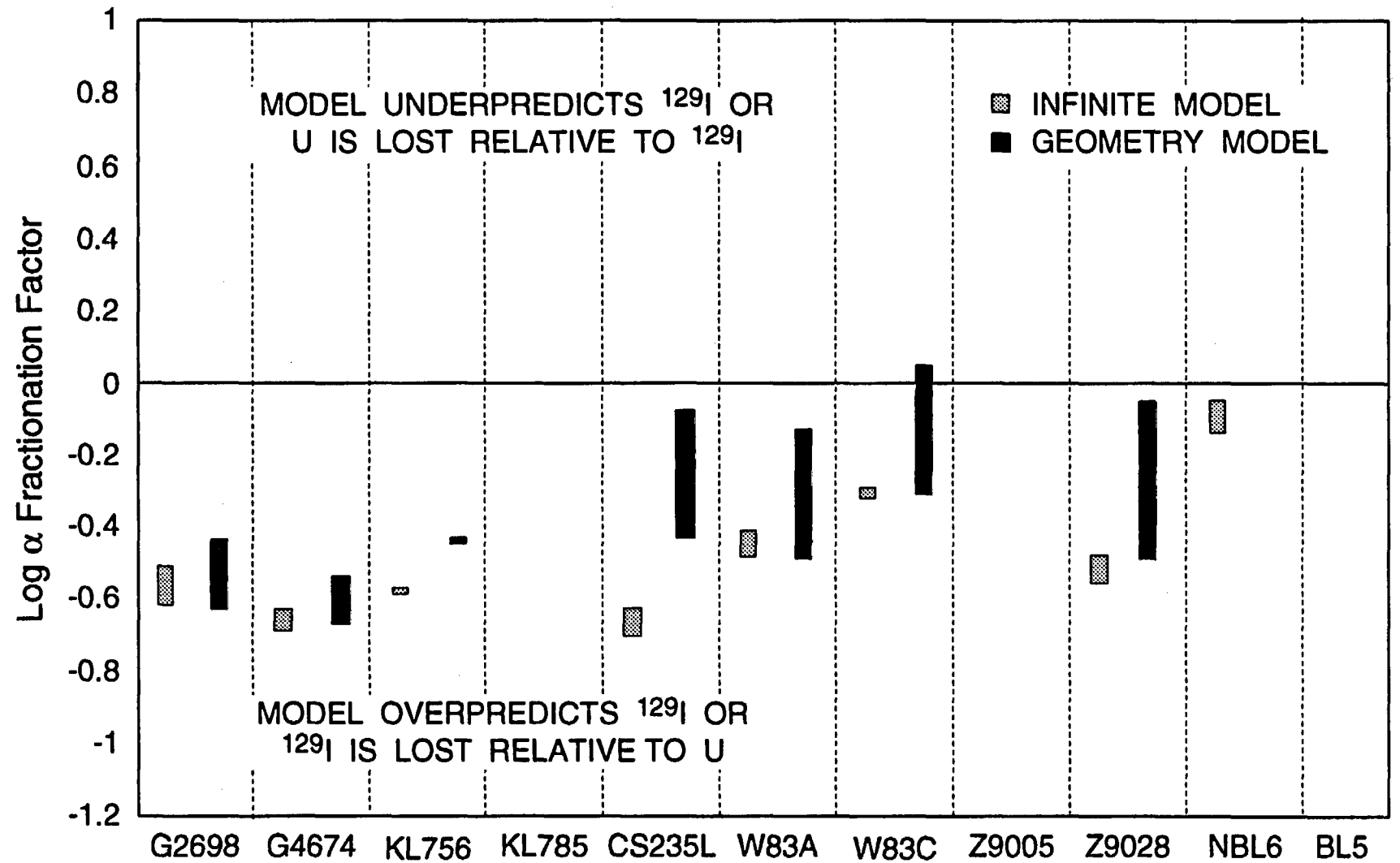


Figure 4.5 Comparison of measured and predicted ^{129}I concentrations for primary uranium ores. Calculated from data in Tables 4.4 and 4.5; see table footnotes for definition of α . No measurements available for KL785, Z9005, or BL5.

TABLE 4.5

EFFECTS OF ORE GEOMETRY ON NRP ABUNDANCE PREDICTIONS

Ore Deposit	Sample	$^{36}\text{Cl}/\text{Cl}$ $\times 10^{-12}$	$^{99}\text{Tc}/\text{U}$ $\times 10^{-12}$	$^{129}\text{I}/\text{U}$ $\times 10^{-12}$	$^{239}\text{Pu}/\text{U}$ $\times 10^{-12}$
RANGE OF PREDICTED VALUES					
Koongarra	G2698	51 - 84	1.9 - 2.1	3.6 - 5.6	2.3 - 4.0
	G4674	52 - 73	1.8 - 2.0	3.5 - 4.7	1.8 - 3.2
Key Lake	KL756	7 - 15	1.7	2.0 - 2.1	1.2 - 1.8
	KL785	15 - 18	1.7	1.7 - 2.1	1.6 - 3.1
Cigar Lake	Bulk average, 15 - 20% U	31 - 44	1.8 - 1.9	2.8 - 3.7	2.4 - 4.0
	Hole 220, intervals with $\geq 25\%$ U	21 - 56	1.7 - 2.0	2.5 - 5.7	2.1 - 4.8
Oklo	Z9-005	27 - 121	1.8 - 2.4	3.3 - 9.3	1.3 - 7.2
	Z9-028	27 - 121	1.8 - 2.3	3.1 - 8.5	1.3 - 7.2
LOG α FRACTIONATION FACTORS					
Koongarra	G2698	n.m.	≤ -0.02	-0.63 to -0.44	-0.19 to 0.02
	G4674	0.06 to 0.21	n.m.	-0.67 to -0.54	-0.36 to -0.11
Key Lake	KL756	n.m.	n.m.	-0.45 to -0.43	0.16 to 0.34
	KL785	n.m.	n.m.	n.m.	-0.42 to -0.09
Cigar Lake	CS235L	n.m.	n.m.	-0.43 to -0.08	-0.40 to -0.04
	W83A	n.m.	≤ 0.06	-0.50 to -0.14	-0.20 to 0.15
	W83C	n.m.	n.m.	-0.31 to 0.05	-0.23 to 0.12
Oklo	Z9-005	n.m.	n.m.	n.m.	-0.96 to -0.21
	Z9-028	n.m.	n.m.	-0.50 to -0.06	-0.38 to 0.36
<p>Note:</p> <p>n.m. - not measured</p> <p>α-fractionation factor: $\alpha = (\text{NRP}/\text{Target})_{\text{M}} / (\text{NRP}/\text{Target})_{\text{SE}}$, where</p> <p>NRP = nuclear reaction product (e.g., ^{239}Pu, ^{36}Cl)</p> <p>Target = elemental target for reaction (e.g., U, Cl)</p> <p>subscript M = measured ratio</p> <p>subscript SE = ratio calculated assuming secular equilibrium</p> <p>Log $\alpha < 0$ suggests that either the model is overpredicting NRP production, or else the NRP is being lost from the sample at a greater rate than is its target.</p> <p>Log $\alpha > 0$ suggests that either the model is underpredicting NRP production, or else the NRP is being lost from the sample at a lesser rate than is its target.</p>					

4.3.1 Koongarra

NRP production rates were calculated for two 2.5-m profiles centred on G2698 and G4674 (Figures 4.6 and 4.7). Uranium concentrations and interval lengths were taken from drillhole log records provided to ARAP by the Denison mining company. The elemental composition of intervals above and below the samples were estimated in the following manner:

- (a) The ore in each interval was assumed to represent a two-component mixture. End-member compositions of the dry mixtures were estimated from elemental analyses of G2698 and G4674. The uraninite component was assumed to be UO_2 ; concentrations of ancillary Pb, Sm, and Gd were established by assuming that Pb/U, Sm/U, and Gd/U ratios were invariant throughout the profile. The end-member composition of the non-uraninite component was estimated by assuming it had an O content of 47% (typical of silicate rocks) and an H content of either 0.75% or 1.3% by weight (see footnote, Table 4.1), and by adjusting all other elements in the sample (excluding those included in the uraninite component) upwards to add to 100%.
- (b) The amount of the uraninite component in each interval was determined by the measured U concentration. The non-uraninite component comprised the remainder of each interval.
- (c) Grain densities were estimated in the manner described in Table 4.1. Ranges in H contents were estimated by assuming 0 and 5% porosity, in conjunction with the H associated with the mineral phases.
- (d) Neutron emission rates in each interval were scaled to the measured rates for these samples according to the U concentration.
- (e) Limits for NRP production rates were calculated by running two cases for each profile: one case with 0% porosity, minimum H content in the mineral phase, and Sm + Gd/U at 120% of the measured values; and a second case with 5% porosity, maximum H content in the mineral phase, and Sm + Gd/U at 80% of the measured values.

The results are tabulated in Table 4.5 and plotted in Figures 4.6 and 4.7. Maximum production rates are obtained in the centre of the G2698 and G4674 profiles, but these rates are generally less, and with a wider range, than the rates estimated for the infinite model. The results of the two modelling approaches are contrasted in Figures 4.4 and 4.5 for ^{239}Pu and ^{129}I , in which $\log \alpha$ values for the geometry model are plotted as black bars for each sample. The general result is that of lowered production rates with increased uncertainty ranges, relative to the infinite case. The variability in NRP production rates emphasizes the danger of comparing analytical results obtained on grab samples from coarsely crushed drillpulp, and the need to homogenise any sample before splitting it for NRP analyses. The variability seen in replicate ^{239}Pu analyses of G2698 and G4674 (Table 3.1) is probably inherent in the raw samples. (However, this explanation cannot be used to explain the variability observed in the ^{129}I results (Table 3.3) because these were all obtained on the homogenised material.)

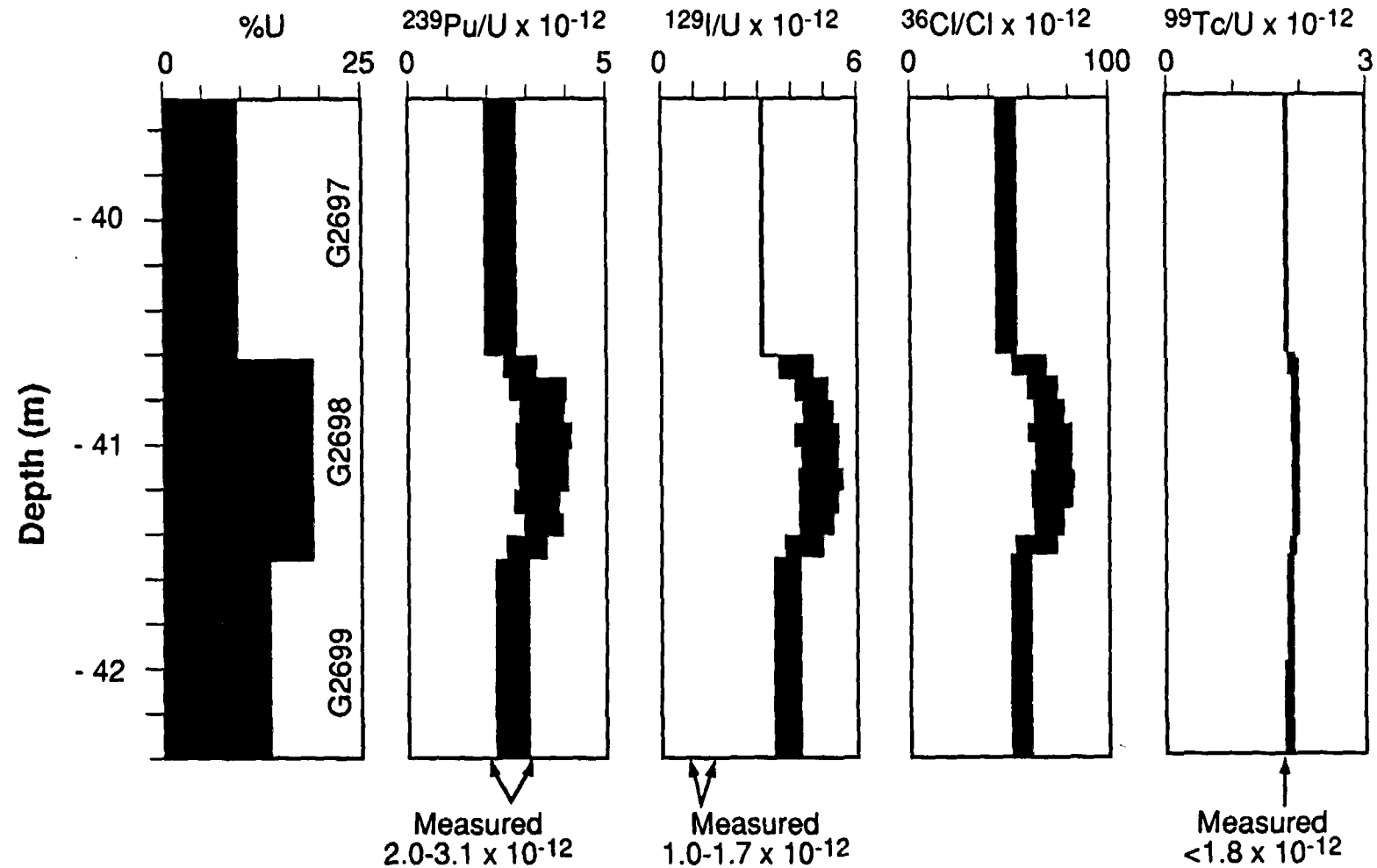


Figure 4.6 Geometry model: Predicted distribution of $^{239}\text{Pu}/\text{U}$, $^{129}\text{I}/\text{U}$, $^{36}\text{Cl}/\text{Cl}$, and $^{99}\text{Tc}/\text{U}$ ratios in a profile through G2698. Uranium contents for samples above and below G2698 were taken from the Denison mining company data base. Lower limits for NRP abundances were estimated by assuming 5% porosity, maximum H content of minerals (Table 4.1), and 120% of the measured Sm/U and Gd/U values. Upper limits were established by assuming 0% porosity, minimum H content of minerals, and 80% of the measured Sm/U and Gd/U values for G2698.

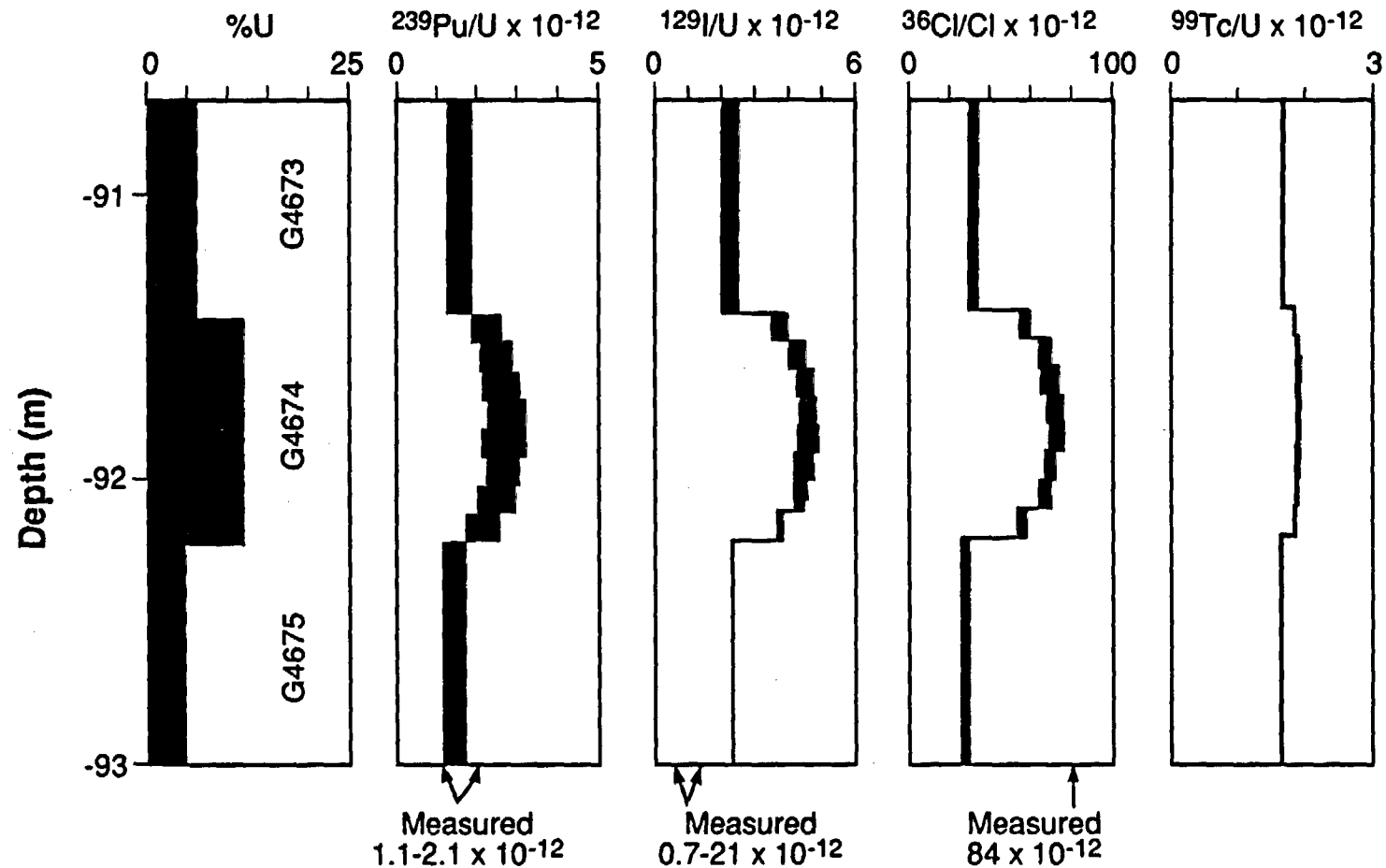


Figure 4.7 Geometry model: Predicted distribution of $^{239}\text{Pu}/\text{U}$, $^{129}\text{I}/\text{U}$, $^{36}\text{Cl}/\text{Cl}$, and $^{99}\text{Tc}/\text{U}$ ratios in a profile through G4674. Uranium contents for samples above and below G4674 were taken from the Denison mining company data base. Lower limits for NRP abundances were estimated by assuming 5% porosity, maximum H content of minerals (Table 4.1), and 120% of the measured Sm/U and Gd/U values. Upper limits were established by assuming 0% porosity, minimum H content of minerals, and 80% of the measured Sm/U and Gd/U values for G4674.

4.3.2 Key Lake

Profiles were also modelled for the two Key Lake samples. Uranium concentrations for the intervals above and below each sample were reported by V. Sopuck (Key Lake Mining Company) to be about 12% U above and below KL756 (with 22% U), and about 8 and 17% U above and below KL785 (with 9% U). The profiles were modelled by assuming that the sampled cores were 8-cm long (Trocki et al., 1984), and that the intervals above and below the samples were infinite in extent. Elemental compositions for the intervals adjacent intervals to KL785 were estimated in a manner similar to that described for the Koongarra profiles and two cases were run (by varying H, Sm, and Gd contents) to establish a range in NRP production rates. The composition of material neighboring KL756 was more difficult to estimate because of the large Ni-As-S fraction. Consequently, this material was assumed to be composed of a three-component mixture: a uraninite fraction (UO_2 , Pb, Sm, Gd), a sulfide fraction (Ni, As, S), and a silicate fraction (all other elements). The quantity of the uraninite fraction in the surrounding material was fixed by the reported U concentration and by assuming constant Pb/U, Sm/U and Gd/U ratios throughout the profile. Two different compositions were then devised: (a) the sulfide fraction was assumed to be constant throughout the profile, and the silicate fraction was adjusted to make the element weights sum to 100%, and (b) the silicate fraction was assumed to remain constant throughout the profile, with the sulfide fraction adjusted as needed. Each composition was modelled twice, varying the H, Sm, and Gd contents each time in order to arrive at a range of NRP production rates.

The results are tabulated in Table 4.5. Again, production rates are generally less, and with a wider range, than the rates estimated for these samples by the infinite model. The results of the two modelling approaches are contrasted in Figures 4.4 and 4.5 for ^{239}Pu and ^{129}I , in which $\log \alpha$ values for the geometry model are plotted as black bars for each sample. The geometry model still appears to overpredict ^{129}I production in KL756 (although loss of this fission product from the matrix is also a possibility); ^{239}Pu production is overpredicted in KL785 but, in contrast to the infinite model, underpredicted in KL756.

4.3.3 Cigar Lake

Two approaches were taken to incorporate geometry effects into the modelling of NRP production in the three Cigar Lake ore samples. One approach was to model the NRP production rate in an ore assumed to represent the average composition of the richest part of the deposit. The average ore grade is 15-20% U, and its composition was estimated by assuming a two-component mixture with the end-member compositions extracted from the elemental analysis of CS235L in the same manner used for the Koongarra profiles. A total of 4 cases were run each assuming 15% and 20% U concentrations, with each case independently varying H and Sm+Gd contents in the same manner as was used for the sensitivity study for the infinite model (section 4.2.3).

A second approach was to model NRP production profiles in a 6.2-m section of Hole 220, a drillhole through one of the richest parts of the orebody. The section was divided into 31 unevenly spaced intervals by J. Cramer (AECL) on the basis of U content and mineralogy. Elemental compositions of the intervals were estimated using the two-

component mixing approach (section 4.3.1), again using CS235L as the starting point. Neutron production rates were assumed to scale directly with the U content. Only one case was run, in which 2% porosity was assumed throughout the profile. In the model, some of the thicker intervals, particularly those comprised of high-grade material, were subdivided in order to examine spatial variabilities and boundary effects in the NRP production rates.

Figure 4.8 shows the resulting NRP profiles in Hole 220. From this profile, the ranges of NRP production rates to be used for comparison with CS235L, W83A and W83C, were established by examining the predicted rates for any interval containing at least 20% U. In this manner, a number of different geometries are sampled. The modelled Hole 220 profile contains several abrupt boundaries between high-grade and low-grade ores as well as variable thicknesses of individual strata. Thus a wider range is expected in the predicted NRP production rates for the Cigar Lake modelling than for the Koongarra and Key Lake modelled profiles.

Table 4.5 tabulates the results of the representative average ore cases and of the high-grade portions of the Hole 220 profile. The production rate ranges predicted by the average cases are narrower than, but included within, the ranges predicted by the Hole 220 profile. Log α factors for ^{239}Pu (black bars in Figure 4.4) indicate that the geometry model predictions probably bracket the true production rate values for the Cigar Lake samples. Log α factors for ^{129}I (black bars in Figure 4.5) indicate that the geometry model may still be overpredicting U fission rates, although to a much lesser extent than did the infinite model.

4.3.4 Oklo

The approach used in the Koongarra, Key Lake and Cigar Lake profile studies could be termed the "infinite sandwich model." In each case, the sample was modelled as a seam of variable thickness, sandwiched between two other seams, all of which were assumed to extend infinitely in the planar direction. However, high-grade samples are probably more appropriately modelled as lenses, seams or nuggets in a low-grade matrix, not as extensive thick layers of high-grade ore. Depending upon the dimensions of the pocket, and the composition of the surrounding material, a considerable fraction of the neutrons could leak out of the sample to be absorbed by the surrounding material; neglecting this neutron leakage would obviously lead to overestimates of the true NRP production rates. However, the size of these lenses or seams is impossible to estimate unless the orebody is exposed in a mine wall, as is the case for some parts of the Oklo deposit.

The effect of neutron leakage on NRP production rate modelling was investigated for the Oklo samples. Oklo reactor zone 9 was a disk-shaped feature with an average UO_2 concentration of 64% (Curtis et al., 1989) surrounded by shale and sandstone containing less than 1% UO_2 (Loss et al., 1989). The uranium-rich disk was metres in extent in two dimensions, but only 30-50 cm thick. NRP/Target ratios were calculated as a function of location through a cross-section of the disk. The calculations were done by simulating the reactor zone as a homogeneous seam with the composition of Z9-005. The seam is 50 cm thick and of infinite dimension in the other dimensions. It is surrounded on three sides by shale containing no uranium.

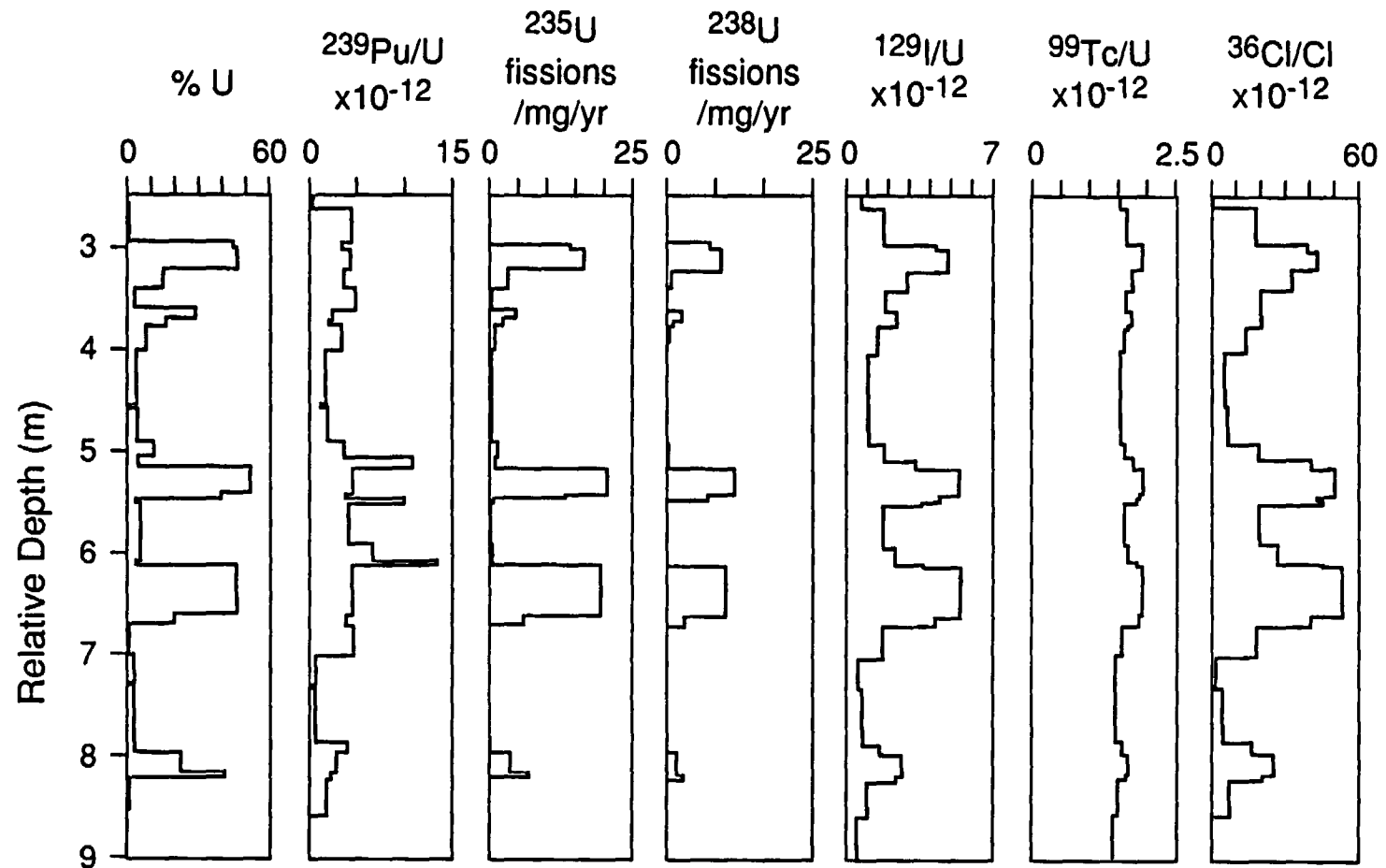


Figure 4.8 Geometry model: predicted distribution of ^{235}U and ^{238}U induced fission rates, and $^{239}\text{Pu}/\text{U}$, $^{129}\text{I}/\text{U}$, $^{99}\text{Tc}/\text{U}$ and $^{36}\text{Cl}/\text{Cl}$ ratios in a profile of Cigar Lake Hole 220. The U profile was provided by J. Cramer (Atomic Energy of Canada, Ltd.). Calculations are based on the elemental composition of CS235L, adjusted as a function of U content as described in the text, and assume 2% porosity, 0.75% H in the silicate mineral phase, and the measured Pb/U, Sm/U and Gd/U values for CS235L.

Figure 4.9A-D is a schematic representation of the model reactor zone. The lines are contours of calculated ^{235}U and ^{238}U induced fission rates, and $^{239}\text{Pu}/\text{U}$ and $^{36}\text{Cl}/\text{Cl}$ ratios. The contoured values demonstrate that samples with identical compositions will have dramatically different NRP compositions depending on their location relative to the boundary of the ore seam with the low-U shale. The effect of neutron leakage at the shale/ore boundary can clearly be seen in all four profiles. The highest $^{239}\text{Pu}/\text{U}$ ratios and the highest ^{235}U induced fission rates are at the centre of the seam where the neutron flux is largely the result of nuclear processes involving uranium. Near the edges, a large proportion of neutrons produced in the ore diffuse into the adjacent shale, resulting in lower local neutron fluxes and hence lower $^{239}\text{Pu}/\text{U}$ ratios. The energy spectrum of the neutrons is also dramatically changed by the adjacent shale due to its higher H content and hence greater ability to thermalise neutrons. The lowest $^{239}\text{Pu}/\text{U}$ ratios are at the corners, where neutron losses are greatest. In contrast, ^{235}U induced fission rates and $^{36}\text{Cl}/\text{Cl}$ ratios are greater along the boundary than in the interior of the ore seam because the thermalization of the neutrons more than offsets the effect of neutron leakage. The effects of neutron leakage on these reactions are only obvious at the corners.

A model of production in a homogeneous medium with the composition of the ore will only describe the measured NRP/Target ratio if the sample was taken from the middle of the fossil reactor zone. Samples from the periphery will have ratios considerably different than those calculated by the model of production in an infinitely homogeneous medium. The Oklo samples available in the LANL archival collection are fairly large, about 10 cm on a side; Z9-005 and Z9-028 were taken as small chips from these larger blocks. The low $^{239}\text{Pu}/\text{U}$ ratios measured in these two samples suggests that their original orientations were on the outermost edge of the uranium ore seam.

4.4 Conclusions about Modelling Capability

4.4.1 Capability to predict absolute NRP abundances

The source-term model is most useful as a predictive tool in cases where the sample represents a volume of material that is large relative to the mean pathlength of a neutron, e.g. NBL-6 and BL-5, or where the sample is derived from relatively homogeneous material. The model also provides useful predictions, although with greater uncertainties, of NRP abundances in samples taken from well-specified locations in geometrically well-defined environments. In the latter case, realistic results are only obtained when the model incorporates additional information about sample environs. The largest uncertainties attend calculations of NRP abundances in small samples taken from heterogeneous geologic systems; for these samples, even with detailed compositional information, the source-term model is not able to predict absolute NRP abundances with the accuracy needed to calculate NRP retention or losses unless the fractionation between uranium and its reaction products is substantial, i.e., $\alpha > 0.1$ or $\alpha < -0.1$.

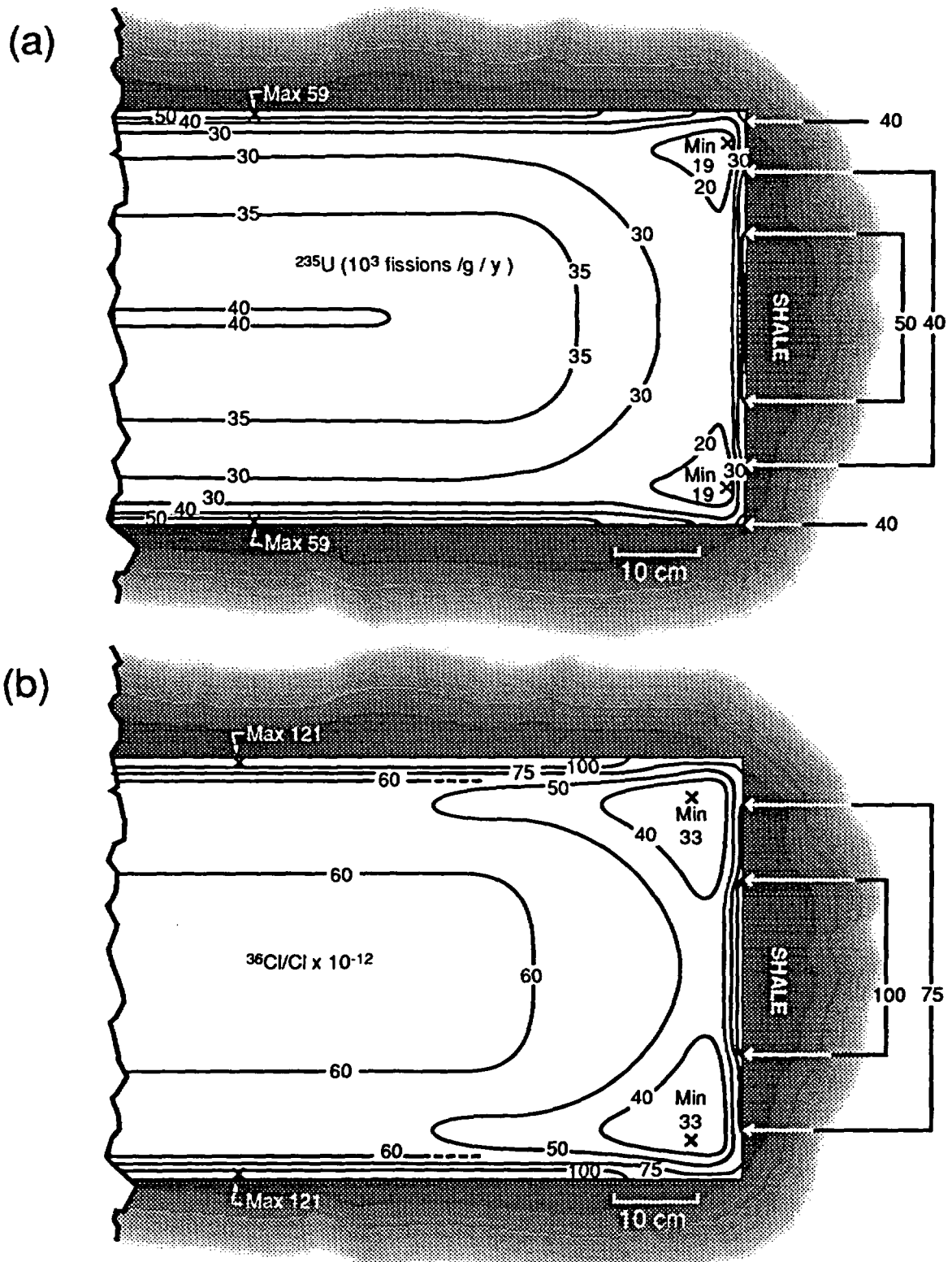
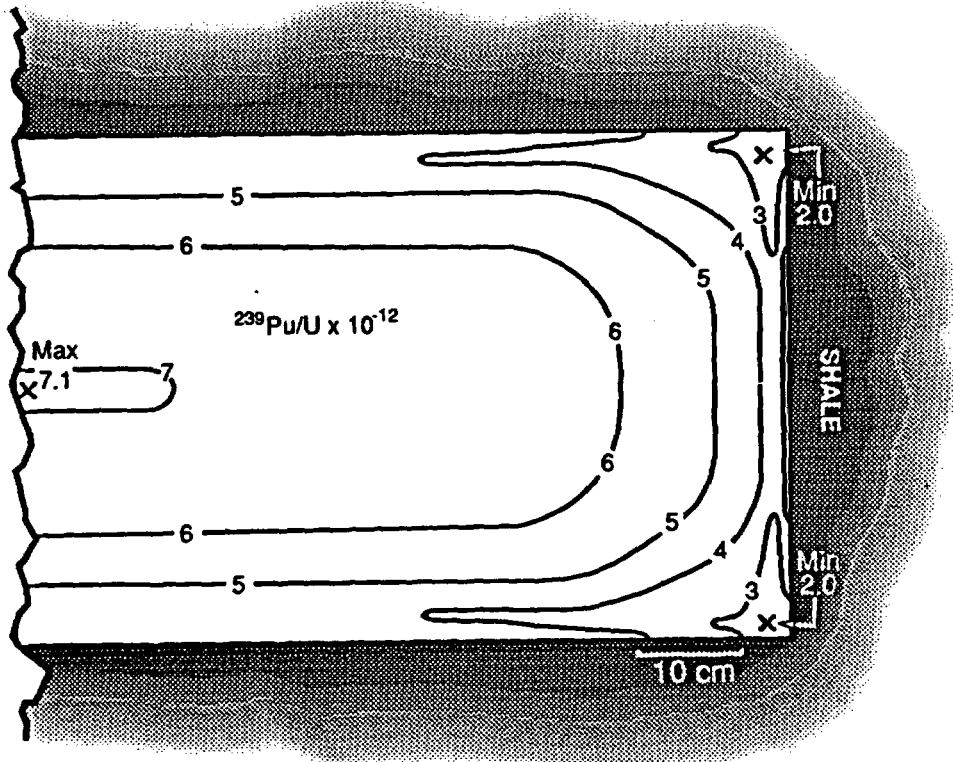


Figure 4.9 Geometry model: predicted distribution of (a) ^{235}U induced fission rates, (b) $^{36}\text{Cl}/\text{Cl}$ ratios, (c) $^{239}\text{Pu}/\text{U}$ ratios, and (d) ^{238}U induced fission rates in the Oklo reactor zone 9 ore seam.

(c)



(d)

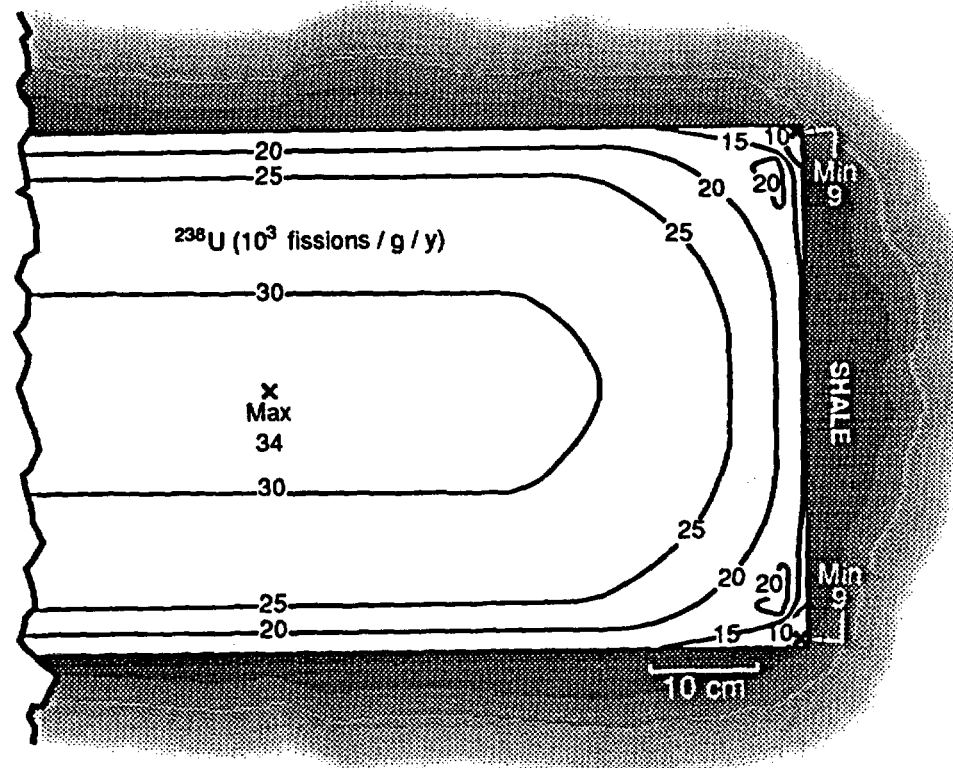


Figure 4.9 (continued)

4.4.2 Uncertainties in predictions of absolute abundances

Calculated uncertainties for the various source-term models in section 4.2.3 range from low for ^{99}Tc (uncertainties about 10%) to moderate for ^{129}I and ^{239}Pu (uncertainties about 20-50%). These uncertainties are almost certainly underestimated. For example, Gd/U ratios are shown by the model results to be a critical parameter in controlling ^{235}U fission rates. However, the supporting information is quite scant for the critical assumption that Gd/U ratios are relatively constant in the vicinity of any given sample; this assumption is based solely on the correlation seen between HREE and U concentrations in the handful of high-grade uranium ores studied by Ferguson and Winer (1980). Varying Gd/U ratios within the range of 80 to 120% of the measured values may not sufficiently reflect the uncertainty in their true concentrations. The effect of varying other elemental concentrations, such as B, F or Fe, which might also have a major influence on the neutron flux for some of the ores, was not investigated. For the geometry model, an infinite number of cases could be proposed to model the lateral extent, thickness, and elemental heterogeneities in stratigraphic intervals, e.g. with barren, high-porosity seams cutting through dense, high-grade material or vice versa.

4.4.3 Capability to predict relative NRP abundances

Even in those cases where the source-term model has not been able to provide precise estimates of the true NRP production rates, it has been invaluable for identifying the critical elemental parameters controlling these rates and establishing the nature of and the conditions under which various NRP production rates should correlate with or constrain one another. Three examples are given in the following subsections.

4.4.3.1 Chlorine-36 as an in-situ monitor of the ^{235}U fission rate

Figure 4.10A shows that the $^{36}\text{Cl}/\text{Cl}$ ratio should be an effective in-situ monitor of the ^{235}U fission rate in a sample, provided that the H/U atom ratio is greater than 6, which corresponds roughly to 6000 ppm U. The correlation may even hold true when the H/U ratio is less than 6 provided the sampled interval is thin relative to the pathlength of a neutron and is adjacent to material with a H/U ratio greater than 6; for example, nearly all of the samples from the Hole 220 profile plot on the correlation line despite the fact that the H/U ratios of the high-grade ore sections are less than 6, because they are adjacent to intervals with H/U ratios of 100. For a similar reason, all of the Oklo ore seam samples (H/U < 2) within 5 cm of the shale/ore boundary also plot on the correlation line (Figure 4.11A-B, black squares).

The constant of proportionality between the modelled NRP production rates is the ratio of their effective cross-sections, about 13 for samples with H/U > 6 (Figure 4.10B). This ratio is close to the ratio of the thermal cross-sections for the two reactions (13.5) and considerably less than the ratio of their resonance integrals (16), suggesting that most of the modelled production is caused by low-energy neutrons when the H/U ratio exceeds 6. The predictive relationship between the two NRP rates is:

$$\begin{aligned} &^{235}\text{U fissions/yr} = (^{36}\text{Cl}/\text{Cl}) (13) \lambda_{36} / 0.7577 \\ &\text{per } ^{235}\text{U atom} \end{aligned} \tag{4.5}$$

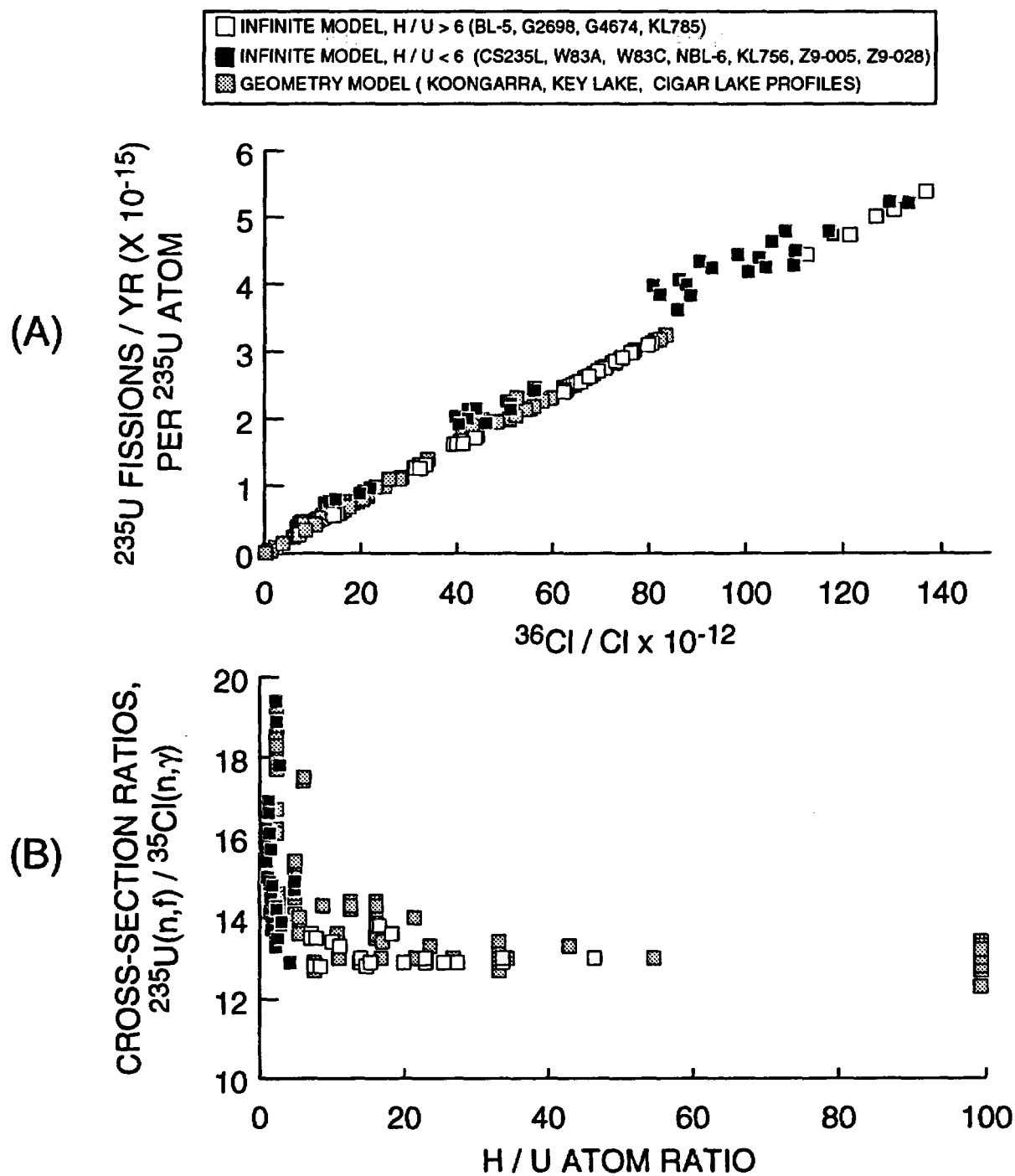


Figure 4.10 Predicted correlation between ^{235}U fission rate and $^{36}\text{Cl}/\text{Cl}$ in primary uranium ores, as a function of H/U atom ratio. Plot A indicates that the ^{235}U fission rate and ^{36}Cl production rate are directly proportional to one another for H/U ratios > 6. Plot B shows that the proportionality constant, or slope, corresponds to an effective cross-section ratio of 13 for these reactions. For comparison, the ratio of their thermal cross-sections is 12.9.

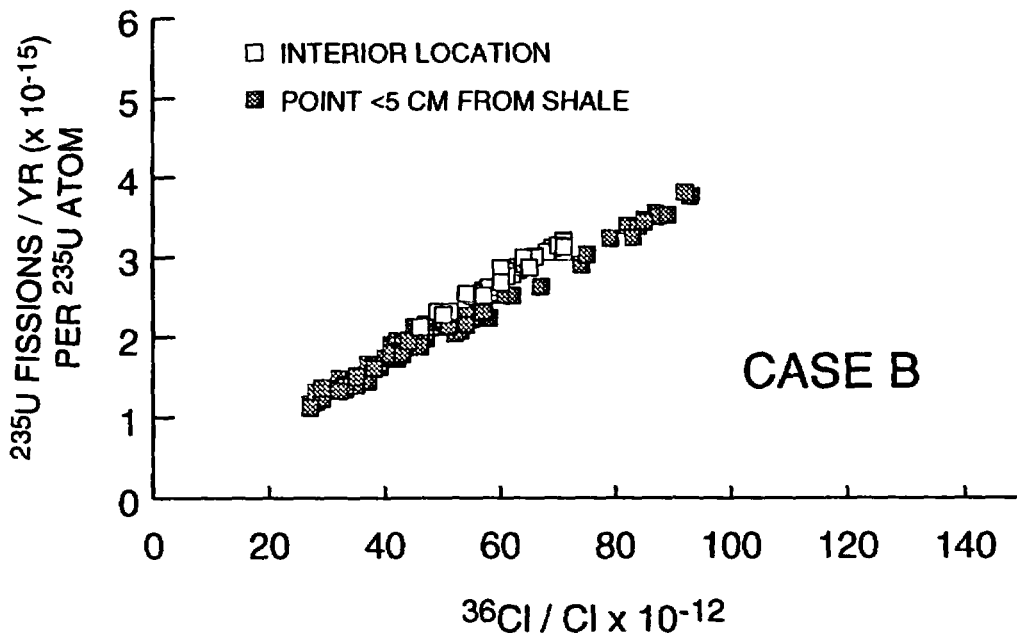
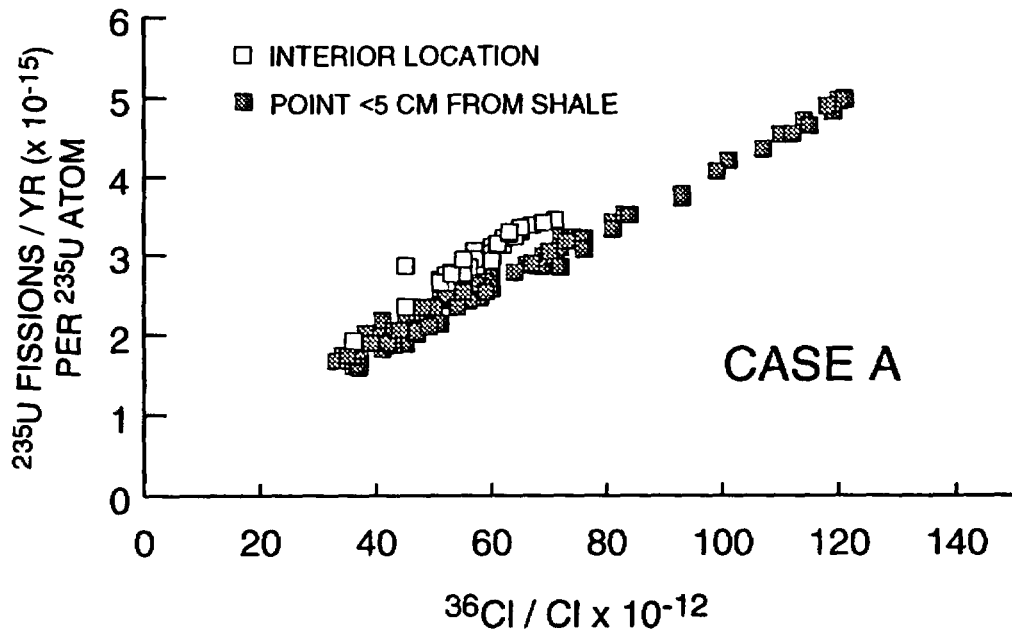


Figure 4.11 Predicted correlation between ^{235}U fission rate and $^{36}\text{Cl}/\text{Cl}$ in the Oklo Reactor Zone 9 ore seam, as a function of location. Calculations are based on the elemental composition of Z9-005. Case A - 80% measured Sm+Gd content, 1850 ppm H in the ore and 12230 ppm H in the surrounding shale; Case B - 120% measured Sm + Gd content in the ore, 3490 ppm H in the ore and 17600 ppm H in the shale.

For H/U ratios less than 6, the appropriateness of $^{36}\text{Cl}/\text{Cl}$ ratio as a monitor of ^{235}U induced fission is less useful.

4.4.3.2 Negligible importance of ^{238}U induced fissions for ^{99}Tc production

For H/U ratios greater than 10, the model predicts that induced fission of ^{238}U will contribute no more than 4% to the total production rate of ^{99}Tc (Figure 4.12A). Because ^{99}Tc fission yields are essentially the same for each of the three fission processes, the ratio of ^{238}U fissions to the total fissions in the sample is the same as the ratio of ^{99}Tc atoms produced by this process to the total production rate of this nuclide.

In contrast, even for large H/U ratios, the model results predict that ^{238}U induced fission could account for up to 30% of the ^{129}I production rate (Figure 4.12B). In uranium ore samples, spontaneous fission of ^{238}U is negligible compared to neutron-induced fission of U isotopes. Because the ^{129}I fission yields are approximately the same for the two induced fission processes, the ratio of ^{238}U induced fissions to the total induced fission rate in a sample is approximately the same as the ratio of ^{129}I atoms produced by this process to the total production rate of this nuclide.

4.4.3.3 Plutonium-239 to establish a constraint on ^{129}I production from ^{238}U induced fission

For H/U ratios greater than 10, measured $^{239}\text{Pu}/\text{U}$ ratios may be used to constrain the predicted rate of ^{238}U induced fission (Figure 4.13). The samples in the present study, with the exception of NBL-6, have $^{239}\text{Pu}/\text{U}$ ratios $\leq 3 \times 10^{-12}$. Figure 4.13A suggests that the ^{238}U induced fission rate in these samples is probably $\leq 4 \times 10^{-18}$ fissions/yr per ^{238}U atom. At this rate, and taking into account the three-fold difference in fission yields, the contribution of ^{129}I from this fission process is equal to that from the spontaneous fission process (8.5×10^{-17} fissions/yr per ^{238}U atom). Both are negligible relative to that produced by ^{235}U fission.

Table 4.6 tabulates the predicted $^{99}\text{Tc}/\text{U}$ and $^{129}\text{I}/\text{U}$ ratios under the assumption that production from ^{238}U induced fission is negligible; Figure 4.14 plots the corresponding log α values for ^{129}I . Measured ^{129}I concentrations are seen to be well within range of predicted values for the Cigar Lake and Oklo samples and NBL-6, but still far depleted in the Koongarra samples and in the Key Lake sample. Because the model appears to be fairly reasonable in predicting ^{239}Pu production in these samples, the apparent ^{129}I depletion in them is probably a real effect and not a consequence of the model overpredicting production. Stronger evidence that the model is not overpredicting ^{235}U fission is that it slightly underpredicts the $^{36}\text{Cl}/\text{Cl}$ ratio, which should track the ^{235}U fission rate very well in this sample.

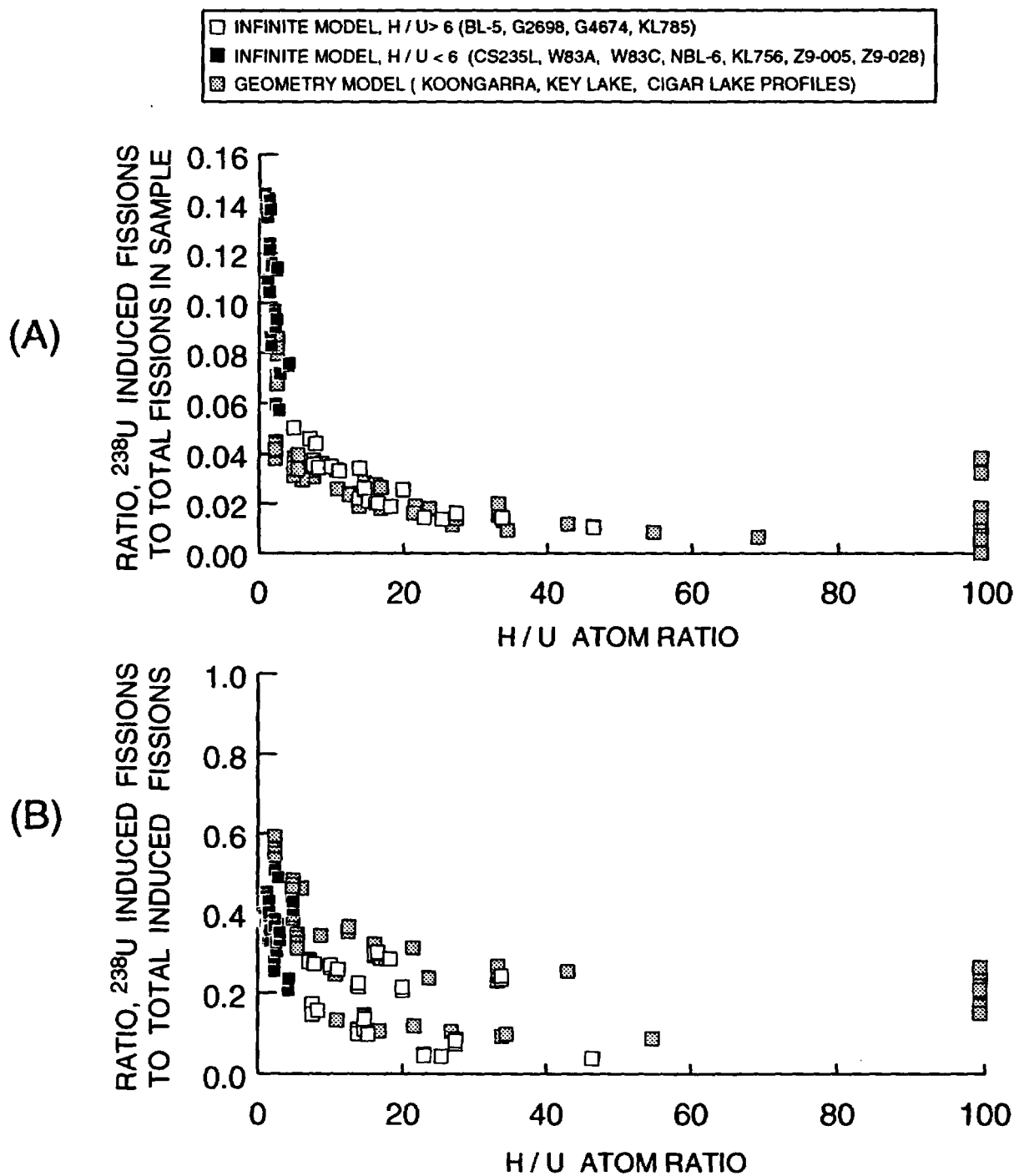


Figure 4.12 Predicted fraction of (A) total and (B) induced fissions attributable to ^{238}U induced fission in primary uranium ores, as a function of H/U atom ratio. The two figures indicate that ^{238}U induced fission contributes negligible quantities to the ^{99}Tc inventory in samples with or adjacent to material with H/U ratios > 6, but that it may contribute as much as 30% to the ^{129}I production rate in the same samples.

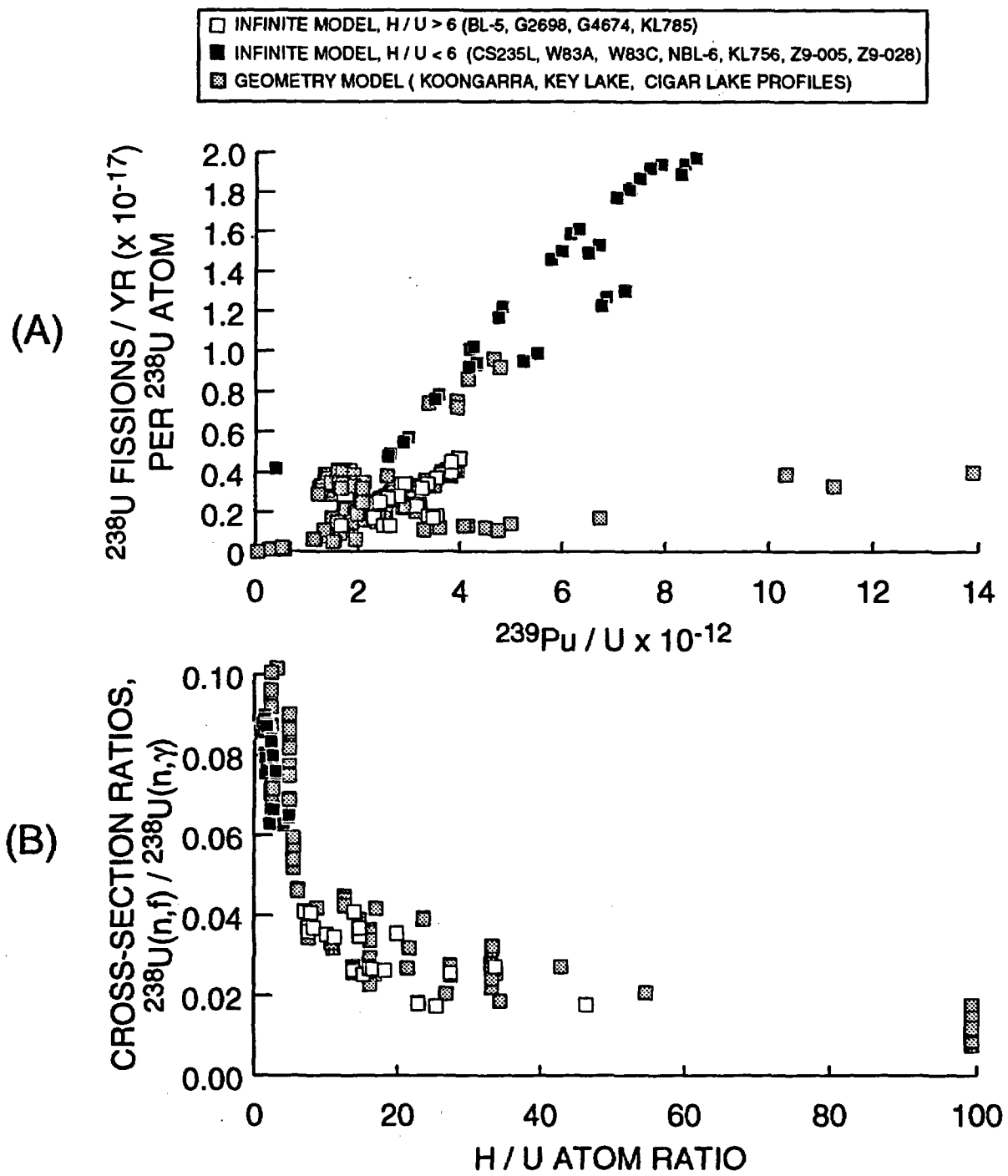


Figure 4.13 Predicted correlation between $^{239}\text{Pu}/\text{U}$ ratios and ^{238}U fission rates, as a function of H/U atom ratio. The figures suggest that measured $^{239}\text{Pu}/\text{U}$ ratios may be used to establish constraints on the estimated ^{238}U induced fission rate.

TABLE 4.6

PREDICTED PRODUCTION RATE OF ^{129}I AND ^{99}Tc ,
ASSUMING NEGLIGIBLE CONTRIBUTION FROM INDUCED FISSION OF ^{238}U

Ore Deposit	Sample	$^{129}\text{I}/\text{U}$ $\times 10^{-12}$ Infinite model	$^{129}\text{I}/\text{U}$ $\times 10^{-12}$ Geometry model	$^{99}\text{Tc}/\text{U}$ $\times 10^{-12}$ Infinite model	$^{99}\text{Tc}/\text{U}$ $\times 10^{-12}$ Geometry model
RANGE OF PREDICTED VALUES					
Koongarra	G2698	3.6 - 4.5	3.1 - 4.6	1.9 - 2.0	1.8 - 2.0
	G4674	3.9 - 4.3	3.2 - 4.1	1.9	1.8 - 1.9
Key Lake	KL756	1.6 - 1.9	1.1 - 1.4	1.6 - 1.7	1.6
	KL785	1.4	1.4 - 1.6	1.6	1.6
Cigar Lake	CS235L	5.9 - 6.5	1.8 - 3.7	2.1 - 2.2	1.7 - 1.9
	W83A	3.0 - 3.5	1.8 - 3.7	1.8	1.7 - 1.9
	W83C	3.2 - 3.6	1.8 - 3.7	1.8 - 1.9	1.7 - 1.9
Oklo	Z9-005	4.9 - 5.6	2.0 - 6.5	2.1	1.7 - 2.2
	Z9-028	4.3 - 4.8	1.7 - 5.4	2.0	1.7 - 2.1
Shinkolobwe	NBL-6	5.9 - 7.1	---	2.1 - 2.2	---
Beaverlodge	BL-5	6.1 - 7.3	---	2.1 - 2.3	---
LOG α FRACTIONATION FACTORS					
Koongarra	G2698	-0.54 to -0.44	-0.55 to -0.38	n.m.	n.m.
	G4674	-0.63 to -0.59	-0.61 to -0.51	≤ 0.02	≤ 0.00
Key Lake	KL756	-0.40 to -0.33	-0.27 to -0.17	n.m.	n.m.
	KL785	n.m.	n.m.	n.m.	n.m.
Cigar Lake	CS235L	-0.49 to -0.45	-0.25 to 0.07	n.m.	n.m.
	W83A	-0.28 to -0.22	-0.31 to 0.00	≤ 0.00	≤ 0.02
	W83C	-0.11 to -0.06	-0.12 to 0.19	n.m.	n.m.
Oklo	Z9-005	n.m.	n.m.	n.m.	n.m.
	Z9-028	-0.25 to -0.20	-0.30 to 0.20	n.m.	n.m.
Shinkolobwe	NBL-6	0.01 to 0.09	---	n.m.	---
Beaverlodge	BL-5	n.m.	---	n.m.	---
Notes:					
n.m. - not measured					
α -fractionation factor: $\alpha = (\text{NRP}/\text{Target})_{\text{M}} / (\text{NRP}/\text{Target})_{\text{SE}}$					
(See Tables 4.4 or 4.5 for full definition)					
Log $\alpha < 0$ suggests that either the model is overpredicting NRP production, or else the NRP is being lost from the sample at a greater rate than is its target.					
Log $\alpha > 0$ suggests that either the model is underpredicting NRP production, or else the NRP is being lost from the sample at a lesser rate than is its target.					

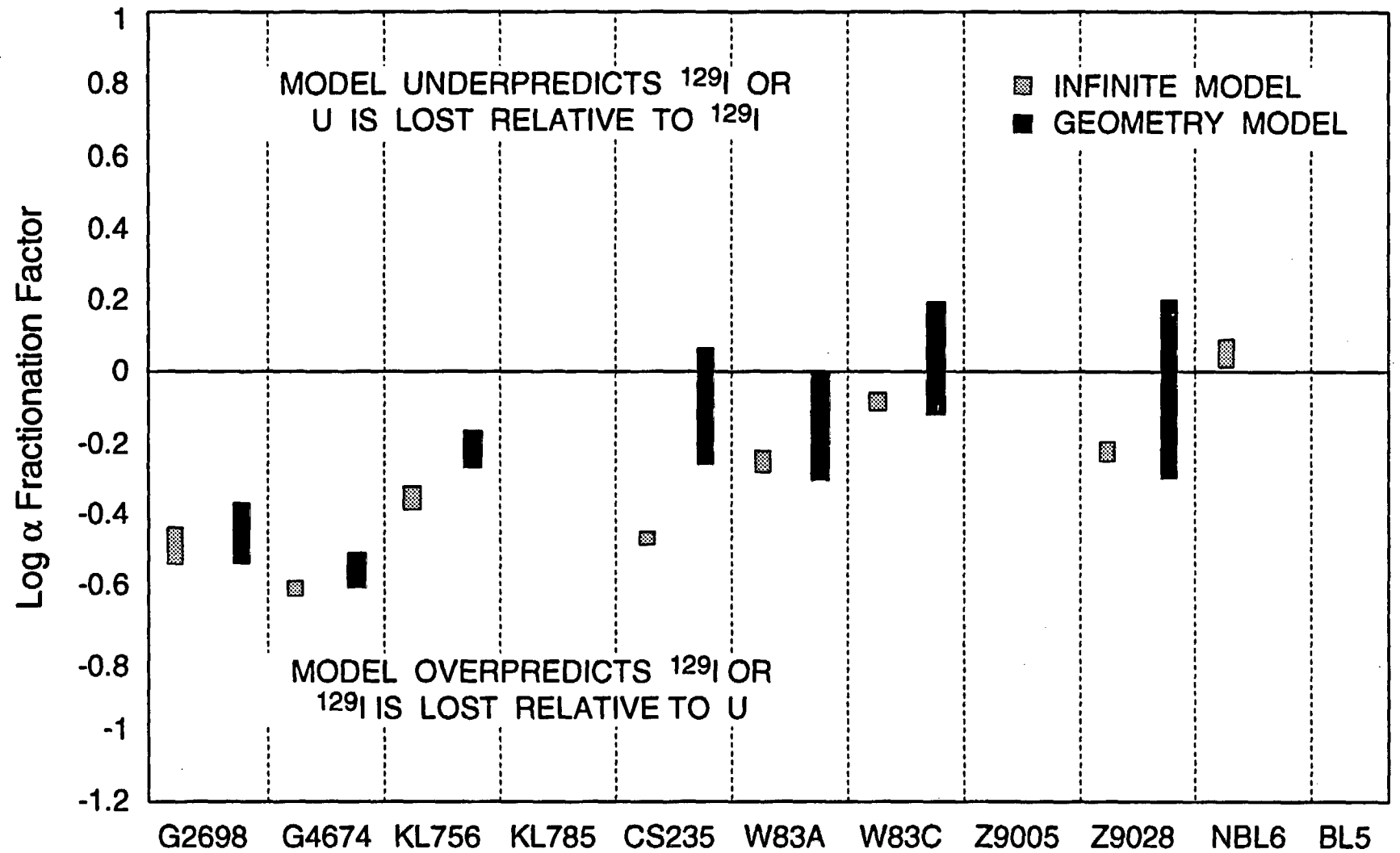


Figure 4.14 Comparison of measured and predicted ^{129}I concentrations for primary uranium ores, assuming negligible contribution from induced fission of ^{238}U . Plotted using data from Table 4.8; see table footnote for definition of α .

4.5 Other Radionuclides in Koongarra Groundwaters

The source-term model is also useful for establishing constraints on the production rates of tritium and ^{14}C in uranium orebodies, and the extent to which in-situ production may contribute to measured concentrations of these nuclides in the groundwater flowing through the deposit. The following sections evaluate the magnitude of the in-situ source term for Koongarra.

4.5.1 Tritium

Tritium is produced by ternary fission of U isotopes, with a fractional yield of 1.25×10^{-4} (Hyde, 1964, p. 131) and by neutron-capture by ^6Li . The former reaction is negligible in comparison to the latter in natural systems. No lithium analyses are available for the Koongarra groundwaters, and concentrations in Koongarra ores G4674 and G2698 are at the detection limit of 100 ppm. An upper limit of 2 TU is obtained for in-situ produced tritium levels in Koongarra groundwaters under the following assumptions. First, a limit of 15 TU is calculated by assuming ore with the elemental composition of G4674, a concentration of 100 ppm Li, complete transfer of all in-situ produced tritium to the groundwater, and 2% porosity. This value is then scaled downward because the average grade of the richest part of the ore body is about 10% of the uranium content of G4674 (12% U), i.e., on the order of 1% U. Measured values would be expected to be lower than the upper limit of 2 TU because of the effects of dilution and because the transfer of tritium from the minerals to the water would be far less than 100%. Thus, observed tritium concentrations in the primary ore zone, which average 0.3 TU (Volume 7 of this series), could possibly be due to in-situ production as opposed to residual meteoric tritium.

4.5.2 Carbon-14

Carbon-14 is produced by neutron-capture by ^{17}O and ^{14}N . Direct production in ground water by other mechanisms, such as neutron capture by ^{13}C , exotic fission of Ra isotopes, and α -capture by ^{11}B (Andrews et al., 1989), is comparatively negligible in the Koongarra system. An upper limit of 0.02 percent modern Carbon (pmC) is obtained for in-situ produced ^{14}C levels in Koongarra groundwaters under the following assumptions. First, a limit of 0.2 pmC is calculated by assuming ore with the elemental composition of G4674, 10 ppm dissolved N_2 in the water, and 0.4 moles/L total dissolved inorganic carbon (DIC). This DIC value is the lowest measured at Koongarra (Volume 7 of this series); the average for the orebody is in the range of 2.6 moles/L (Table 4.1 in Volume 12 of this series). The calculated ^{14}C production limit is then scaled downward to 0.02 pmC--far below detection limits--because the average grade of the richest part of the ore body is about 10% of the uranium content of G4674 (12% U), i.e., on the order of 1% U. Thus, observed ^{14}C concentrations in the primary ore zone, the lowest of which is 55 pmC (Volume 7 of this series), must be residual meteoric ^{14}C .

5 CONCLUSIONS: APPLICABILITY OF URANIUM OREBODIES AS NATURAL ANALOGUES FOR HLW REPOSITORIES

5.1 Applicability for Testing Release-Rate Models

One objective of this research programme has been to evaluate the applicability of uranium orebodies as natural analogues for testing radionuclide release-rate models used in performance assessment activities. The investigated nuclides included three of the most persistent radioactive constituents of high-level wastes from nuclear fission power reactors: plutonium-239 ($t_{1/2}$, 24,100 a), iodine-129 ($t_{1/2}$, 1.6×10^7 a), and technetium-99 ($t_{1/2}$, 2.1×10^5 a). The feasibility of uranium minerals as analogues for the behavior of these nuclear reaction products (NRP) in spent fuel relies upon a capability to characterise NRP concentrations in the source minerals. Measured abundances of natural ^{239}Pu , ^{99}Tc and ^{129}I in uranium ores are compared to calculated abundances in order to evaluate the degree of retention of these radionuclides by the ore.

Measured ^{129}I concentrations in unweathered primary ores investigated in this study exceed minimum concentrations predicted from spontaneous fission of ^{238}U . However, concentrations are variably less than amounts predicted by the source-term model under a wide variety of assumptions. Although production of ^{129}I by neutron-induced fission of ^{235}U and ^{238}U is difficult to estimate with any accuracy, the measurements suggest that ^{129}I may be depleted to a larger extent in samples from Koongarra than in samples from Cigar Lake. Samples from weathered primary ore from Koongarra contain quantities of ^{129}I that are well below the minimum abundance, an unambiguous indicator of loss of this fission product from its site of production. The mobility of radioiodine is also apparent by its high concentrations in groundwaters flowing through the Koongarra deposit, and has also been found to be true in other uraniferous environments (e.g., Fabryka-Martin et al., 1987d, 1989).

Predictions of the source-term model indicate that ^{99}Tc production in uranium ores is dominated by spontaneous fission of ^{238}U . Production of ^{99}Tc by induced fission of ^{235}U is 5-25% of the total for the samples studied, and that by neutron-induced fission of ^{238}U is generally $\leq 4\%$. The dominance of the spontaneous fission component should simplify interpretation of measured ^{99}Tc concentrations in uranium minerals. The validity of the source-term model prediction is borne out by two analyses of ^{99}Tc in primary ores, which had ^{99}Tc abundances at the levels predicted by the model, about 10% above that expected for spontaneous fission alone. Release of ^{99}Tc from the Koongarra ore during weathering is suggested by its presence at measurable concentrations in one of the Koongarra boreholes. Mobility in an oxidising environment such as that in the weathered zone at Koongarra is expected based upon speciation calculations which indicate the pertechnetate anion as the stable species (e.g., Brookins, 1978), and upon results of field studies in other oxidising groundwaters (e.g., Schroeder et al., 1993).

Source-term models predicting ^{239}Pu abundances in uranium minerals lead to ambiguous conclusions. Measured abundances are generally, but not always, within the range of predicted values, suggesting that this nuclide has been largely retained in most, if not all, of the studied samples. The only other study addressing the retention of ^{239}Pu at its point of production in uranium ore was that by Frejacques and Hagemann

(1976). These authors concluded that ^{239}Pu in the Oklo orebody was stable, based upon the good correlations observed between neutron fluences and depletions in ^{235}U along cores, without any discontinuity or irregularity attributable to ^{239}Pu migration. In addition, no sample enriched in ^{235}U has been found around the Oklo reactor zones, and ion-probe data show ^{235}U and ^{238}U occurring in the same positions, which would not be the case if ^{239}Pu had moved more than a few microns from its point of production.

In very heterogeneous media such as that typical of uranium ore deposits, chemical parameters critical for determination of ^{239}Pu production rates are difficult to characterise with sufficient accuracy to use the results for evaluating degree of retention or loss of ^{239}Pu from the orebody. Alternative methods for evaluating Pu mobility are being investigated, including its measurement in groundwaters. Attempts to characterise the aqueous geochemistry of plutonium in Koongarra groundwater indicated the presence of the element at very low concentrations, on the order of 10^{-18} M. In well PH146, the source of the plutonium is ambiguous and may be anthropogenic fallout rather than natural plutonium derived from the nearby deposits. The results suggest that mobile plutonium may be present in particulate matter and in anionic form. Establishing the validity of these observations, and a less ambiguous interpretation, would require additional, more sophisticated, sampling.

This modelling study also shows the extent to which various NRP are correlated, such that one provides a constraint on the production rates of others. Under most conditions, ^{36}Cl ($t_{1/2}$, 3.0×10^5 a), another long-lived neutron-capture product found in uranium ores, is shown to be an ideal in-situ monitor of the ^{235}U fission rate, which is the dominant source term for ^{129}I and possibly a significant one for ^{99}Tc . Similarly, $^{239}\text{Pu}/\text{U}$ ratios can be used to establish limits on the ^{238}U neutron-induced fission rate; the ratios measured in this study suggest that ^{238}U induced fission comprises $< 4\%$ of the total fissions in most of the ore samples studied and hence can be neglected as a source of ^{129}I and ^{99}Tc .

5.2 Directions for Future Work

The applicability of uranium orebodies as analogues for testing NRP release-rate models could be maximised by focussing future work on approaches that are relatively independent of source-term model assumptions. Some promising areas for investigation are as follows:

- (a) Relative distributions of NRP and U could be studied in separable co-existing uranium mineral phases in environments where such phases could be assumed to be exposed to the same neutron flux. This assumption should be valid for samples within a centimetre or so of one another, provided they are not located near an abrupt boundary between two materials with significantly different neutron generation and transport properties.
- (b) Relative distributions of NRP and U could be studied in a profile across a water-bearing fracture, in order to ascertain the extent to which the NRP have been mobilised by the water. Again, this approach minimises dependence upon source-term model predictions to the extent that samples taken within close proximity to one

another within a fairly homogeneous system should be subject to the same neutron flux.

- (c) Chlorine-36/Cl ratios should be routinely measured for all uranium samples in which the long-lived fission products are measured. The $^{36}\text{Cl}/\text{Cl}$ measurements can then be used as an in-situ measure of ^{235}U fission rates--subject to the limitations identified in this report--and hence ^{129}I and ^{99}Tc abundances, thereby reducing the uncertainties inherent in the source-term model predictions.
- (d) Particularly in those cases where analyses of mineral studies suggest large-scale losses of the fission products ^{129}I or ^{99}Tc , efforts should be made to collect sufficient quantities of groundwater from these environs to test such hypotheses.

To maximise benefits of analogue research, close coordination is needed between natural analogue research groups and those involved in the development and application of HLW release-rate models used in performance assessment. The Alligator Rivers Analogue Project has provided an excellent forum for such interaction, and additional such integrated efforts would continue to benefit the performance assessment community.

6 REFERENCES

- Airey P.L. (1986) Radionuclide migration around uranium ore bodies in the Alligator Rivers region of the Northern Territory of Australia: analogue of radioactive waste repositories - a review. *Chemical Geology* 55, 255-268.
- Airey P.L., Duerden P., Roman D., Golian C., Nightingale T., Payne T., Davey B., and Gray D. (1987) The Koongarra ore body: a natural analogue of radionuclide migration in the far field of HLW repositories. B. Côme and N. Chapman, eds., *Commission of the European Communities Natural Analogues in Radioactive Waste Disposal - A Symposium*. Brussels: CEC:175-215.
- Airey P.L. and Ivanovich M. (1986) Geochemical analogues of high-level radioactive waste repositories, *Chem. Geol.* 55, 203-213.
- Andrews J.N., Davis S.N., Fabryka-Martin J., Fontes J-Ch., Lehmann B.E., Loosli H.H., Michelot J-L., Moser H., Smith B., Wolf M. (1989) The in-situ production of radioisotopes in rock matrices with particular reference to the Stripa granite. *Geochim. Cosmochim. Acta* 53, 1803-1815.
- Arino H. and Kuroda P.K. (1968) Spontaneous fission-produced strontium isotopes in uranium minerals and salts. *J. Inorg. Nucl. Chem.* 30, 677-683.
- Attrep M., Jr. (1965) The radiochemical measurement of promethium isotopes in nature, Ph.D. thesis, University of Arkansas.
- Attrep M., Jr., and Kuroda P.K. (1968) Promethium in pitchblende. *J. Inorg. Nucl. Chem.* 30, 699-703.
- Attrep M., Jr., Roensch F.R., Aguilar R., and Fabryka-Martin J. (1992) Separation and purification of plutonium in uranium ores for mass spectrometric measurement. *Radiochim. Acta* 57, 15-20.
- Birchard G.F. and Alexander D.H. (1983) Natural analogues - a way to increase confidence in predictions of long-term performance of radioactive waste disposal. In: *Scientific Basis for Nuclear Waste Management, Vol. 6* (D.G. Brookins, ed.), North Holland, New York, pp 323-329.
- Brauer F.P., and Strebin R.S., Jr. (1982) Environmental concentration and migration of ^{129}I , in: *Environmental Migration of Long-Lived Radionuclides*, 465-475, Int. Atomic Energy Agency IAEA, Vienna, IAEA-SM-257/43.
- Briesmeister J. (ed.) (1986) MCNP -- A General Monte Carlo Code for Neutron and Photon Transport, Version 3A, Los Alamos National Laboratory, LA-7396-M, Rev. 2 (manual), 583 p.
- Brookins D.G. (1976) Shale as a repository for radioactive waste: the evidence from Oklo. *Environ. Geol.* 1, 255-259.

Brookins D.G. (1978) Application of Eh-pH diagrams to problems of retention and/or migration of fissionogenic elements at Oklo, pp 243-266 in: Natural Fission Reactors (I.A.E.A., Vienna), STI/PUB/475.

CANMET (Canada Centre for Mineral and Energy Technology) (no date) BL-5 certificate of analysis.

Chapman N., McKinley I.G., and Smellie J.A.T. (1984) The potential of natural analogues in assessing systems for deep disposal of high-level radioactive waste. Swedish Nuclear Fuel and Waste Management Company (SKB) and the Swiss Radioactive Waste Cooperative (NAGRA). NTB 84-41. KBS 84-16. Eir Ber 545.

Chapman N., and Smellie J.A.T. (1986) Natural analogues to the conditions around a final repository for high-level radioactive waste. Chem. Geol. 55, 167-173.

Cramer J.J. (1986) Sandstone-hosted uranium deposits in northern Saskatchewan as natural analogs to nuclear fuel waste disposal vaults. Chem. Geol. 55, 269-279.

Cramer J.J., Vilks P., and Larocque J.P.A. (1987) Near-field analog features from the Cigar Lake uranium deposit. B. Côme and N. Chapman, eds., Commission of the European Communities Natural Analogues in Radioactive Waste Disposal - A Symposium. Brussels: CEC:59-72.

Curtis D.B., Fabryka-Martin J., Aguilar R., Attrep M., Roensch F. (1992) Plutonium in uranium deposits: natural analogues of geologic repositories for plutonium-bearing nuclear wastes. Proc., 3rd Annual Intl. High-Level Radioactive Waste Management Conf., Vol. 1, pp 338-344.

Curtis D., Benjamin T., Gancarz A., Loss R., Rosman K., DeLaeter J., Delmore J.E., and Maeck W.J. (1989) Fission product retention in the Oklo natural fission reactors. Appl. Geochem. 4, 49-62.

Dahlkamp F.J. (1978) Geologic appraisal of the Key Lake U-Ni deposits, Northern Saskatchewan, Economic Geology 73, 1430-1449.

DeCarvalho H.G., Martins J.B., Medeiros E.L. and Tavares O.A.P. (1982) Decay constant for the spontaneous fission process in ^{238}U . Nucl. Instrum. Meth. 197, 417-426.

Deer W.A., Howie R.A., and Zussman J. (1966) An Introduction to the Rock-Forming Minerals. Longmans, Green and Co., Ltd., London.

DeLaeter J.R. (1985) The Oklo reactors: Natural analogues to nuclear waste repositories, Search 16, 193-196.

Dickson B.L. and Snelling A.A. (1980) Movements of uranium and daughter isotopes in the Koongarra uranium deposit, pp 499-507 in: Proc. Intl. Uranium Symp. on the Pine Creek Geosyncline 1980 (J. Ferguson and A.B. Goleby, eds.), Intl. Atomic Energy Agency, Vienna.

Ehrhardt K.C. and Attrep M. Jr. (1978) Technetium-99 in the environment, *Environ. Sci. Technol.* 12, 55-57.

Elmore D., Fluton B.R., Clover M.R., Marsden J.R., Gove H.E., Naylor H., Purser K.H., Kilius L.R., Beukens R.P., and Litherland A.E. (1979) Analysis of ^{36}Cl in environmental water samples using an electrostatic accelerator, *Nature* 277, 22.

Elmore D., Gove H.E., Ferraro R., Kilius L.R., Lee H.W., Chang K.H., Beukens R.P., Litherland A.E., Russo C.J., Purser K.H., Murrell M.T., and Finkel R.C. (1980) Determination of ^{129}I using tandem accelerator mass spectrometry, *Nature* 286, 138-139.

Ewing R.C. and Jercinovic M.J. (1987) Natural analogues: their application to the prediction of the long-term behavior of nuclear waste forms. *Materials Research Society Symposia Proc.* 84, 67-83.

Fabryka-Martin J. (1988) Production of radionuclides in the earth and their hydrogeologic significance, with emphasis on chlorine-36 and iodine-129. Unpub. Ph. D. dissertation, Dept. of Hydrology and Water Resources, Univ. of Arizona, Tucson AZ, 400 p.

Fabryka-Martin J., Bentley H., Elmore D. and Airey P.L. (1985) Natural iodine-129 as an environmental tracer. *Geochim. Cosmochim. Acta*, 49, 337-347.

Fabryka-Martin J., Davis S.N., and Elmore D. (1987a) Applications of ^{129}I and ^{36}Cl in hydrology. *Nucl. Instr. Meth. Phys. Res.*, B29, 361-371.

Fabryka-Martin J., Davis S.N., Wirt L., Elmore D., Kubik P.W. (1987b) Comparison of theoretical and measured deep subsurface production of ^{36}Cl (abstr.). *Geol. Soc. Amer., Abstr. with Programs*, 19, 658.

Fabryka-Martin J., Roman D., Airey P.L., Elmore D. and Kubik P.W. (1987c) Redistribution of natural iodine-129 among mineral phases and groundwater in the Koongarra uranium ore deposit, N.T., Australia. *Proc., Natural Analogues in Radioactive Waste Disposal: a Symposium* (B. Côme, ed.), Commission of the European Communities, Brussels, Belgium. CEC report EUR 11037 EN.

Fabryka-Martin J., Davis S.N., Roman D., Airey P.L., Kubik P.W. (1988) Iodine-129 and chlorine-36 in uranium ores, 2. Discussion of AMS measurements. *Chem. Geol. (Isot. Geos. Sect.)*, 72, 7-16.

Fabryka-Martin J., Davis S.N., Elmore D., and Kubik P.W. (1989) In-situ production and migration of iodine-129 in the Stripa granite, Sweden. *Geochim. Cosmochim. Acta*, 53, 1817-1823.

Fabryka-Martin J., Baker M., and Eccleston G. (1993, in prep.) Neutron production in uranium ores.

Feige Y., Oltman B.G., and Kastner J. (1968). Production rates of neutrons in soils due to natural radioactivity. *J. Geophys. Res.*, 73, 3135-3142.

Ferguson J. and Winer P. (1980) Pine Creek Geosyncline: statistical treatment of whole-rock chemical data, pp 191 + appendix in: Proc. Intl. Uranium Symp. on the Pine Creek Geosyncline 1980 (J. Ferguson and A.B. Goleby, eds.), Intl. Atomic Energy Agency, Vienna.

Finch R.J., and Ewing R.C. (1989) Alteration of natural UO₂ under oxidizing conditions from Shinkolobwe, Katanga, Zaire: a natural analogue for the corrosion of spent fuel. Swedish Nuclear Fuel and Waste Management Company (SKB). Technical Report 89-37.

Frejaques C. and Hagemann R. (1976) Conclusions from studies of the Oklo natural reactors, Proc. Intl. Symp. on the Mgmt. of Wastes from the LWR Fuel Cycle, Denver CO, 11-16 July 1976, CONF-760701, pp 678-685.

Fronde! C. (1958) Systematic Mineralogy of Uranium and Thorium, Geological Survey Bulletin 1064 (U.S. Govt. Printing Office, Washington, D.C.)

Garber D. (ed.) (1975) ENDF/B-V, Report BNL-17541 (ENDF-201), National Nuclear Data Center, Brookhaven National Laboratory, Upton NY.

Gardner M.A. and Howerton R.J. (1978) ACTL: Evaluated Neutron Activation Cross-Section Library - Evaluation Techniques and Reaction Index, Lawrence Livermore National Laboratory report UCRL-50400, Vol. 18.

Gascoyne M. and Larocque J.P.A. (1984) A rapid method of extraction of uranium and thorium from granite for alpha spectrometry. Nucl. Instrum. Meth. Phys. Res., 223, 250-252.

Gauthier-Lafaye F. and Ohmoto H. (1989) Natural fission reactors of Oklo. Econ. Geol., 84, 2286-2295.

Gole M.J., Butt C.R.M., and Snelling A.A. (1986) A groundwater helium survey of the Koongarra uranium deposits, Pine Creek Geosyncline, Northern Territory, Uranium, 2, 343-360.

Goodwin B.W., Cramer J.J., and McConnell D.B. (1988) The Cigar Lake uranium deposit: an analogue for nuclear fuel waste disposal. B. Côme and N. Chapman, eds., Commission of the European Communities Natural Analogue Working Group, Third Meeting, Snowbird, Utah: CEC:180-189.

Heaton R., Lee H., Skensved P., and Robertson B.C. (1989) Neutron production from thick-target (α,n) reactions, Nucl. Instrum. Meth. Phys. Res., A276, 529-538.

Hebeda E.H., Schultz L., and Freundel M. (1987) Radiogenic, fissionogenic and nucleogenic noble gases in zircon, Earth Planet. Sci. Lett., 85, 79-90.

Holden N.E. (1981) The uranium half-lives: a critical review, Brookhaven National Laboratory, National Nuclear Data Center, Report BNL-NC8-51320.

Hyde E.K. (1964) *The Nuclear Properties of the Heavy Elements, Vol. III, Fission Phenomena*. Prentice-Hall, Inc., Englewood Cliffs, New Jersey, 519 p.

Ingles J.C., Sutarno R., Bowman W.S. and Faye G.H. (1977) Radioactive ores DH-1, DL-1, BL-1, BL-2, BL-3 and BL-4 -- certified reference materials. Prepared by Minerals Research Program; Mineral Sciences Laboratories; Energy, Mines and Resources Canada; Canada Centre for Mineral and Energy Technology (CANMET). CANMET Report 77-64.

Kenna B.T. and Attrep M., Jr. (1966) The ratio of induced fission vs. spontaneous fission and the trace element analysis in pitchblende. *J. Inorg. Nucl. Chem.*, 28, 1491-1500.

Kenna B.T. and Kuroda P.K. (1960) The ratio of induced fission vs. spontaneous fission in pitchblende, and natural occurrence of radiochlorine. *J. Inorg. Nucl. Chem.*, 16, 1-7.

Kenna B.T. and Kuroda P.K. (1964) Technetium in nature. *J. Inorg. Nucl. Chem.*, 26, 493-499.

Kleinberg J. and Cowan G.A. (1960) *The Radiochemistry of Fluorine, Chlorine, Bromine and Iodine*. Report NAS-NS-3005, Subcommittee on Radiochemistry, National Academy of Sciences--National Research Council, Washington D.C., 42 p.

Kuhn M.W., Davis S.N., Bentley H.W., and Zito R. (1984) Measurement of thermal neutrons in the subsurface, *Geophys. Res. Lett.*, 11, 607-610.

Lehmann B.E., Davis S.N., and J.T. Fabryka-Martin J.T. (1993) Atmospheric and subsurface sources of stable and radioactive nuclides used for groundwater dating, *Water Resources Research* (in press).

Levine C.A. and Seaborg G.T. (1951) The occurrence of plutonium in nature, *J. Am. Chem. Soc.*, 73, 3278-3283.

Loss R.D., Rosman K.J.R., DeLaeter J.R., Curtis D.B., Benjamin T.M., Gancarz A.J., Maeck W.J., and Delmore J.E. (1989) Fission-product retentivity in peripheral rocks at the Oklo natural fission reactors, Gabon, *Chemical Geology*, 76, 71-84.

McLennan S.M. and Taylor S.R. (1980) Rare earth elements in sedimentary rocks, granites, and uranium deposits of the Pine Creek Geosyncline, in *Proc. Intl. Symp. on the Pine Creek Geosyncline 1980*, pp 175-190. Intl. Atomic Energy Agency, Vienna.

Myers W.A. and Lindner M. (1971) Precise determination of the natural abundance of ^{237}Np and ^{239}Pu in Katanga pitchblende, *J. Inorg. Nucl. Chem.*, 33, 3233-3238.

NCRP (National Council of Radiation Protection and Measurements), 1983. Iodine-129: evaluation of releases from nuclear power generation. NCRP Rep. No. 75 (Washington D.C.), 74 p.

Payne T.E. and Waite T.D. (1991) Uranium and thorium migration in Koongarra groundwater - implications to nuclear waste disposal, *Chemistry in Australia*, 58, 281-283.

Pearcy E.C., and Manaktala H.K. (1992) Occurrence of metallic phases in spent nuclear fuel: significance for source term predictions for high-level waste disposal, *Proc., 3rd Annual Intl. High-Level Radioactive Waste Management Conf.*, Vol. 1, pp 131-136.

Pearcy E.C., and Murphy W.M. (1991) *Geochemical Natural Analogues Literature Review*. Center for Nuclear Waste Regulatory Analyses (San Antonio, Texas), Report CNWRA 90-008.

Peppard D.F., Studier M.H., Gergel M.V., Mason G.W., Sullivan J.C. and Mech J.F. (1951) Isolation of microgram quantities of naturally-occurring plutonium and examination of its isotopic composition, *J. Am. Chem. Soc.* 73, 2529-2531.

Perrin R.E., Knobeloch G.W., Armijo V.M. and Efurud D.W. (1985) Isotopic analysis of nanogram quantities of plutonium by using a SID ionization source, *Intl. J. Mass Spectrometry and Ion Proc.* 64, 17-34.

Petit J.-C. (1991) Natural analogues aspects of radionuclide transport in the geosphere, *Radiochim. Acta*, 52/53, 337-340.

Rider B.F. (1981) *Compilation of fission product yields*, Vallecitos Nuclear Center report NEDO-12154-3(C), Pleasanton, California.

Rokop D.J., Schroeder N.C., and Wolfsberg K. (1990) Mass spectrometry of technetium at the subpicogram level, *Analytical Chem.*, 62, 1271-1274.

Schroeder N.C., Morgan D., Rokop D.J., and Fabryka-Martin J. (1993, in press) Migration of technetium-99 in the alluvial aquifer at the Nevada Test Site, Nevada. *Radiochim. Acta*.

Silker W.B., Perkins R.W., and Rieck H.G. (1971) A sampler for concentrating radionuclides from natural waters, *Ocean Engng.*, 2, 49-55.

Steger H.F. (compiler) (1986) *Certified reference materials*. Prepared by Canadian Certified Reference Materials Project; Energy, Mines and Resources Canada; Canada Centre for Mineral and Energy Technology (CANMET). Report CM84-14E, 42 p.

Sunder S., Taylor P., and Cramer J.J (1987) XPS and XRD studies of uranium rich minerals from Cigar Lake, Saskatchewan. *Proc., 11th Mat. Res. Soc. Symp. on Scientific Basis for Nuclear Waste Management*, Boston.

Trocki L.K., Curtis D.B., Gancarz A.J., and Banar J.C. (1984) Ages of major uranium mineralization and lead loss in the Key Lake uranium deposit, Northern Saskatchewan, Canada, *Economic Geology*, 79, 1378-1386.